European Journal of Taxonomy 810: 1–95
https://doi.org/10.5852/ejt.2022.810.1723
ISSN 2118-9773
www.europeanjournaloftaxonomy.eu
2022 · Nethupul H. *et al.*

This work is licensed under a Creative Commons Attribution License (CC BY 4.0).

Monograph

urn:lsid:zoobank.org:pub:67E0CCF7-F768-4C5F-9F02-55EBFFADD3D5

New species, redescriptions and new records of deep-sea brittle stars (Echinodermata: Ophiuroidea) from the South China Sea, an integrated morphological and molecular approach

Hasitha NETHUPUL [1], Sabine STÖHR [2] & Haibin ZHANG [3,*]

[1,3] Institute of Deep-sea Science and Engineering, Chinese Academy of Sciences, CAS, 57200 Sanya, China.
[1] University of Chinese Academy of Sciences, Beijing 100039, China.
[2] Swedish Museum of Natural History, Department of Zoology, Box 50007, 10405 Stockholm, Sweden.

[*] Corresponding author: hzhang@idsse.ac.cn
[1] Email: Nethupul@idsse.ac.cn
[2] Email: sabine.stohr@nrm.se

[1] urn:lsid:zoobank.org:author:947FC889-2FAA-465B-8F4C-93E4DF21BD00
[2] urn:lsid:zoobank.org:author:412800EB-AACE-4313-9810-61F89B740405
[3] urn:lsid:zoobank.org:author:42C09E82-18C5-446D-B4F4-A2C8F2367AC9

Abstract. Deep-sea ophiuroids were collected by the manned submersible 'Shenhaiyongshi' from the South China Sea at depths of 500–3550 m, in 2017 to 2020. A total of 18 species were identified, including three new species and eight new records, increasing the total number of species known from the South China Sea to 304. Most of the ophiuroids recorded from the South China Sea were found in shallow waters (77.9%) and a few of them occurred only in deep water (20.4%). Three new species are described as *Ophiacantha aster* sp. nov., *Ophiomoeris petalis* sp. nov. and *Ophiopristis shenhaiyongshii* sp. nov. We provide comprehensive descriptions of morphological features, including characteristics of the arm skeletons, and a phylogenetic analysis based on COI and 16S sequences. Overall intraspecific and interspecific genetic distance variations among the families found in this study were 0.5% to 2.47% and 1.16% to 44.16%, respectively, along the South Pacific region to the South China Sea. Our phylogenetic analysis suggested that COI partial genes resolved the interspecies complexity in the class Ophiuroidea better than 16S partial genes. The order Euryalida had low interspecies genetic distance variation within the class Ophiuroidea. The present study suggests a high probability that species of *Asteroschema* and *Gorgonocephalus* are more widely spread around the Indo-Pacific region than previously expected.

Keywords. Taxonomy, faunistic, scanning electron microscope, COI, 16S.

Nethupul H., Stöhr S. & Zhang H. 2022. New species, redescriptions and new records of deep-sea brittle stars (Echinodermata: Ophiuroidea) from the South China Sea, an integrated morphological and molecular approach. *European Journal of Taxonomy* 810: 1–95. https://doi.org/10.5852/ejt.2022.810.1723

Introduction

The class Ophiuroidea contains more than 2100 accepted species (Stöhr *et al.* 2021) and new species are discovered frequently. This class includes 259 genera, 34 families and six orders. Ophiuroidea are widespread across all oceans and occur in various physiochemical environments. They have a range of lifestyles, adapted to a wide range of marine environments. The majority of ophiuroids are bottom dwellers on the seafloor, buried in mud or hidden in crevices of rocks and corals, but some species are epizoic, living on various kinds of hosts, such as corals, gorgonians and glass sponges (Stöhr *et al.* 2012). It has been suggested that ophiuroids and corals may have a parasitic, commensal association or a mutualistic relationship (Girard *et al.* 2016). Deep-sea ophiuroids represent a high percentage of the biomass in deep-sea environments (Frensel *et al.* 2010).

DNA barcoding is an effective tool for the identification of ophiuroid species and has become useful for rapid assessment of biodiversity in combination with field surveys (Ward *et al.* 2008; Hoareau & Boissin 2010). Previous molecular studies indicated that interspecies genetic distances within the class Ophiuroidea range approximately from 2.2% to 31.6% for the COI partial gene (Muths *et al.* 2006, 2009; Boissin *et al.* 2008, 2011, 2017; Pérez-Portela *et al.* 2013; Richards *et al.* 2015; Sands *et al.* 2015) and intraspecies genetic distances approximately range from 0.5% to 6.4%, with a mean of 2.2% (Boissin *et al.* 2017). Recently, advanced molecular technology and a large amount of molecular data being collected have become a major advantage in the identification of ophiuroid species (Okanishi *et al.* 2011a; Okanishi & Fujita 2013; O'Hara *et al.* 2014, 2016, 2019; Boissin *et al.* 2017; Christodoulou *et al.* 2019). However, no molecular analysis of deep-sea ophiuroids in the South China Sea has been done yet.

The South China Sea covers 3.5 million km^2 and is part of the Western Pacific Ocean. It includes over 200 islands and islets with coral reefs in waters shallower than 200 m, to deep-sea basins, reaching nearly 5000 m in depth (Teh *et al.* 2019). The ophiuroids in the South China Sea have still not been completely studied and most of the previous expeditions hardly covered the area. The deep-sea exploring voyage of HMS 'Challenger' (1873–1876) was the first major expedition that explored the South China Sea, but only at two localities. The South China Sea ophiuroids from the 'Challenger' and 'Albatross' voyages were described by several authors (Lyman 1882; Koehler 1922a). Deep-sea exploration began in China by launching the first manned submersible, 'Jiaolong', used to discover the biodiversity of deep waters from Chinese seas and the Mariana trench and finding new deep-water fauna and flora communities in recent years (Li 2017).

Recent studies done in the Japan Sea indicated new species of Euryalida and new records of species that had previously only been reported from the South Pacific region, Australia and New Zealand (Okanishi *et al.* 2011a, 2011b, 2001c; Kim & Shin 2015; Okanishi & Fujita 2018a, 2018b; Okanishi *et al.* 2018). Previous explorations of the ophiuroid community in the South China Sea compiled three comprehensive species checklists (Lane *et al.* 2000; Liao 2004; Putchakarn & Sonchaeng 2004), but few studies have been published since 2004 (Sirenko *et al.* 2019; Chen *et al.* 2020; Li *et al.* 2021). Therefore, the checklist of the Ophiuroidea of the South China Sea is considered outdated.

The present study covers deep waters around Hainan Island, the Xisha Islands and the Zhongsha Islands complex in the South China Sea. Here, we present an account of the ophiuroids collected, with descriptions of new records and new species. Our goal is to present a diagnosis of the morphological features of these species combined with molecular details, to complement the limited original descriptions and the lack of figures, with many morphological variations presented in the literature. Three new species are described and 15 species are redescribed, including eight new records from the South China Sea; all are richly illustrated.

Material and methods

Sample collecting

Most of the specimens of this study were collected by the manned submersible vehicle 'Shenhaiyongshi' on South China Sea deep-sea seamounts, at depths of 516 to 3500 m (Fig. 1; Table 1). Most of the specimens were frozen without preservation fluid, but some of them were stored in ethanol (95%) at room temperature, then transported to the Institute of Deep-sea Science and Engineering, Chinese Academy of Sciences (CAS), Sanya, China, for further analysis. The samples were sorted and the species identified by using summaries, keys, various original descriptions (Lyman 1875, 1878, 1879, 1882, 1883; Lütken & Mortensen 1889; Koehler 1897, 1899, 1900, 1904, 1905, 1907, 1922a, 1922b; Döderlein 1902, 1911, 1927; H.L. Clark 1911, 1915, 1923; Matsumoto 1917; Mortensen 1924; Baker 1980; Hendler 1988, 2018; Liao & Clark 1995; McKnight 2000; Liao 2004; O'Hara & Stöhr 2006; Martynov 2010; Stöhr 2011, 2012; Stöhr *et al.* 2012; Thuy & Stöhr 2016; O'Hara *et al.* 2017, 2018; Stöhr & O'Hara 2021) and molecular analysis.

Morphological analysis

To document morphological characters and color patterns, most of the specimens were photographed through a dissecting stereo microscope (OLYMPUS SZX7) and larger specimens with a digital camera (Canon EOS 6DII). Micro-morphological features and smaller specimens were examined with a Phenom ProX scanning electron microscope (SEM). For SEM examination, household bleach was used to remove the outer integument (skin) from the specimens. The animal was held with tweezers and submerged in NaOCl (household bleach) diluted with water (1:1) for 20 seconds. This was repeated until the skin of the specimen had been removed. The specimens were then gently washed in distilled water and left to dry, before mounting them on a stub with carbon tape. Ethanol was used to dissolve

Table 1. Deep-sea ophiuroids found in the South China Sea; damaged unidentified specimens recorded under generic name. New records for South China Sea marked with an asterisk.

Family	Species name	Station (specimens)
Asteronychidae	*Asteronyx loveni*	SC002 (1)
	*Asteronyx luzonicus**	SC002 (2)
Euryalidae	*Asteroschema horridum**	SC013 (1), SC019 (1)
Gorgonocephalidae	*Gorgonocephalus chilensis novaezelandiae**	SC013 (1)
	Gorgonocephalus cf. *dolichodactylus*	SC008 (1)
Ophiomusaidae	*Ophiomusa lymani*	SC017 (1), SC015 (1), SC005 (1)
	Ophiomusa sp. (damaged)	SC006 (1)
Ophiotomidae	*Ophiotreta eximia**	SC022 (1)
	***Ophiopristis shenhaiyongshii* sp. nov.**	SC012 (1)
Ophiacanthidae	*Ophientrema scolopendrica**	SC003 (1), SC017 (2), SC018 (3), SC022 (2), SC023 (1)
	Ophiurothamnus clausa	SC020 (2), SC021(1)
	Ophioplinthaca plicata	SC014 (1)
	*Ophiacantha bathybia**	SC016 (3)
	*Ophiacantha vorax**	SC001 (1), SC020(1), SC021(1)
	***Ophiacantha aster* sp. nov.**	SC011 (30)
	***Ophiomoeris petalis* sp. nov.**	SC013 (5)
	Ophiomoeris sp.	SC013 (1)
Ophiactidae	*Ophiactis* cf. *perplexa**	SC012 (3)
	Ophiactis profundi	SC013 (7)
	Ophiactis cf. *brachygens*	SC013 (2)

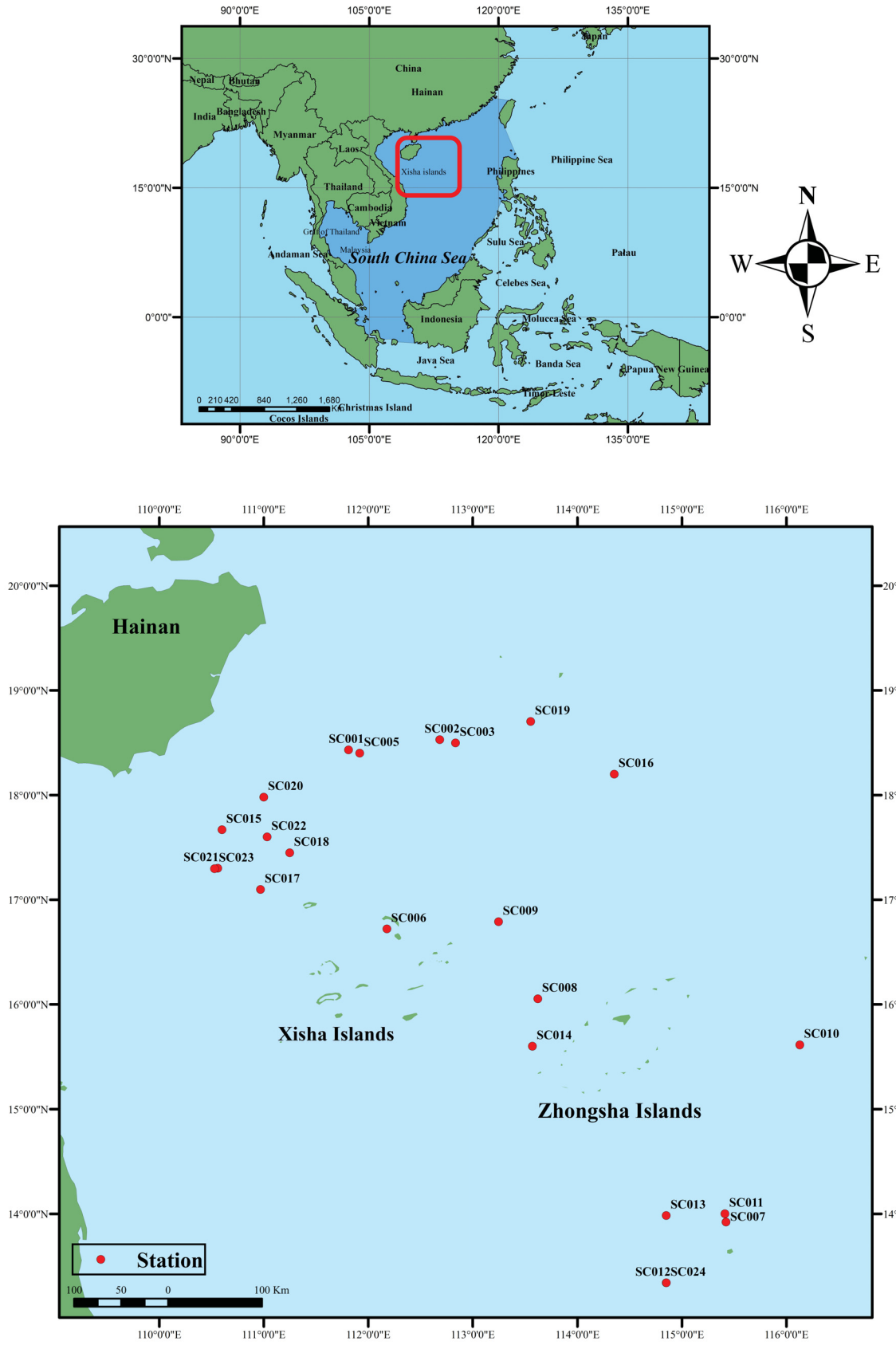

Fig. 1. Map of collecting stations in the South China Sea (Hainan, Xisha and Zhongsha Islands) in this study. Note: Gulf of Thailand included as part of the South China Sea. (Source: IHO & Sieger 2012)

the carbon tape to remove the specimen safely from the stub after SEM and for further analysis of the specimen. Skeletal elements of specimens were prepared by dissolving the soft tissue of part of an arm in undiluted NaOCl. The excess NaOCl was removed from the dissociated skeletal elements (ossicles) by repeated flushing with distilled water, to avoid formation of crystals on the surface of the ossicles. After drying, the ossicles were mounted on a stub using dissolved carbon tapes.

Holotypes, paratypes and all other specimens are deposited at the Institute of Deep-sea Sciences and Engineering (CAS), Sanya, China. The terms used to describe ophiuroids follow previous authors (Martynov 2010; Stöhr 2011, 2012; O'Hara *et al.* 2017; Hendler 2018; Stöhr & O'Hara 2021) The interpretation of oral structures follows Hendler (2018) as much as is possible without ontogenetic data. The lateral oral papillae are considered in a broad sense, the term 'apical papilla' is replaced by the more appropriate terms 'ventralmost tooth' and 'tooth papillae', as applicable. In Gorgonocephalidae, the term 'girdle bands' is replaced by 'pedicellarial bands' and 'girdle hooklets' are interpreted as pedicellariae following Turner *et al.* (2021).

DNA extraction, PCR amplification and DNA sequencing

We extracted DNA from the identified specimens from the South China Sea and two additional specimens from the East China Sea (*Asteronyx loveni* Müller & Troschel, 1842 and *Asteronyx reticulata* Okanishi *et al.*, 2018). Extraction was done by using the TIANamp Marine Animals DNA kit (TianGen, Beijing) following the manufacturer's protocol. We sequenced the mitochondrial 16S rRNA and cytochrome c oxidase I (COI) partial genes for phylogenetic analysis. The forward primer 16Sar (5′-CGCCTGTTTATCAAAAACAT-3′) and reverse primer 16Sbr (5′-CCGGTCTGAACTCAGATCACGT-3′) were used for PCR analysis of the 16S rRNA partial gene (Palumbi 1996a). Primer sets COI005 (5′- TTAGGTTAAHWAAACCAVYTKCCTTCAAAG-3′) and COI008 (5′- CCDTANGMDATCATDGCRTACATCATTCC-3′), COI007 (5′- TGATTYTTTGGN-CAYCCYGAKGTMTATAT-3′) and COI031 (5′-CGAAAMCWBTKGTTTTMDTTAAACTAAC-3′), and COIceF (5′- ACTGCCCACGCCCTAGTAATGATATTTTTTATGGTNATGCC-3′) and COIceR (5′-TCGTGTGTCTACGTCCATTCCTACTGTRAACATRTG-3′) were used for amplification of the COI partial gene (Hoareau & Boissin 2010; Okanishi & Fujita 2013).

The total volume of the PCR mixture was 50 μL, containing 25 μL Premix Taq with 1.25 U Taq, 0.4 mM each of dNTP and 4 mMMg2+ (Ex Taq version, Takara, Dalian, China), 0.5 μM each of the primers and approximately 100 ng template DNA. The PCR temperature profile for 16Sar/br primers was as follows: an initial denaturation at 95°C for 2 min, followed by 40 cycles of denaturation at 95°C for 30 s, annealing temperature at 49°C to 51°C for 40 s, extension at 72°C for 60 s, and a final extension at 72°C for 7 min. For COI005/008 and COI007/031 the primer settings were as follows: an initial denaturation at 94°C for 2 min, followed by 40 cycles of denaturation at 94°C for 30 s, annealing temperature at 49°C to 52°C for 90 s, extension at 72°C for 60 s, and a final extension at 72°C for 10 min. For COIceF/ceR the primer settings were as follows: an initial denaturation at 95°C for 3 min, followed by 42 cycles of denaturation at 94°C for 45 s, annealing temperature at 51°C to 55°C for 70 s, extension at 72°C for 80 s, and a final extension at 72°C for 5 min.

PCR product quality was assessed by electrophoresis using a 1.0% agarose gel and the NanoDrop 1000 (Thermo Scientific, Waltham, MA, USA). PCR products were sequenced in both directions on an ABI3730 DNA Analyzer. The SeqMan ver. 7.2.1 program (DNAStar Inc., Madison, WI, USA) was used to assemble and trim the raw COI sequences. All the new sequences were deposited at NCBI GenBank (Table 2).

Phylogenetic analysis

We analyzed the sequences from 16 specimens of deep-sea ophiuroids for 16S and 23 specimens of deep-sea ophiuroids for COI, compared to 64 published sequences (COI and 16S) from various families

Table 2 (continued on next two pages). List of species used in this study to reconstruct molecular phylogeny trees (sources: Ward *et al.* 2008; Corstorphine 2010; Cho & Shank 2010; Okanishi *et al.* 2011a, 2018; O'Hara *et al.* 2013, 2014, 2016; Okanishi & Fujita 2013; Gallego *et al.* 2014; Summers & Rouse 2014; Hunter *et al.* 2016; Galaska *et al.* 2019; Na *et al.* 2022) (new species in bold).

Species (origin)	**16S**	**COI**	**Reference**
Family Euryalidae			
Asteroschema horridum	–	MZ198759	This study
Asteroschema horridum (Reunion Isl.)	–	AB758764	Okanishi & Fujita 2013
Asteroschema edmondsoni	–	AB758831	Okanishi & Fujita 2013
Asteroschema tubiferum	–	KU895076	O'Hara *et al.* 2016
Asteroschema bidwillae	–	KU895077	O'Hara *et al.* 2016
Ophiocreas glutinosum	–	AB758815	Okanishi & Fujita 2013
Ophiocreas caudatus	–	AB758814	Okanishi & Fujita 2013
Euryale aspera	–	AB758808	Okanishi & Fujita 2013
Asteromorpha rousseaui	–	AB758756	Okanishi & Fujita 2013
Astroceras spinigerum	–	AB758786	Okanishi & Fujita 2013
Asterostegus tuberculatus	–	AB758769	Okanishi & Fujita 2013
Sthenocephalus indicus	–	KU895091	O'Hara *et al.* 2016
Sthenocephalus anopla	–	AB758825	Okanishi & Fujita 2013
Family Gorgonocephalidae			
Gorgonocephalus chilensis novaezelandiae	–	MZ198761	This study
Gorgonocephalus chilensis (New Zealand)	–	KU895116	O'Hara *et al.* 2016
Gorgonocephalus chilensis (Antarctica)	–	AB758812	Okanishi & Fujita 2013
Gorgonocephalus chilensis (Southern Ocean)	–	MH671879	Galaska *et al.* 2019
Gorgonocephalus eucnemis	–	AB758809	Okanishi & Fujita 2013
Gorgonocephalus arcticus	–	HM543017	Corstorphine 2010
Gorgonocephalus sundanus	–	KU895115	O'Hara *et al.* 2016
Gorgonocephalus cf. *dolichodsactylus*	–	MZ198760	This study
Gorgonocephalus pustulatum	–	KU895114	O'Hara *et al.* 2016
Astrodendrum sagaminum	–	AB758795	Okanishi & Fujita 2013
Asteroporpa australiensis	–	KU895095	O'Hara *et al.* 2016
Astrocrius parens	–	AB758794	Okanishi & Fujita 2013
Astrotoma agassizii	–	KU895112	O'Hara *et al.* 2016
Family Asteronychidae			
Asteronyx luzonicus	MZ203265	MZ198757	This study
Asteronyx loveni	MZ203264	MZ198756	This study
Asteronyx loveni (East China Sea)	MZ203263	MZ198755	This study
Asteronyx reticulata (East China Sea)	MZ203266	MZ198758	This study
Asteronyx reticulata (Japan)	LC276351	–	Okanishi *et al.* 2018
Asteronyx longifissus	KM014337	–	Summers & Rouse 2014
Asteronyx loveni (Japan)	LC276347	–	Okanishi *et al.* 2018
Astrodia tenuispina	AB605077	–	Okanishi *et al*. 2011a
Asteronyx loveni (Japan)	–	AB758757	Okanishi *et al.* 2011a
Astrodia tenuispina	–	AB758828	Okanishi & Fujita 2013

Table 2 (continued).

Species (origin)	**16S**	**COI**	**Reference**
Family Ophiacanthidae			
Ophientrema scolopendrica 01	MZ203270	MZ198774	This study
Ophientrema scolopendrica 02	MZ203271	MZ198775	This study
Ophiacantha bathybia 01	MZ203273	–	This study
Ophiacantha bathybia 02	MZ203274	–	This study
Ophiacantha vorax 01	MZ203267	MZ198765	This study
Ophiacantha vorax 02	MZ203268	MZ198766	This study
Ophiacantha antarctica 1	KU672408	–	Hunter *et al.* 2016
Ophiacantha antarctica 2	–	KU895384	O'Hara *et al.* 2016
Ophiacantha bidentata	KU672412	–	Hunter *et al.* 2016
Ophiacantha yaldwyni	–	KU895385	O'Hara *et al.* 2016
***Ophiacantha aster* sp. nov.** 01	MZ203275	–	This study
***Ophiacantha aster* sp. nov.** 02	MZ203275	–	This study
Ophioplinthaca plicata (New Zealand)	–	KU895133	O'Hara *et al.* 2016
Ophioplinthaca plicata (Tasman Sea)	–	EU869989	Ward *et al*. 2008
Ophioplinthaca plicata	MZ203269	MZ198773	This study
Ophioplinthaca pulchra	–	KU895136	O'Hara *et al.* 2016
Ophioplinthaca rudis	–	KU895135	O'Hara *et al.* 2016
Ophioplinthaca abyssalis	HM587819	–	Cho & Shank 2010
Ophioplinthaca defensor 1	MT031947	–	Na *et al.* 2022
Ophioplinthaca defensor 2	–	MT025778	Na *et al.* 2022
Ophiurothamnus clausa	MZ203272	MZ198777	This study
Ophiomoeris obstricta	AB605125	–	Okanishi *et al.* 2011a
***Ophiomoeris petalis* sp. nov.**	MZ203278	–	This study
Ophiomoeris sp.	MZ203277	–	This study
Ophiolimna antarctica	KF713452	–	Gallego *et al*. 2014
Ophiomitrella conferta	–	HQ946174	O'Hara *et al.* 2013
Family Ophiotomidae			
***Ophiopristis shenhaiyongshii* sp. nov.**	–	MZ198776	This study
Ophiacantha spectabilis	–	KU895369	O'Hara *et al.* 2016
Ophiopristis luctosa	–	KU895397	O'Hara *et al.* 2016
Ophiopristis procera	–	KU895396	O'Hara *et al.* 2016
Ophiotreta matura	–	KU895401	O'Hara *et al.* 2016
Ophiotreta eximia	–	KU895398	O'Hara *et al.* 2016
Ophiomitra leucorhabdota	–	KU895394	O'Hara *et al.* 2016
Ophiotoma alberti	–	KU895356	O'Hara *et al.* 2016
Ophiotoma assimilis	–	KU895355	O'Hara *et al.* 2016
Ophiocopa spatula	–	KU895393	O'Hara *et al.* 2016
Family Ophiactidae			
Ophiactis perplexa (Tasman Sea)	–	KF663482	O'Hara *et al.* 2014
Ophiactis cf. *perplexa* 01	–	MZ198767	This study
Ophiactis cf. *perplexa* 02	–	MZ198768	This study

Table 2 (continued).

Species (origin)	**16S**	**COI**	**Reference**
Ophiactis perplexa (New Zealand)	–	KU895159	O'Hara *et al.* 2016
Ophiactis flexuosa	–	KU895160	O'Hara *et al.* 2016
Ophiactis profundi 01	–	MZ198771	This study
Ophiactis profundi 02	–	MZ198772	This study
Ophiactis profundi (Tasman Sea)	–	KF663474	O'Hara *et al.* 2014
Ophiactis plana	–	KU895161	O'Hara *et al.* 2016
Ophiactis definita	–	KU895158	O'Hara *et al.* 2016
Ophiactis definita (Australia)		KF663481	O'Hara *et al.* 2014
Ophiactis cf. *brachygens* 01	–	MZ198769	This study
Ophiactis cf. *brachygens* 02	–	MZ198770	This study
Ophiactis affinis	–	KU895154	O'Hara *et al.* 2016
Ophiactis macrolepidota	–	KU895155	O'Hara *et al.* 2016
Ophiactis hirta	–	KU895147	O'Hara *et al.* 2016
Ophiactis abyssicola	–	KU895138	O'Hara *et al.* 2016
Ophiactis amator	–	KU895142	O'Hara *et al.* 2016
Family Ophiomusaidae			
Ophiomusa lymani 01	–	MZ198762	This study
Ophiomusa lymani 02	–	MZ198763	This study
Ophiomusa lymani (New Zealand)	–	KU895250	O'Hara *et al.* 2016
Ophiomusa sp. (South China Sea)	–	MZ198764	This study
Ophiomusa anisacantha	–	KU895254	O'Hara *et al.* 2016
Ophiomusa miranda	–	KU895255	O'Hara *et al.* 2016
Ophiomusa lunare	–	KU895253	O'Hara *et al.* 2016
Ophiomusa australe	–	KU895261	O'Hara *et al.* 2016
Ophiomusa simplex	–	KU895260	O'Hara *et al.* 2016
Ophiomusa aspera	–	KU895262	O'Hara *et al.* 2016
Ophiomusa scalare	–	KU895263	O'Hara *et al.* 2016
Ophiomusium eburneum	–	KU895266	O'Hara *et al.* 2016
Ophiosphalma laqueatum	–	KU895363	O'Hara *et al.* 2016
Outgroups			
Astrodia tenuispina	–	AB758828	Okanishi & Fujita 2013
Asteronyx loveni	–	KU895062	O'Hara *et al.* 2016
Asteroschema intectum	AB758484	–	Okanishi *et al.* 2011a
Asteroschema horridum	AB758487	–	Okanishi *et al.* 2011a
Asteroschema tubiferum	–	KU895076	O'Hara *et al.* 2016
Asteroschema bidwillae	–	KU895077	O'Hara *et al.* 2016
Ophiomyxa vivipara	KU672420	–	Hunter *et al.* 2016
Ophiomyxa flaccida	KU672429	–	Hunter *et al.* 2016
Ophiomyxa neglecta	–	KU895174	O'Hara *et al.* 2016
Bathypectinura heros	–	KU895207	O'Hara *et al.* 2016
Ophiothamnus biocal	–	KU895365	O'Hara *et al.* 2016
Ophiothamnus habrotatus	–	KU895366	O'Hara *et al.* 2016

(Table 2). We constructed six Maximum Likelihood (ML) phylogenetic trees from COI, representing the families Euryalidae, Gorgonocephalidae, Asteronychidae, Ophiacanthidae, Ophiotomidae, Ophiactidae and Ophiomusaidae and two ML phylogenetic trees from 16S, one for each of the families Asteronychidae and Ophiacanthidae.

Families Euryalidae and Gorgonocephalidae: to construct the COI ML tree, we used three species from our collection and additionally 23 sequences from GenBank, including 12 COI sequences of the family Euryalidae and 11 COI sequences of the family Gorgonocephalidae. As outgroup we used COI sequences from *Astrodia tenuispina* (Verrill, 1884) and *Asteronyx loveni*. Family Asteronychidae: to construct ML trees for both 16S and COI sequences, we used four species from our collection and additionally four 16S sequences and two COI sequences from GenBank. As outgroup we used *Asteroschema intectum* Lyman, 1878 and *Asteroschema horridum* Lyman, 1879 for the 16S ML tree, and *Asteroschema tubiferum* Matsumoto, 1911 and *Asteroschema bidwillae* McKnight, 2000 for the COI ML tree. Family Ophiomusaidae: to construct the ML tree from COI sequences, we used three species from our collection and additionally 10 COI sequences from GenBank. As outgroup we used *Asteroschema tubiferum* and *Asteroschema bidwillae.* Family Ophiotomidae: to construct the COI ML tree, we used one species from our collection and additionally 9 COI sequences from GenBank. As outgroup we used *Astrodia tenuispina* and *Asteronyx loveni*. Family Ophiacanthidae: to construct the ML tree for both 16S and COI sequences, we used 12 species for 16S and six species for COI from our collection and additionally six 16S sequences and eight COI sequences from GenBank. As outgroup we used *Ophiomyxa flaccida* (Say, 1825) and *Ophiomyxa vivipara* Studer, 1876 for the 16S ML tree and *Bathypectinura heros* (Lyman, 1879) and *Ophiomyxa neglecta* (Koehler, 1904) for the COI ML tree. Family Ophiactidae: to construct the ML tree from COI sequences, we used six species from our collection and additionally 12 COI sequences from GenBank. As outgroup we used *Ophiothamnus biocal* O'Hara & Stöhr, 2006 and *Ophiothamnus habrotatus* (H.L. Clark, 1911) (Table 2).

All sequences were aligned using the Clustal W algorithm in MEGA X (Kimura 1980; Thompson *et al.* 1994; Kumar *et al.* 2016, 2018). The best-fit substitution model of each gene in the ML trees was estimated by the 'Find Best DNA/Protein Models' option of MEGA X. The GTRGAMMA (GTR+G) model and the GTRGAMMAI (GTR+G+I) model were selected for the 16S and COI sequences, respectively (Tavaré 1986; Rodriguez *et al.* 1990; Edler *et al.* 2021). Phylogenetic trees were reconstructed for each partial 16S and COI gene by using the maximum likelihood bootstrap method. ML analysis was run with RaxML GUI ver. 2.0 by using raxmlHPC-PTHREADS-SSE3 (Edler *et al.* 2021). ML trees were constructed for COI and 16S with a rapid bootstrap likelihood analysis, including 1000 bootstrap replicates. Phylogenetic trees were visualized by FigTree ver. 1.4.4.

The genetic distances were analyzed according to the Kimura 2-parameter model (Kimura 1980) by using MEGA X. The overall genetic distance between and among clades that was clearly visible on the reconstructed phylogenetic trees was calculated. The standard error of each group was discovered by performing 1000 bootstrap replications.

Abbreviations

Morphology

ap = articular pad of the base
ars = arm spine
as = adoral shield
asa = arm spine articulation
au = auricle
cs = calcified scale
D = dorsal

dap = dorsal arm plate
das = dorsal arm spine
Dist = distal
dl = dorsal lobe
drs = distal end of radial shield
ds = disc spine
dsc = disc scale
fo = foramina of the base
fs = fossa between adjacent tubercles
gra = granular
gs = genital slit
hd = head of the apophysis
lap = lateral arm plate
lp = lateral pores of the blade
m = madreporite
mo = muscle opening
no = nerve opening
os = oral shield
oss = oral shield spine
ots = oral tentacle scale
pb = pedicellarial band
pd = pedicle of the apophysis
Prox = proximal
pt = primary tooth of the blade
rs = radial shield
sh = sheath of the baseplate
st = secondary tooth
su = sulcus of tubercle head
t = teeth
tf = tube foot
tp = tentacle pore
ts = tentacle scale
tts = thin transparent skin
uas = uppermost arm spine
V = ventral
vap = ventral arm plate
vas = ventral arm spine
vl = ventral lobe
vs = volute-shaped

Other

AN = Antarctica
AUS = Australia
C = Clade
COI = Cytochrome C oxidase subunit 1
E = East
ECS = East China Sea
IC = Inter Clade
IDSSE = Institute of Deep-sea Science and Engineering
JP = Japan
ML = Maximum Likelihood

MSV = manned submersible vehicle
NZ = New Zealand
PNG = Papua New Guinea
RI = Reunion Island
SC = Sub-Clade
SCS = South China Sea
SE = Southeast
SO = Southern Ocean
TS = Tasman Sea

Results

A total of 80 deep-sea ophiuroid specimens were examined in this study and identified to 18 species, including three new species and eight new records. These species represent 12 genera within seven families in the class Ophiuroidea. The most common deep-water ophiuroid species from our collection was *Ophientrema scolopendrica* Lyman, 1883 (Table 1).

Taxonomic account

Class Ophiuroidea Gray, 1840
Superorder Euryophiurida O'Hara, Hugall, Thuy, Stöhr & Martynov, 2017
Order Euryalida Lamarck, 1816
Family Asteronychidae Ljungman, 1867
Genus *Asteronyx* Müller & Troschel, 1842

Asteronyx loveni Müller & Troschel, 1842
Figs 2–3

Asteronyx loveni Müller & Troschel, 1842: 119–120, pl. 10 figs 3–5.
Ophiuropsis lymani Studer, 1884: 55–46, pl. 5 fig. 12a–d.
Asteronyx dispar Lütken & Mortensen, 1889: 185, pls 21–22.
Asteronyx locardi Koehler, 1895: 470–471, fig. 10.
Asteronyx cooperi Bell, 1909: 22.
Ophiuraster patersoni Litvinova, 1998: 441–444, fig. 3.

Asteronyx loveni – Döderlein 1927: 59, 97, pl. 7 figs 7–8. — Baker 1980: 12, 16–18, figs 2–3. — Liao & Clark 1995: 165–166, fig. 71. — McKnight 2000: 8, 13–15, pl. 1. — Olbers *et al.* 2019: 49–50, fig. 23.
Ophiuraster patersoni – Stöhr 2005: 545–546, fig. 1.

Material examined

CHINA • 1 spec.; South China Sea, SE of Hainan Island, seamount; 18°31.76′ N, 112°40.56′ E; depth 1167 m; 27 Jun. 2019; collection event: stn SC002; MSV Shenhaiyongshi leg.; preserved in -80°C; GenBank: MZ198756, MZ203264; IDSSE EEB-SW0002.

Remarks

Disc diameter 11 mm and collected attached to a gorgonian species. Our specimen is similar to the holotype description by Müller & Troschel (1842) and later published descriptions (Baker 1980; McKnight 2000; Olbers *et al.* 2019) (Fig. 2). Vertebrae with a streptospondylous articulation and the lateral arm plate bears four to five spine articulations, which lack a separate nerve opening (Fig. 3). Species of *Asteronyx* are usually found on mud and sand, associated with gorgonians and pennatulids. In 1959 and from 1976 to 1981, 52 specimens of *A. loveni* were collected from the East and South China

seas, at depths of 510–1100 m. *Asteronyx loveni* was first reported from the South China Sea by Chang *et al.* (1962).

Distribution

62–4721 m depth. Global, except Arctic and Antarctic (Olbers *et al.* 2019; OBIS 2021).

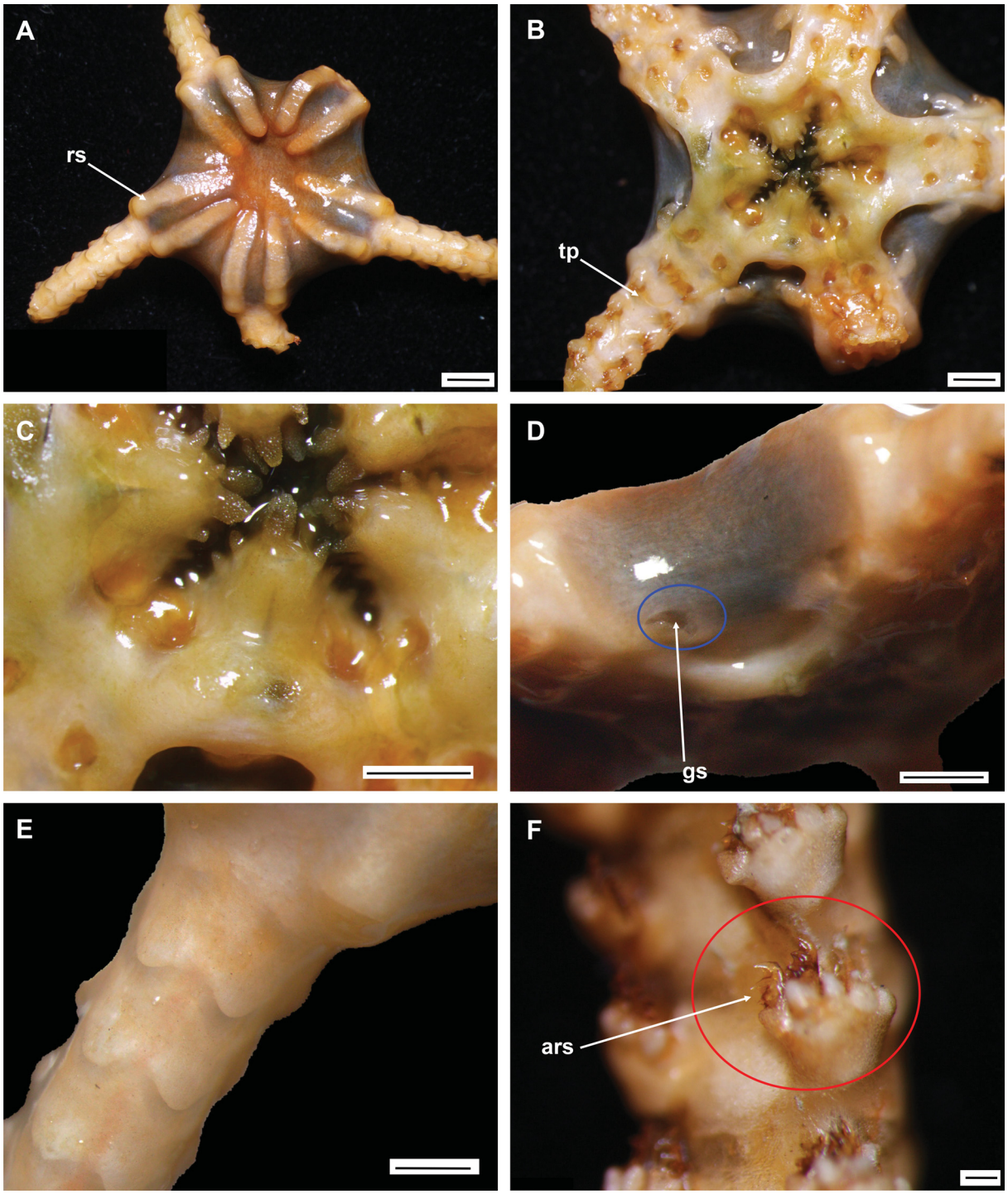

Fig. 2. *Asteronyx loveni* Müller & Troschel, 1842 (IDSSE EEB-SW0002). **A**. Dorsal disc. **B**. Ventral disc. **C**. Oral frame. **D**. Genital slit. **E**. Dorsal arm. **F**. Arm spines. Abbreviations: ars = arm spines; gs = genital slit; rs = radial shield; tp = tentacle pore. Scale bars: A–B = 2 mm; C–E = 1 mm; F = 200 µm.

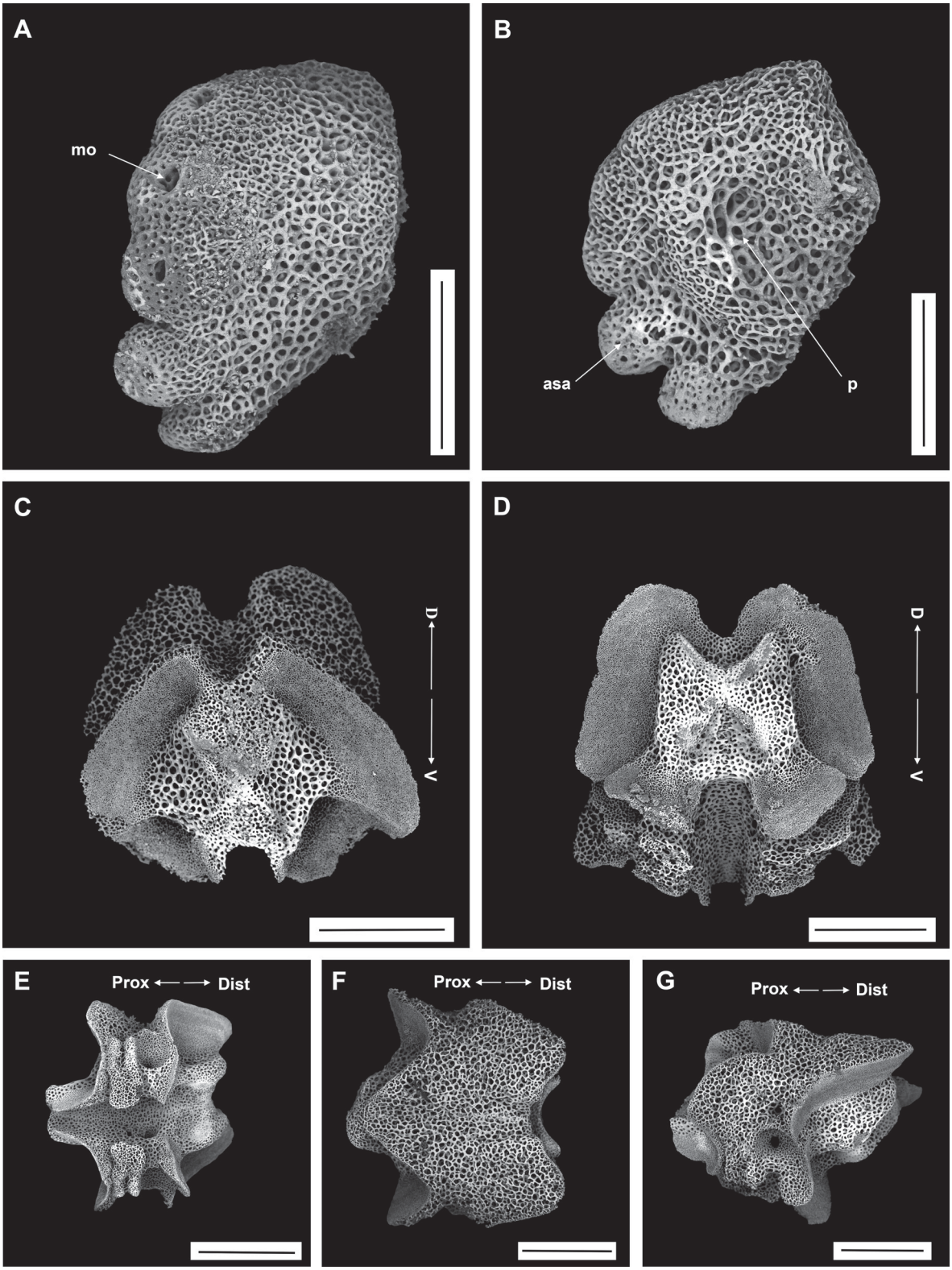

Fig. 3. *Asteronyx loveni* Müller & Troschel, 1842, SEM (IDSSE EEB-SW0002). **A–B**. Lateral arm plates (external, internal). **C–G**. Vertebrae. **C**. Proximal view. **D**. Distal view. **E**. Ventral view. **F**. Dorsal view. **G**. Lateral view. Abbreviations: asa = arm spine articulation; D = dorsal; Dist = distal; mo = muscle opening; p = perforation of inner side; Prox = proximal; V = ventral. Scale bars: A–B = 300 μm; C–D, F–G = 500 μm; E = 800 μm.

Asteronyx luzonicus Döderlein, 1927
Figs 4–6

Asteronyx luzonicus Döderlein, 1927: 64, pl. 7 figs 4–5, 6a–d.

Asteronyx luzonicus – Baker *et al.* 2018: 7–8, figs 4–5.

Material examined

CHINA • 1 spec.; South China Sea, SE of Hainan Island, seamount; 18°31.76′ N, 112°40.56′ E; depth 1167 m; 27 Jun. 2019; collection event: stn SC002; MSV Shenhaiyongshi leg.; preserved in -80°C; GenBank: MZ198757, MZ203265; IDSSE EEB-SW0003 • 1 spec.; same collection data as for preceding; depth 1162 m; 8 Jul. 2019; collection event: stn SC002; MSV Shenhaiyongshi leg.; preserved in -80°C; IDSSE EEB-SW0032.

Description (IDSSE EEB-SW0003)

Measurements. Disc diameter 13.5 mm.

Disc. Flat, pentagonal. Entire dorsal disc covered by smooth, transparent, naked skin, but some small calcified scales between radial shields. Skin on center of dorsal disc becoming mesh-like and less smooth than at periphery of disc. Radial shields narrow, elongate, separate, covered by skin and extending to near disc center, but not meeting in center (Fig. 4A). Ventral (oral) surface of disc also covered by smooth skin (Fig. 4B). Oral shields slightly triangular. Adoral shield large, wider than long and slightly concave at distal margin, bordering proximal end of a depressed area near genital slit. Two tooth papillae, large and pointed, three smaller pointed lateral oral papillae, teeth also pointed. Two small, short, well separated genital slits in each ventral interradius (Fig. 4C–D).

Arms. Simple, similar in size and length, five in number, with no abrupt change in width proximally, gradually tapering toward arm tip. No dorsal arm plates, arm covered with smooth translucent skin, leaving vertebrae visible (Fig. 4E). Ventral and lateral arm plates concealed by thick skin but slightly visible on proximal arm (Fig. 4F). Lateral arm plates meet at ventral midline, spines at ventrolateral margin extending onto ventral surface (Figs 4F–G, 5A–B). Starting from first free arm segment beyond disc, first two to three arm segments without spines at tentacle pores (Fig. 4B–C); third to fourth arm segments with one or two short arm spines, becoming hook-shaped or with one secondary tooth (Fig. 4C). Following tentacle pores with two to five hook-shaped arm spines and only uppermost arm spine elongated to simple hook shape, but ventralmost spines with one secondary tooth (Fig. 5D). Length of all arm spines decreasing to approximately half length of corresponding arm segment in middle of arm. On distal third of arm, arm spines half as long as corresponding arm segment and transforming into hooks without secondary tooth, except ventralmost arm spine. Ventralmost arm spine becoming cylindrical, blunt with thorny tip, as long as one arm segment (Fig. 5A–F). Tube foot elongate, cylindrical, slender, as long as an arm segment and positioned close to ventralmost arm spine (Fig. 5A–C).

Color. Dorsal disc light brown in center, naked skin between radial shields darker, radial shields whitish brown; ventral interradial areas light brown; arms whitish brown above and below (Fig. 4).

Ossicle morphology. Lateral arm plate curved around vertebrae, bearing five spine articulations, each with small muscle opening, but lacking a separate nerve opening (Fig. 6A–C). Arm spine articulations at distal edge of lateral plate, raised outwards, pointing distalwards. A depression on inner side of lateral arm plate (Fig. 6B). Vertebrae with streptospondylous articulation, ventral side with a longitudinal groove along midline and no oral bridge (Fig. 6D–H).

Remarks

The here examined specimens were collected on a deep-sea seamount, attached to a gorgonian. *Asteronyx luzonicus* was first described by Döderlein (1927) from the Philippines. However, there are few published descriptions of *A. luzonicus* (Baker *et al.* 2018) and the species has not been imaged well before. Döderlein (1927) mentioned an elongated, slender ventralmost arm spine, as long as an arm segment, parallel to the longitudinal arm axis, as a distinguishing morphological feature of *A. luzonicus*, because in other species of *Asteronyx*, the ventralmost spine is usually placed transversally to the longitudinal axis of the arm and often reaches twice the length of an arm segment. Dried specimens

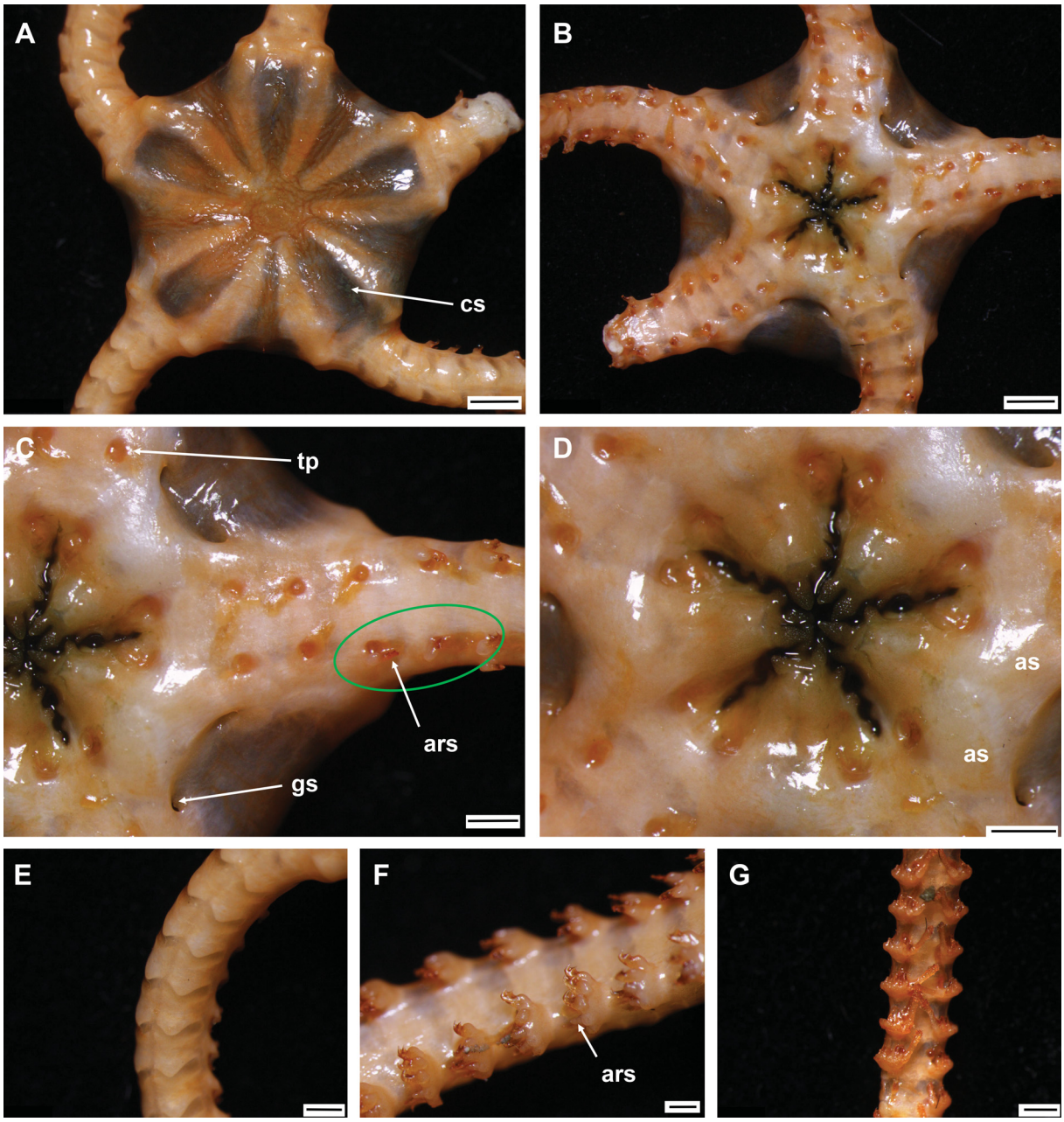

Fig. 4. *Asteronyx luzonicus* Döderlein, 1927 (IDSSE EEB-SW0003). **A**. Dorsal disc. **B**. Ventral disc. **C**. Ventral arm base (start of first arm spine highlighted). **D**. Oral frame. **E**. Dorsal arm. **F–G**. Ventral arm (proximal and distal region). Abbreviations: ars = arm spine; as = adoral shield; cs = calcified scales; gs = genital slit; tp = tentacle pore. Scale bars: A–B = 2 mm; C–E, G = 1 mm; F = 500 µm.

of *A. luzonicus* are particularly strikingly dark and a main distinguishing morphological feature of *A. luzonicus* is the presence of black spots on the disc of sexually mature specimens (Baker *et al.* 2018). Specimens from our collection were not sexually mature and only had darker skin on both the dorsal and ventral disc, but they concur with a Baker *et al.* (2018) in the calcified scales.

Recent studies on species of *Asteronyx* suggested that features of the dorsal disc surface, as well as the position and length of the genital slit may be important characters to distinguish the six species in this genus (Okanishi *et al.* 2018). Döderlein did not describe the dorsal disc surface and mentioned few morphological characters to distinguish his new species from other species in the genus *Asteronyx*, i.e., in characters of the tentacle scale and darker disc spots in sexually mature specimens. Specimens of *Asteronyx* in our collection are immature but similar in size. Therefore, a comprehensive morphological analysis can be used to distinguish *A. loveni* from *A. luzonicus* such as: hook-shaped arm spines with at most one secondary tooth along the arm in *A. luzonicus*, whereas *A. loveni* has hook-shaped arm spines with more than one secondary tooth (Figs 2F, 4F, 5); in *A. luzonicus* the dorsal disc surface is flatter than in *A. loveni* and becoming rough, mesh-like in the center (Figs 2A, 4A); the first two to three arm segments in *A. luzonicus* have only a tentacle foot and no arm spine, but in *A. loveni* only the first arm segment is without a single spine (Figs 2B, 4B). The ventralmost arm spine is as long as one arm segment, cylindrical, tapered, with a blunt, thorny tip (Fig. 5H–J). *Asteronyx reticulata* Okanishi, Martynov & Fujita, 2018 is similar to *A. luzonicus*, but differs in having mesh-like skin on its ventral disc (Okanishi *et al.* 2018).

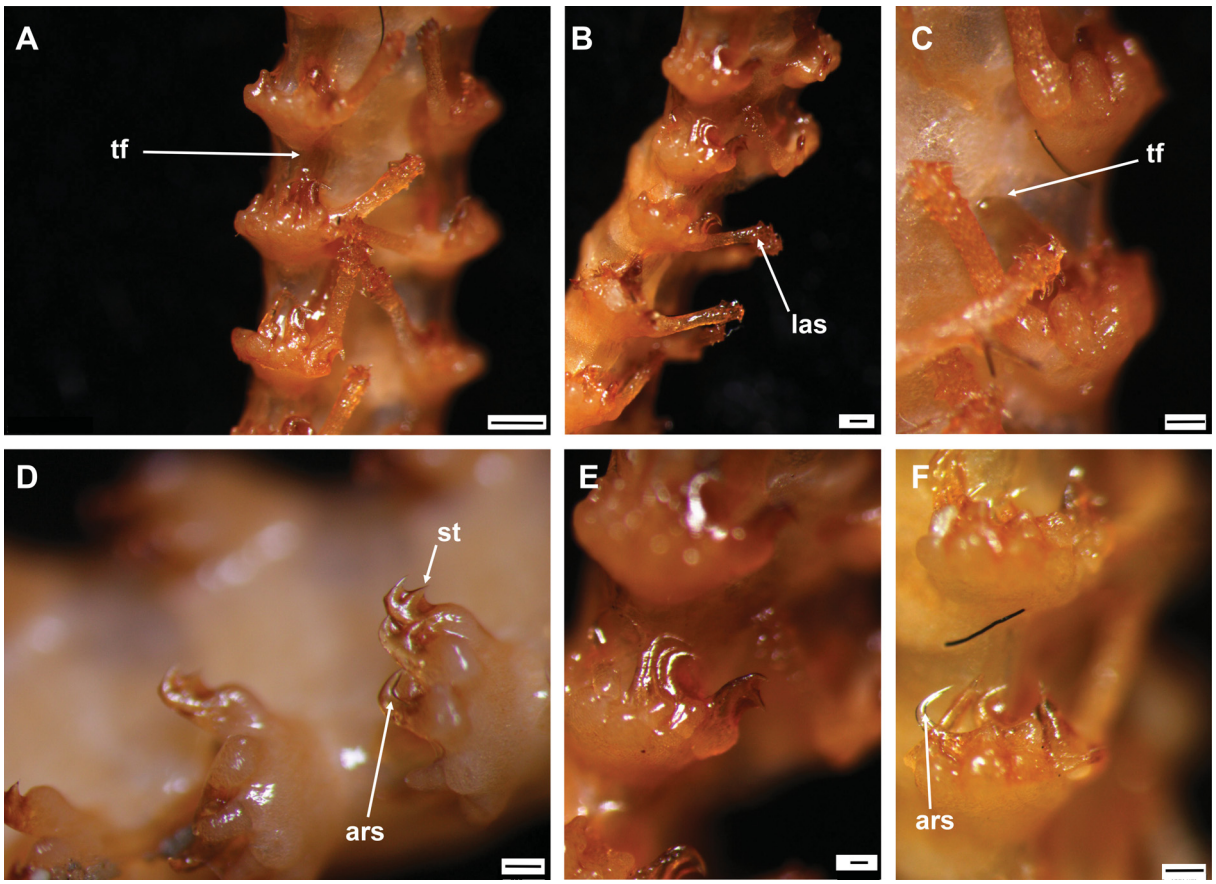

Fig. 5. *Asteronyx luzonicus* Döderlein, 1927 (IDSSE EEB-SW0003). **A–F**. Various shapes of arm spines along the arm. Abbreviations: ars = arm spine; las = lowermost arm spine; st = secondary tooth; tf = tube foot. Scale bars: A = 500 µm; B–F = 200 µm.

Distribution

109–2963 m depth. South China Sea, Sibuyan Sea, Samar Sea, Bohol Sea, East China Sea, Andaman Sea, Southern Mozambique (Baker *et al.* 2018).

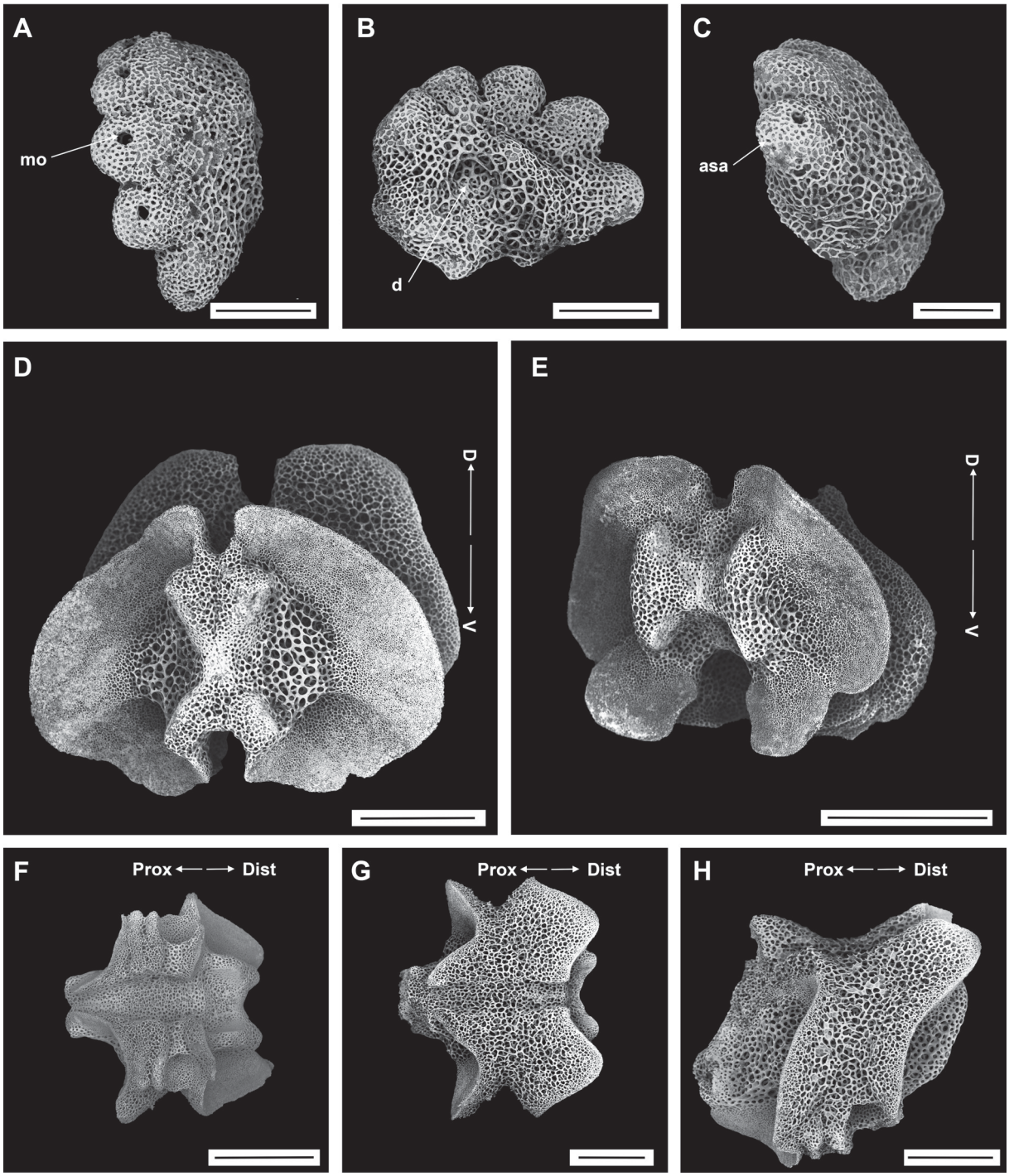

Fig. 6. *Asteronyx luzonicus* Döderlein, 1927, SEM (IDSSE EEB-SW0003). **A–C**. Lateral arm plates (internal, external). **D–H**. Vertebrae. **D**. Proximal view. **E**. Distal view. **F**. Ventral view. **G**. Dorsal view. **H**. Lateral view. Abbreviations: asa = arm spine articulation; D = dorsal; d = depression; Dist = distal; mo = muscle opening; Prox = proximal; V = ventral. Scale bars: A–B = 300 µm; C = 200 µm; D, G–H = 500 µm; E–F = 800 µm.

Family Euryalidae Gray, 1840
Genus *Asteroschema* Örsted & Lütken in Lütken, 1856

Asteroschema horridum Lyman, 1879
Figs 7–8

Asteroschema horridum Lyman, 1879: 66.

Asteroschema horridum – Lyman 1882: 275. — Baker 1980: 20, fig. 4. — McKnight 2000: 17, pl. 3.

Material examined

CHINA • 1 spec.; South China Sea, SE of Zhongsha Islands complex, seamount; 13°58.68′ N, 114°52.09′ E; depth 1550 m; 25 Sep. 2020; collection event: stn SC013; MSV Shenhaiyongshi leg.; preserved in 95% ethanol; GenBank: MZ198759; IDSSE EEB-SW0005 • 1 spec.; South China Sea, SE of Hainan Island, seamount; 18°41.95′ N, 113°33.08′ E; depth 1070 m; 29 Mar. 2018; collection event: stn SC019; MSV Shenhaiyongshi leg.; preserved in -80°C; IDSSE EEB-SW0033.

Description (IDSSE EEB-SW0005)

Measurements. Disc diameter 12.5 mm, length of arms from 180 to 191 mm.

Disc. Flat, interradially deeply excavated and small in relation to total body size of specimen. Disc covered with small, tumid, irregular scales, but larger on ventral than on dorsal disc. Conically tumid scales on radial shields, forming tubercles with finely thorny tip (Fig. 7A–B), both shields and tubercles decreasing in size towards disc center. Radial shields thick, swollen, widely separated distally, convergent proximally and with additional smaller scales and tubercles. Genital slits short, vertical on ventral interradii (Fig. 7D). Seven blunt, spearhead-shaped teeth. Jaws covered with swollen scales and no true oral papillae (Fig. 7C–D). Adoral shield obscured by swollen scales, oral shield absent and oral tentacle pore covered by small tube-shaped scales. Entire oral area covered with tumid scales, higher and pointier towards margin of ventral disc (Fig. 7C).

Arms. Narrow, more cylindrical and slightly swollen in first 14–15 free arm segments (Fig. 7E). Dorsal and ventral arm also covered with more trapezoid tuberculous scales, distally tubercles more rounded and less elongated and arms with increasingly banded appearance distalwards (Fig. 7E–I). Tubercles on ventral arm slightly lower and pointier than on dorsal surface. First tentacle pore with zero to one arm spine, on second to fifth arm segments one arm spine at tentacle pores, thereafter two arm spines per pore (Fig. 7G–H). Arm spines cylindrical with thorny tip, innermost spine slightly swollen, longer than arm width, twice as long as outermost spine, with thorny tip. Outermost spine not swollen, half as long as innermost spine, tapered (Figs 7I–J, 8C).

Color. Pale reddish-brown in alcohol specimen (Fig. 7), slightly stronger color in live specimen.

Ossicle morphology. Lateral arm plates curved around vertebrae, bearing two strongly outwards curved arm spine articulations with large muscle and nerve openings (Fig. 8A–B). Vertebrae with a streptospondylous articulation, with deep slope between proximal and distal end, ventrally with longitudinal groove along midline, no oral bridge (Fig. 8D–H).

Remarks

Asteroschema horridum was first described by Lyman (1879), with the Kermadec Islands as the type locality (HMS ‘Challenger’ Expedition). Baker (1980) and McKnight (2000) redescribed it. The

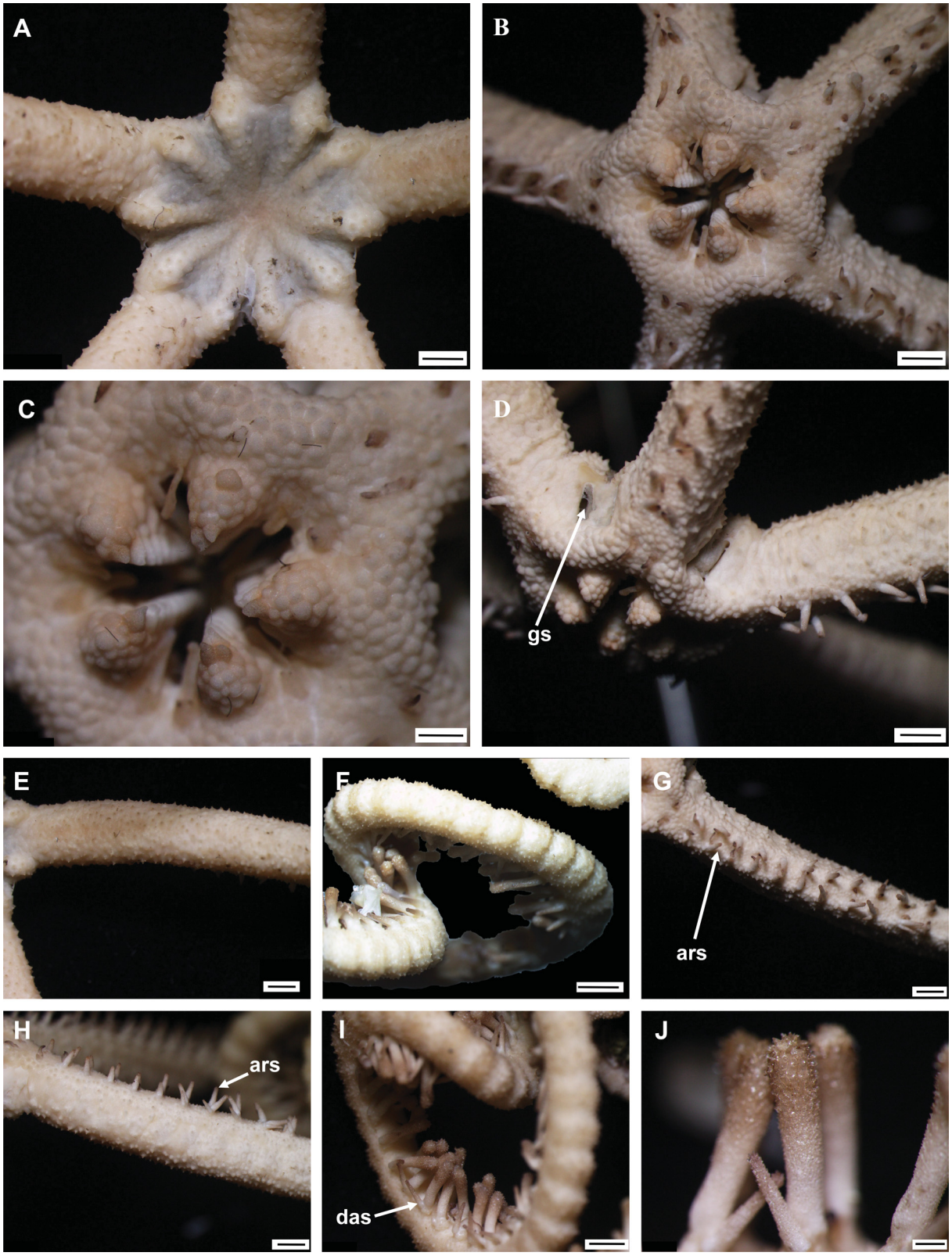

Fig. 7. *Asteroschema horridum* Lyman, 1879 (IDSSE EEB-SW0005). **A**. Dorsal disc. **B**. Ventral disc. **C**. Oral frame. **D**. Lateral disc. **E–F**. Dorsal arm (proximal and distal regions). **G**. Ventral arm. **H**. Lateral arm. **I**. Ventral arm. **J**. Ventral arm spine. Abbreviations: ars = arm spine; das = dorsal arm spine; gs = genital slit. Scale bars: A–B, D–I = 2 mm; C = 1 mm; J = 500 μm.

specimen from our collection was similar to Lyman's holotype description, but differs slightly from the descriptions in Baker (1980) and McKnight (2000) in having the start of the second arm spine at the first few arm segments (beyond segments 3–6, usually beyond segment 2). This character varies among species of *Asteroschema* (Baker 1980). Another morphological variation was shown as the extent of

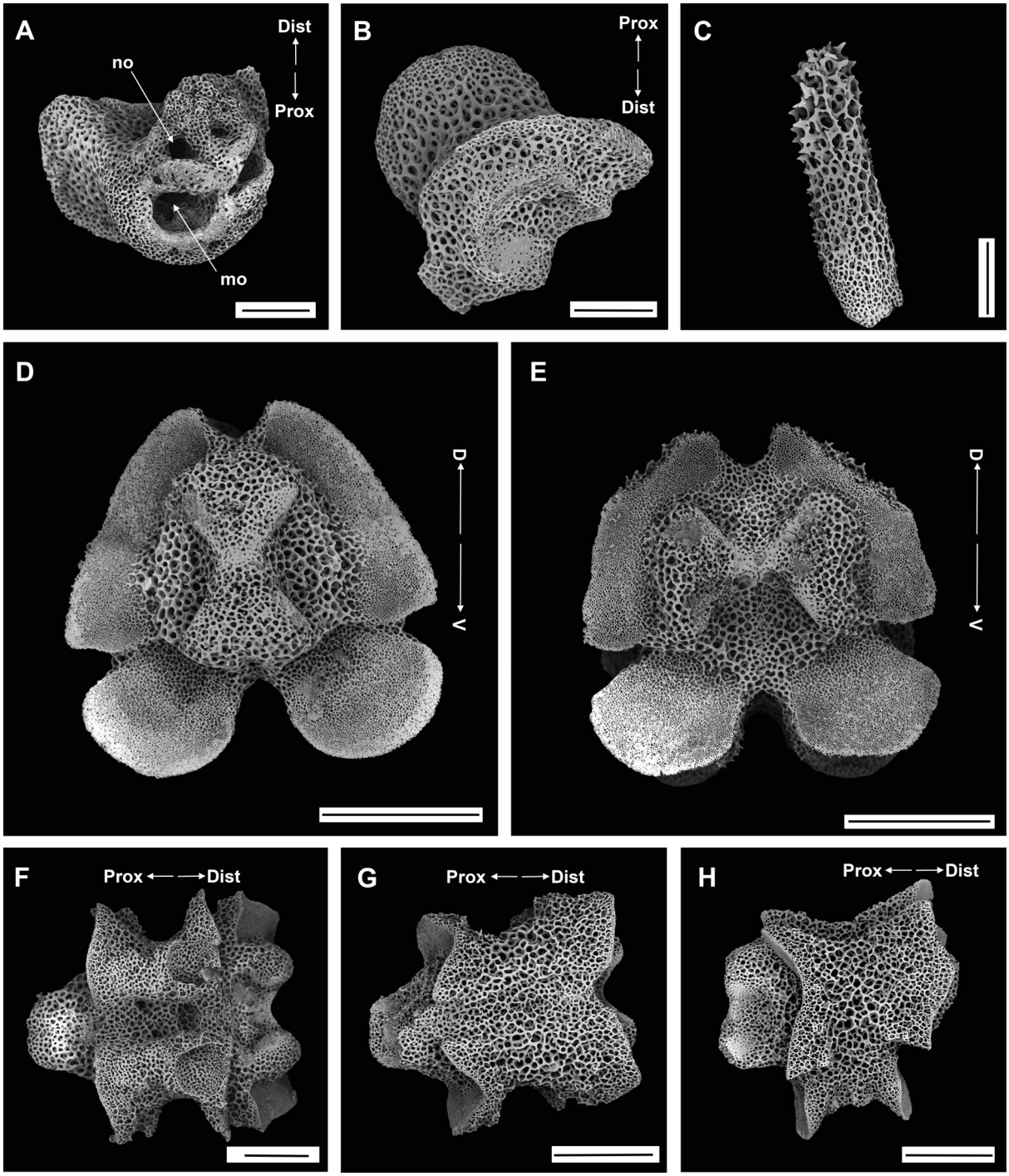

Fig. 8. *Asteroschema horridum* Lyman, 1879, SEM (IDSSE EEB-SW0005). **A–B**. Lateral arm plate (external, internal). **C**. Arm spine. **D–H**. Vertebrae. **D**. Proximal view. **E**. Distal view. **F**. Ventral view. **G**. Dorsal view. **H**. Lateral view. Abbreviations: D = dorsal; Dist = distal; Prox = proximal; mo = muscle opening; no = nerve opening; V = ventral. Scale bars: A–C, F = 300 µm; D–E, G–H = 500 µm.

swelling on the proximal arm. In the present study, the small specimen (8.2 mm) had a swollen arm for five to six segments, which is similar to Baker (1980) and McKnight (2000), but they did not mention the diameter of the disc (size of the specimen). The character of having a small, flat disc with tubercle-shaped scales is one that distinguishes *A. horridum* from other species of *Asteroschema. Asteroschema horridum* is considered a close relative of *A. tumidum* Lyman, 1879 according to morphological aspects (Baker 1980; McKnight 2000). Previously published descriptions suggested that the morphological characters of *A. horridum* may vary with the size and maturity of the specimens (Baker 1980; McKnight 2000).

Distribution

300–2000 m depth. South China Sea, Kermadec Islands and Norfolk Island (New Zealand), New Caledonia, Vanuatu (Coral Sea), French Polynesia (Baker 1980; McKnight 2000; OBIS 2021).

Family Gorgonocephalidae Ljungman, 1867
Subfamily Gorgonocephalinae Döderlein, 1911
Genus *Gorgonocephalus* Leach, 1815

Gorgonocephalus chilensis novaezelandiae Mortensen, 1924
Figs 9–10

Gorgonocephalus chilensis var. *novaezelandiae* Mortensen, 1924: 109–110, pl. 4 fig 1.

Gorgonocephalus chilensis – Baker 1980: 51–52. — McKnight 2000: 45–46, pl. 19. [non *G. chilensis chilensis* Philippi, 1858]

Material examined

CHINA • 1 spec.; South China Sea, SE of Zhongsha Islands, seamount; 13° 58.68′ N, 114° 52.09′ E; depth 1550 m; 25 Sep. 2020; collection event: stn SC013; MSV Shenhaiyongshi leg.; preserved in 95% ethanol; GenBank: MZ198761; IDSSE EEB-SW0007.

Description (IDSSE EEB-SW0007)

Measurements. Disc diameter 15.5 mm.

Disc. Dorsal disc slightly inflated, interradials slightly indented. Radial shields elongated and narrow, extending nearly toward center of disc but not meeting in center, tapering at distal ends, densely covered by large, tall conical granules. Skin between radial shields also covered by conical granules, but less dense and smaller than on radial shields, but disc center covered with compacted conical granules. Disc periphery covered with few larger conical granules (Fig. 9A–F). Ventral disc covered with small, scattered, low granules, extending onto oral area (Fig. 9E). Genital slits conspicuous, interradial margin covered by two irregular rows of larger, higher than wide granules (Fig. 9D). Single madreporite. Oral area covered by smooth skin, partly exposing adoral shield outlines and few scattered smaller granules (Fig. 9E). Adoral shields short, square. Oral papillae spiniform (Fig. 9E).

Arms. Branched at least six to seven times, flexible dorso-ventrally, flat ventrally, high rounded dorsally (Fig. 9A). Ventral arm along first branch and near base covered by smooth skin, distalwards scattered with smaller granules (Fig. 9G). Dorsal arm surface covered by domed scales, on proximal segments

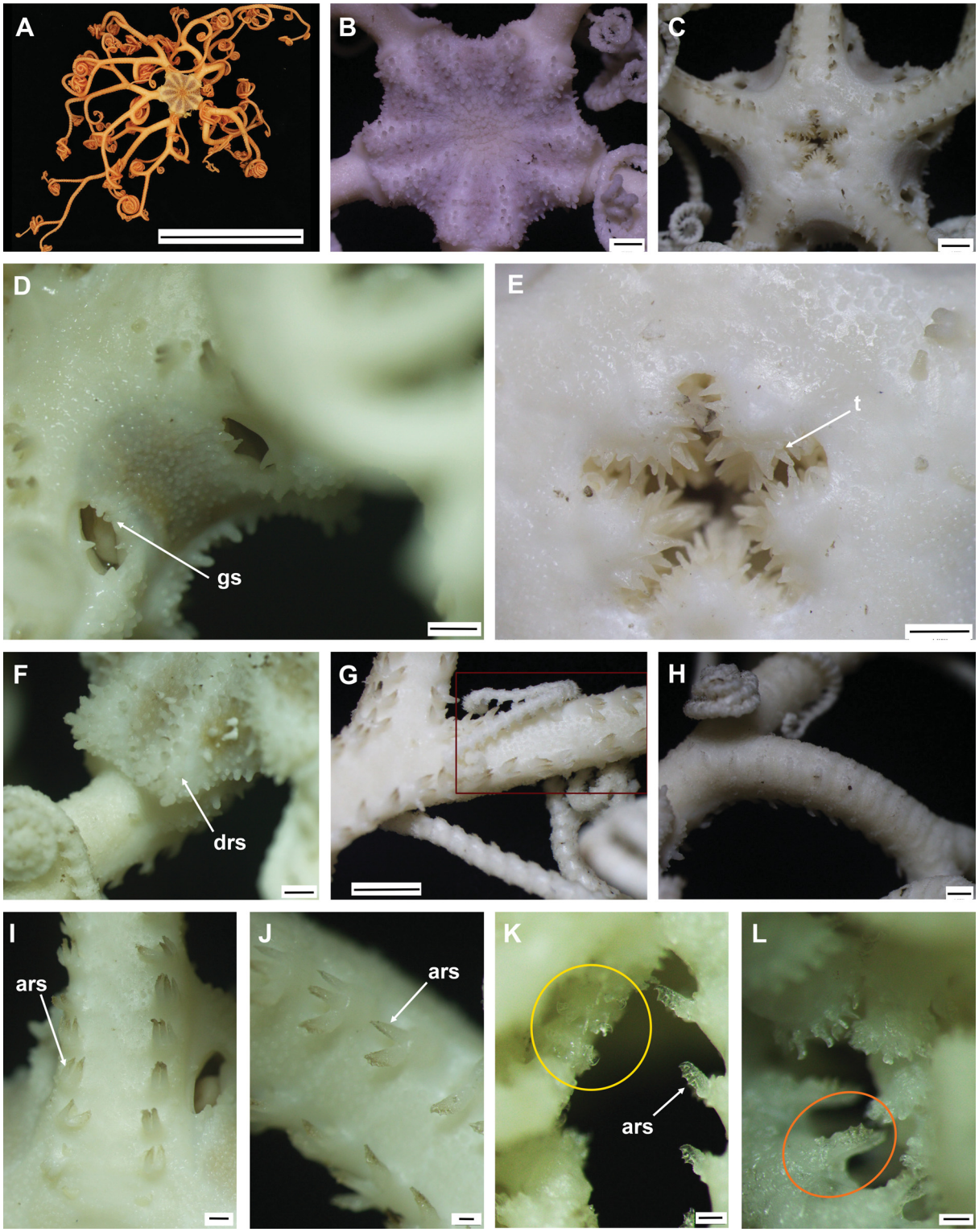

Fig. 9. *Gorgonocephalus chilensis novaezelandiae* Mortensen, 1924 (IDSSE EEB-SW0005). **A**. Live specimen. **B**. Dorsal disc. **C**. Ventral disc. **D**. Lateral disc. **E**. Oral frame. **F**. Dorsal view of disc periphery. **G**. Ventral view of first branch of an arm. **H**. Dorsal view of first branch of an arm. **I**. Ventral view of arm base. **J–L**. Variations of arm spines and pedicellariae along the arm. Abbreviations: ars = arm spine; drs = distal end of radial shield; gs = genital slit; t = teeth. Scale bars: A = 5 cm; B–C, G = 2 mm; D–F, H = 1 mm; I = 500 µm; J–L = 200 µm.

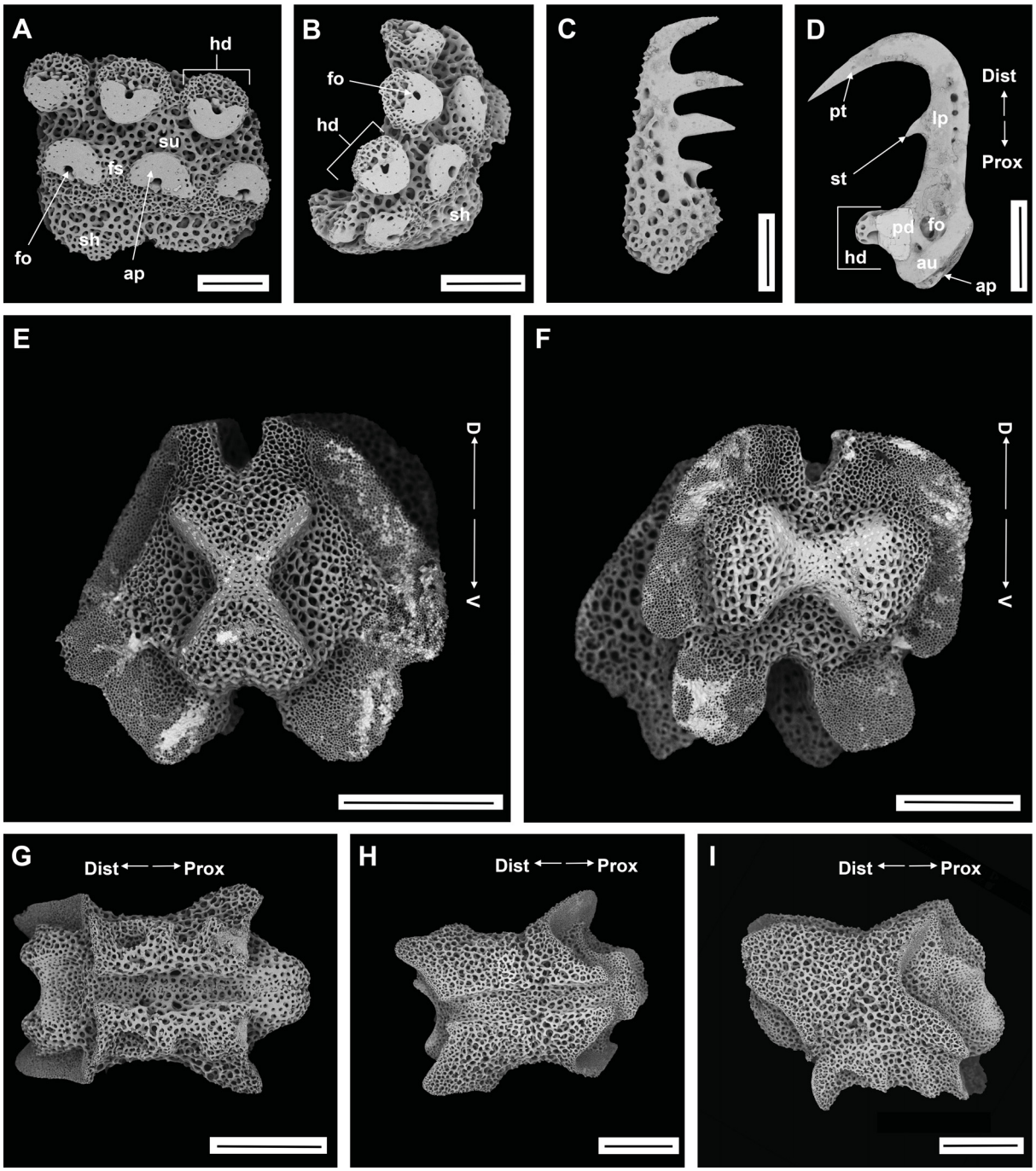

Fig. 10. *Gorgonocephalus chilensis novaezelandiae* Mortensen, 1924, SEM (IDSSE EEB-SW0005). **A**. Plan view of the baseplate. **B**. Distal view of the baseplate. **C**. Arm spine on proximal lateral plate. **D**. Pedicellaria on the pedicellarial band. **E–I**. Vertebrae. **E**. Proximal view. **F**. Distal view. **G**. Ventral view. **H**. Dorsal view. **I**. Lateral view. Abbreviations: ap = articular pad of the base; au = auricle; D = dorsal; Dist = distal; fo = foramen of the base; fs = fossa between adjacent tubercles; hd = head of the apophysis; lp = lateral pores of the blade; pd = pedicel of the apophysis; Prox = proximal; pt = primary tooth of the blade; sh = sheath of the baseplate; st = secondary inner tooth; su = sulcus of tubercle head; V = ventral. Scale bars: A–C = 100 μm; D = 20 μm; E, G–I = 300 μm; F = 200 μm.

with naked scales and naked areas corresponding to pedicellarial bands. Dorsal arm surface densely covered by compact granules after second arm fork. Pedicellarial bands start at second arm fork with three to four isolated clumps on each side of arm and becoming continuous across arm. From sixth arm fork, raised pedicellarial bands give an annulated appearance to arm (Fig 9H). First arm segment lacks spines, next three with two arm spines, next nine to ten with three arm spines and thereafter four arm spines per segment, decreasing to three after fifth branch (Fig. 9G, I–J). Ventral arm spines smaller, slightly flattened, unevenly pointed, distally turning into multi-toothed hooks (Fig. 9J–L). Pedicellariae with small secondary tooth (Fig. 9K–L).

Color. Creamy white in alcohol specimen, with light brown disc and darker arms when alive (Fig. 9A–B).

Ossicle morphology. Pedicellarial band formed by approximately six articulating tubercles on middle arm region and eight articulations at curved distal end (Fig. 10A–B). Tubercles form two parallel rows with single foramen (Fig. 10A–B). Ventral arm spines distally transformed into hooks with two or three secondary teeth (Fig. 10C). Pedicellariae on pedicellarial band with single secondary tooth and apophysis (Fig. 10D). Pedicellariae on pedicellarial band differ from ventral arm spine by smooth apophysis. Vertebrae with hourglass-shaped streptospondylous articulation with smooth lateral furrows (Fig. 10E–I). Paired openings in lateral side of vertebrae for lateral water canals, no oral bridge (Fig. 10F–G).

Remarks

The subspecies *G. chilensis novaezelandiae* is currently unaccepted and considered a junior synonym of *G. chilensis* (Philippi, 1858) (Stöhr *et al.* 2021). Our molecular results (see below) place this specimen with other New Zealand material in a sister clade to *G. chilensis* from Antarctica and the Southern Ocean. We consider the New Zealand clade sufficiently different from the Antarctic clade to reinstate the subspecies name for it, pending further investigation that may result in raising it to full species status. For the Antarctic clade, the name *G. chilensis chilensis* should be used for the time being, although the type locality is in Southern Chile, and if future molecular data find the Chilean population to be in the same clade as the New Zealand and South China Sea material, a new name would need to be found for the Antarctic clade. The only morphological difference between the two subspecies mentioned by Mortensen (1924) is a sparser distribution of the dorsal disc granules in *G. chilensis novaezelandiae*. The specimen from the present study is smaller and thus probably younger than the holotypes of both subspecies and the New Zealand specimens described by Baker (1980) and McKnight (2000). However, McKnight (2000) also reported two specimens of the same size as ours (16 mm disc diameter) with a dense cover of disc granules. This character may either be variable or age-related. We consider it highly likely that the specimens studied by Baker (1980) and McKnight (2000) represent *G. chilensis novaezelandiae*. The morphological characters of our specimen varied slightly from their descriptions, particularly in the number of branches in the arms, which is size dependent. According to Baker (1980) the shields indirectly contributed to thickening the periphery of the disc, but other species of *Gorgonocephalus* showed a distinct gap in granulation at the end of the shields and granules on the periphery of the disc. Therefore, this morphological feature can be used to distinguish *G. chilensis* within the genus *Gorgonocephalus*. Considering other morphological characters, *G. tuberosus* Döderlein, 1902 is similar to *G. chilensis* by having a dense cover of coarse, conical, or hemispherical granules on the disc, small and closely arranged in the dorsal angle of the interradial space (Döderlein 1902).

H.L. Clark (1923), Seno & Irimura (1968) and Mortensen (1936) reported on younger individuals that were attached to the mature adult individuals, which prompted H.L. Clark (1923) to consider *G. chilensis*

as viviparous. Mortensen (1936) suggested that it is not viviparous and these younger specimens simply attached to mature specimens as a host, like larger specimens attach to gorgonians (Olbers *et al.* 2019). This is the first record of *G. chilensis novaezelandiae* from the Indo-Pacific region and far from previously recorded occurrences, which may suggest that other non-Antarctic records also belong to this subspecies. Its true bathymetric and geographic distribution is currently unclear, because most previously recorded specimens were reported as *G. chilensis* and need to be re-examined, preferably with molecular methods. The taxonomic value of the disc granulation should be tested by examination of a large number of specimens, which could also find other distinguishing characters.

Distribution

1550–1830 m depth. New Zealand, South China Sea (Mortensen 1924; this study).

Gorgonocephalus cf. ***dolichodactylus*** Döderlein, 1911
Figs 11–12

Gorgonocephalus dolichodactylus Döderlein, 1911: 34–36, pl. 1 figs 4–5, pl. 7 figs 3, 4a–b.

Gorgonocephalus dolichodactylus – Döderlein 1927: 27, 52. — Matsumoto 1915: 73, fig. 20. — Baker 1980: 52, figs 18a, 20, 30. — Liao & Clark 1995: 171, fig. 75. — McKnight 2000: 45–46, pl. 20.

Material examined

CHINA • 1 spec.; South China Sea, Zhongsha Islands, seamount; 13°36.00′ N, 114°34.49′ E; depth 1340 m; 30 Mar. 2020; collection event: stn SC008; MSV Shenhaiyongshi leg.; preserved in -80°C; GenBank: MZ198760; IDSSE EEB-SW0006.

Remarks

The disc diameter was 67 mm. Our specimen is similar to the holotype description by Döderlein (1911) and the description in Liao & Clark (1995), but showed some morphological variations, especially on the disc (Fig. 11). Therefore, we hesitate to fully associate our specimen with *G. dolichodactylus*. The original description and the description in Liao & Clark (1995) mention small granules on both the dorsal and ventral disc, but the present specimen is completely naked except for the radial shields (Fig. 11A–E), which are covered by scattered granules (Fig. 11F).

Pedicellarial bands are formed by approximately 12 articulating tubercles at the curved distal end of the baseplate (Fig. 12B), and these articulations have a single foramen (Fig. 12C). The distal end of the baseplate internal side becomes curved with perforations on the ventral side of the baseplate (Fig. 12B–C). The vertebrae have a streptospondylous articulation with smooth lateral furrows and no oral bridge (Fig. 12D–H). The external side of the lateral arm plate has three separate tubercle-shaped articulations with a single opening and one large muscle opening at the edge. *Gorgonocephalus dolichodactylus* was first recorded from the South China Sea in southeastern Hainan, at a depth of 1100 m, in 1959.

Distribution

146–1357 m depth. South China Sea, Japan, Korea, Philippines, Australia and New Zealand (Liao 2004; OBIS 2021).

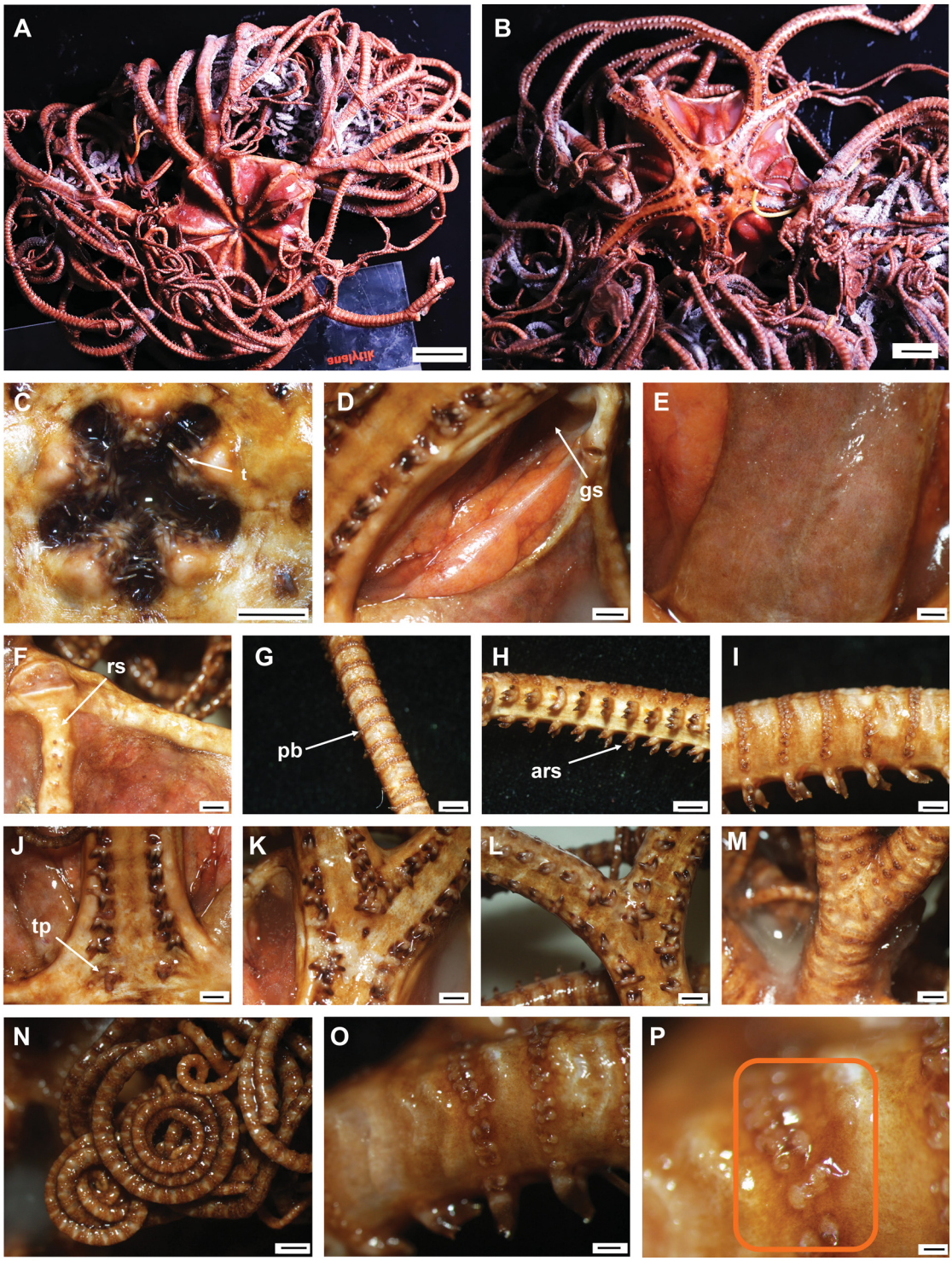

Fig. 11. *Gorgonocephalus* cf. *dolichodactylus* Döderlein, 1911 (IDSSE EEB-SW0006). **A**. Dorsal aspect. **B**. Ventral aspect. **C**. Oral frame. **D**. Genital slit. **E**. Ventral disc. **F**. Radial shield with peripheral plate. **G**. Dorsal arm. **H**. Ventral arm. **I**. Lateral arm. **J**. Ventral view of arm base. **K**. Ventral view of first arm branch. **L**. Ventral view of second arm branch. **M**. Dorsal view of second arm branch. **N**. Coiled distal arm branches. **O**. Pedicellarial band. **P**. Pedicellariae on pedicellarial band. Abbreviations: ars = arm spine; gs = genital slit; pb = pedicellarial band; rs = radial shield; t = teeth; tp = tentacle pore. Scale bars: A = 22 mm; B = 14 mm; C = 5 mm; D, F–H, J–N = 2 mm; E, I = 1 mm; O = 500 µm; P = 200 µm.

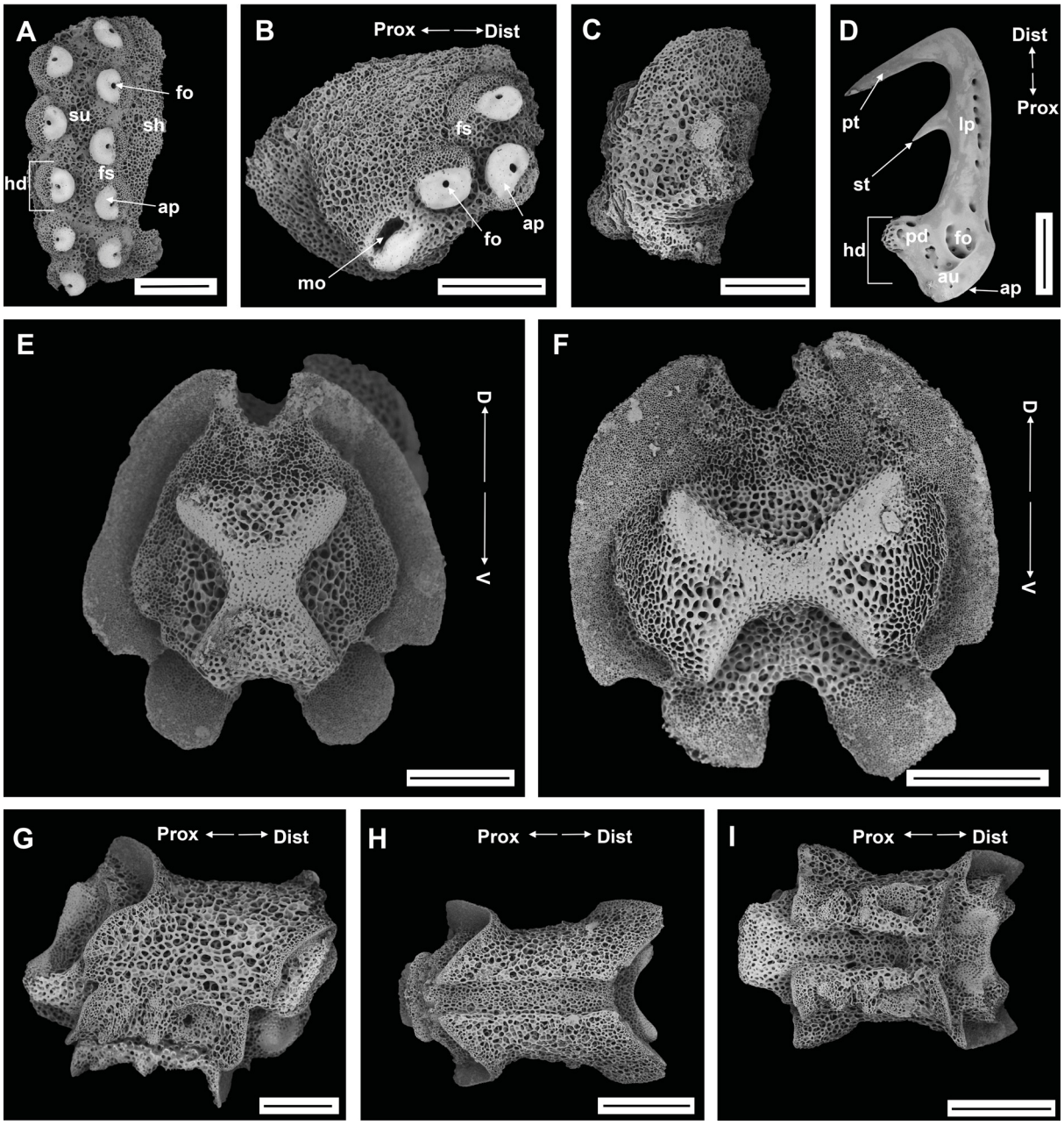

Fig. 12. *Gorgonocephalus* cf. *dolichodactylus* Döderlein, 1911, SEM (IDSSE EEB-SW0006). **A**. Plan view of base plate. **B**. Distal view of base plate. **C**. Internal view of base plate. **D**. Pedicellaria in the pedicellarial band. **E–I**. Vertebrae. **E**. Proximal view. **F**. Distal view. **G**. Lateral view. **H**. Dorsal view. **I**. Ventral view. Abbreviations: ap = articular pad of the base; au = auricle; D = dorsal; Dist = distal; fo = foramen of the base; fs = fossa between adjacent tubercles; hd = head of the apophysis; lp = lateral pores of the blade; mo = muscle opening; pd = pedicel of the apophysis; Prox = proximal; pt = primary tooth of the blade; sh = sheath of the base plate; st = secondary tooth; su = sulcus of tubercle head; V = ventral. Scale bars: A–C, E–F = 300 µm; D = 100 µm; G–I = 500 µm.

Order Ophiurida Müller & Troschel, 1840 sensu O'Hara *et al.* 2017
Suborder Ophiomusina O'Hara, Hugall, Thuy, Stöhr & Martynov, 2017
Family Ophiomusaidae O'Hara, Stöhr, Hugall, Thuy & Martynov, 2018
Genus *Ophiomusa* Hertz, 1927

Ophiomusa lymani (Wyville Thomson, 1873)
Figs 13A–G, 14

Ophiomusium lymani Wyville Thomson, 1873: 174–175, fig. 33.

Ophiomusium lymani – Koehler 1904: 58; 1922b: 411, pl. 86 figs 5, 7–9. — H.L. Clark 1911: 107–108; 1923: 364. — Matsumoto 1915: 289. — Olbers *et al.* 2019: 72–74 fig. 51.
Ophiomusa lymani – Hertz 1927: 103–105.

Material examined

CHINA • 1 spec.; South China Sea, E of Hainan Island, seamount; 18°24.45′ N, 114°52.09′ E; depth 1911 m; 12 Mar. 2020; collection event: stn SC005; MSV Shenhaiyongshi leg.; preserved in -80°C; GenBank: MZ198762; IDSSE EEB-SW0008 • 1 spec.; South China Sea, SE of Hainan Island, seamount; 17°39.60′ N, 110°36.42′ E; depth 917 m; 1 Sep. 2017; collection event: stn SC015; MSV Shenhaiyongshi leg.; preserved in -80°C; GenBank: MZ198763; IDSSE EEB-SW0009 • 1 spec.; South China Sea, SE of Hainan Island, seamount; 17°06.00′ N, 110°58.20′ E; depth 1500 m; 23 Mar. 2018; collection event: stn SC017; MSV Shenhaiyongshi leg.; IDSSE EEB-SW0034.

Remarks

We recorded three specimens from the South China Sea at 917 m to 1911 m depth. Disc diameter ranges from 17 to 20 mm. The specimens are similar to the holotype description by Wyville Thomson (1873) and to the first description from the South China Sea in Liao (2004) (Fig. 13A–G). The arm spine articulations are placed at the distal edge of the lateral arm plate (Fig. 14A–D). The vertebrae have a long zygospondylous articulation, a short, moderately large podial basin at the proximal end, and are small and narrow at the distal end. The dorsal end of the vertebrae is distally triangular and proximally flattened, with a long longitudinal groove along the midline, without furrow (Fig. 14E–H). The ventral end of the vertebrae has a broad midline longitudinal groove without an oral bridge (Fig. 14G). *Ophiomusa lymani* has been recorded from deep waters in both the East and South China Seas.

Distribution

130–4829 m depth. East China Sea, South China Sea, Arabian Sea, Indonesia, Australia, New Zealand, Chile, Gulf of Mexico, Caribbean, Atlantic Ocean and South Africa (Olbers *et al.* 2019; OBIS 2021).

Ophiomusa sp.
Fig. 13H–L

Material examined

CHINA • 1 spec.; South China Sea, near Xisha Islands; 16°39.75′ N, 112°7.43′ E; depth 663 m; 15 Mar. 2020; collection event: stn SC006; MSV Shenhaiyongshi leg.; preserved in -80°C; GenBank: MZ198764; IDSSE EEB-SW0010.

Remarks

We collected a damaged specimen that could only be identified to genus level as *Ophiomusa*. It differs from *O. lymani* by the coverage of irregular scales on the disc center, the radial shields being smaller and more triangular, large ventral disc scales connected to the oral shield entirely covering the interradial space between the genital plates and having an ventral arm plate present on up to seven arm segments from the arm base (Fig. 13H–L). *Ophiomusa* sp. forms a sister clade to *O. lymani* on our molecular tree

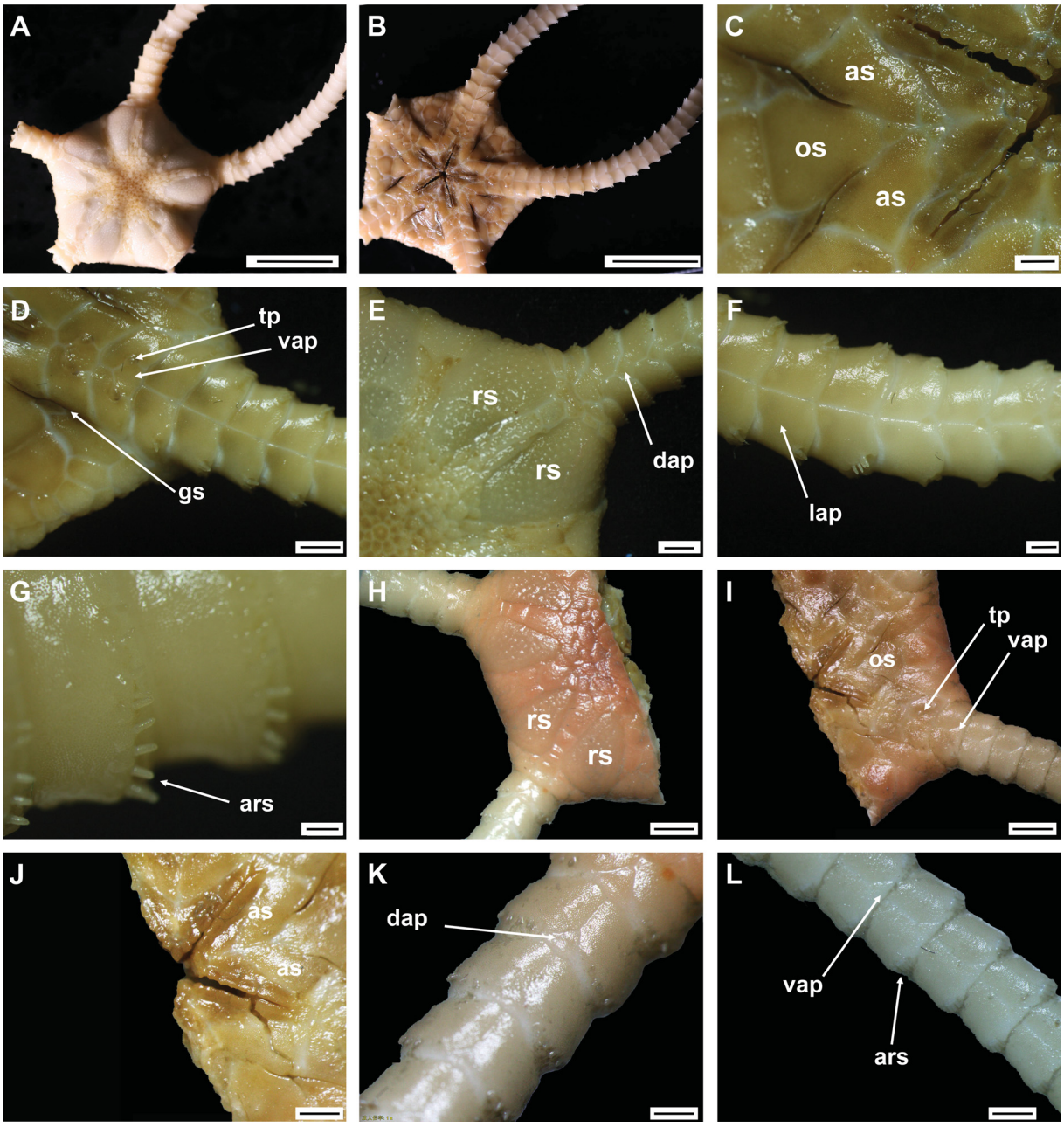

Fig. 13. A–G. *Ophiomusa lymani* (Wyville Thomson, 1873) (IDSSE EEB-SW0008). **A**. Dorsal disc. **B**. Ventral disc. **C**. Oral frame. **D**. Ventral arm base. **E**. Dorsal arm base. **F**. Ventral arm. **G**. Lateral arm plate with arm spines. **H–L**. *Ophiomusa* sp. (IDSSE EEB-SW0010). **H**. Dorsal disc. **I–J**. Ventral disc. **K**. Dorsal arm. **L**. Ventral arm. Abbreviations: as = adoral shield; ars = arm spine; dap = dorsal arm plate; gs = genital slit; lap =lateral arm plate; os = oral shield; rs = radial shield; tp = tentacle pore; vap = ventral arm plate. Scale bars: A = 10 mm; B = 15 mm; C–E = 2 mm; F, H–L = 1 mm; G = 500 µm.

(see below). In the phylogeny by Christodoulou *et al.* (2019), this sister clade is composed of *O. faceta* (Koehler, 1922a) and *O. facunda* (Koehler, 1922a), which suggests that our specimen may also belong to one of these species. *Ophiomusa faceta* is similar to *Ophiomusa* sp. by having irregular disc scales on the disc center and radial shields separated by a single layer of disc scales, but differs by lacking a ventral arm plate beyond the second arm segment, smooth dorsal disc surface and 6–7 arm spines on the lateral arm plate. *Ophiomusa facunda* is similar to *Ophiomusa* sp. by having a rough dorsal disc surface

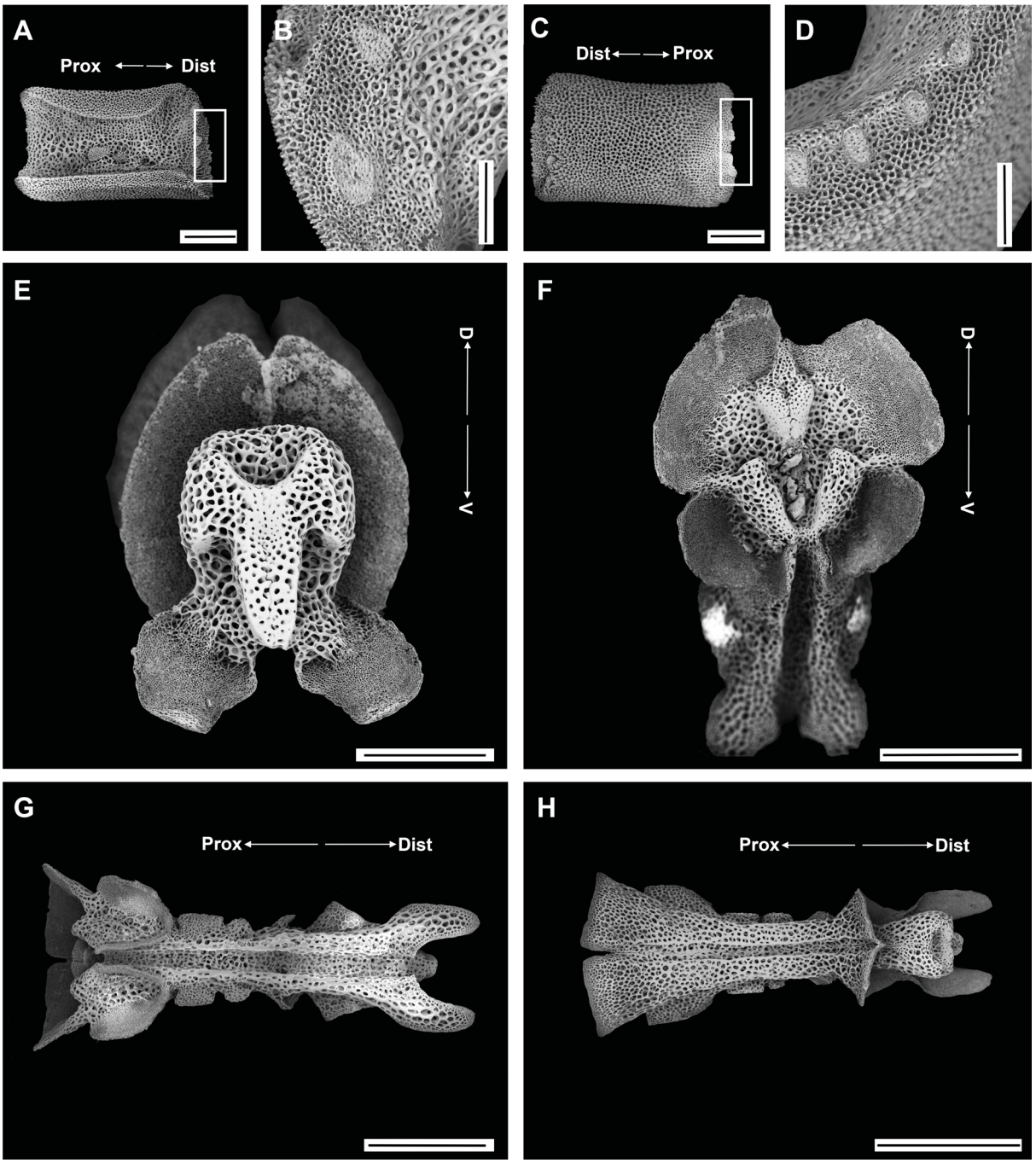

Fig. 14. *Ophiomusa lymani* (Wyville Thomson, 1873), SEM (IDSSE EEB-SW0008). **A–B**. Internal view of lateral arm plate. **C–D**. External view of lateral arm plate. **E–H**. Vertebrae. **E**. Distal view. **F**. Proximal view. **G**. Ventral view. **H**. Dorsal view. Abbreviations: D = dorsal; Dist = distal; Prox = proximal; V = ventral. Scale bars: A, C, E–G = 500 µm; B, D = 300 µm; H = 800 µm.

and radial shields separated by a single layer of disc scales, but differs in having large dorsal disc scales, the entire ventral surface occupied by a large interradial scale, in lacking a ventral arm plate beyond the third arm segment and having 6–7 arm spines on the lateral arm plate. The differences between those species and our specimen prevent us from associating it with either of them.

Superorder Ophintegrida O'Hara, Hugall, Thuy, Stöhr & Martynov, 2017
Order Ophiacanthida O'Hara, Hugall, Thuy, Stöhr & Martynov, 2017
Suborder Ophiacanthina O'Hara, Hugall, Thuy, Stöhr & Martynov, 2017
Family Ophiotomidae Paterson, 1985
Genus *Ophiotreta* Verrill, 1899

Ophiotreta eximia (Koehler, 1904)
Figs 15–16

Ophiacantha eximia Koehler, 1904: 116–117, pl. 21 figs 3–5.
Ophiacantha dilecta Koehler, 1904: 117–118, pl. 22 figs 3–4.

Ophiotreta eximia – H.L. Clark 1915: 216. — Koehler 1922a: 70–71, pl. 8 figs 5–6, pl. 93 fig. 7. — O'Hara & Stöhr 2006: 55–56, fig. 4e–g.
Ophiotreta dilecta – H.L. Clark 1915: 216. — Koehler 1922a: 71.

Material examined

CHINA • 1 spec.; South China Sea, SE of Hainan Island, seamount; 17°35.80′ N, 111°02.00′ E; depth 1750 m; 3 Apr. 2018; collection event: stn SC022; MSV Shenhaiyongshi leg.; preserved in -80°C; IDSSE EEB SW0030.

Description (IDSSE EEB-SW0030)

Measurements. Disc diameter 11.9 mm, arm width 3.0 mm.

Disc. Circular, dorsal side covered by overlapping scales with one or mostly two spines (Fig. 15A–B). Disc spines tall, 0.4–0.6 mm high, 10–11 times as high as wide, slender, thorny, with two to three small, non-flaring terminal thorns (Fig. 15C–G). Few disc spines scattered on first dorsal arm segment (Fig. 15E). Radial shields covered by disc scales and skin (Fig. 15A, E). Ventral disc completely covered by disc spines, two small disc spines at ventralmost margins of three oral shields. Genital slits conspicuous, extending from oral shield to periphery of disc (Fig. 15B–F). Oral shield much wider than long, broadly triangular, with obtuse proximal angle and lobed or convex distal edge. Adoral shield long and narrow, mostly not separated. Adoral shields enclosing proximal edges of oral shield and separating it from first lateral arm plate, reaching just beyond lateral angle of oral shield (Fig. 15F). Jaws longer than wide. Cluster of papillae on jaw with three to five large, pointed, spiniform tooth papillae on dental plate and two rows of pointed papillae on apex of jaw (on oral plates), with large, pointed tip, five to seven lateral oral papillae and distalmost two flat and enlarged (Fig. 15F).

Arms. Dorsal arm plates as long as wide, fan-shaped, triangular with straight proximal end, slightly curved distal margin, covered with minute spines and consecutive plates completely separated (Fig. 15J). Ventral arm plates pentagonal, as wide as long except on first one to two arm segments, straight obtuse triangular proximal end, distal margin truncated to concave, along arm plates thickened distalwards, consecutive plates well separated (Fig. 15H–I). Lateral arm plates meeting above and below (Fig. 15H). 10–12 arm spines at each lateral arm plate; five to six upper arm spines four to six arm segments in length, smooth and meeting across dorsal midline (Fig. 15G); five to six lower arm spines short, two to three shortest, half arm segment in length, thorny (Fig. 15K). Lowermost arm spine on lateral arm

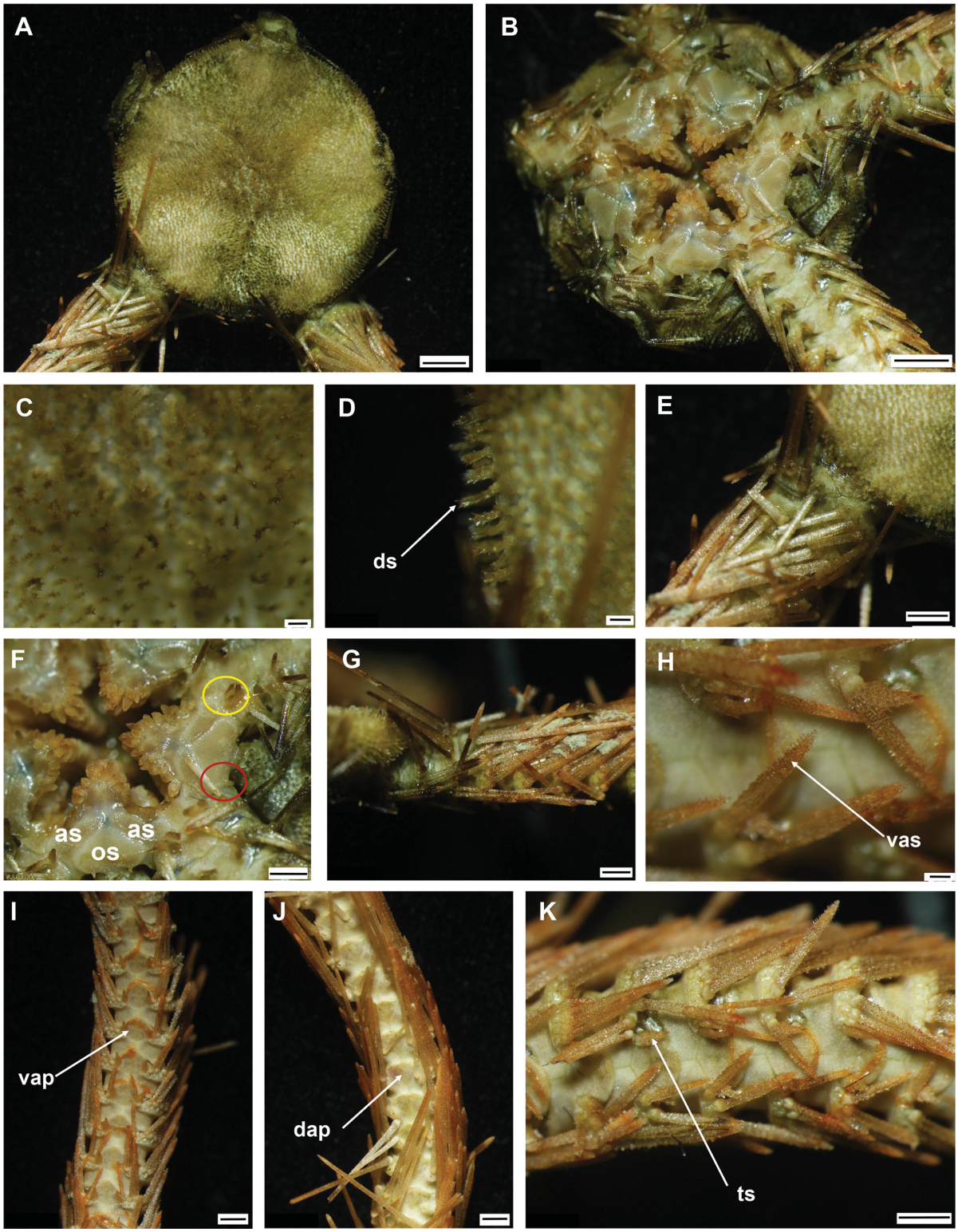

Fig. 15. *Ophiotreta eximia* (Koehler, 1904) (IDSSE EEB-SW0030). **A**. Dorsal disc. **B**. Ventral disc. **C–D**. Disc spines. **E**. Dorsal view of arm base. **F**. Oral frame (yellow circle = tentacle scales on first tentacle pore; red circle = oral shield spine). **G**. Lateral view of arm base. **H**. Ventralmost arm spine. **I**. Ventral arm. **J**. Dorsal arm. **K**. Ventral arm spines. Abbreviations: as = adoral shield; dap = dorsal arm plate; ds = disc spine; os = oral shield; ts = tentacle scale; vap = ventral arm plate; vas = ventral arm spine. Scale bars: A–B = 2 mm; C–D, F, H = 200 µm; E, G, I–K = 1 mm.

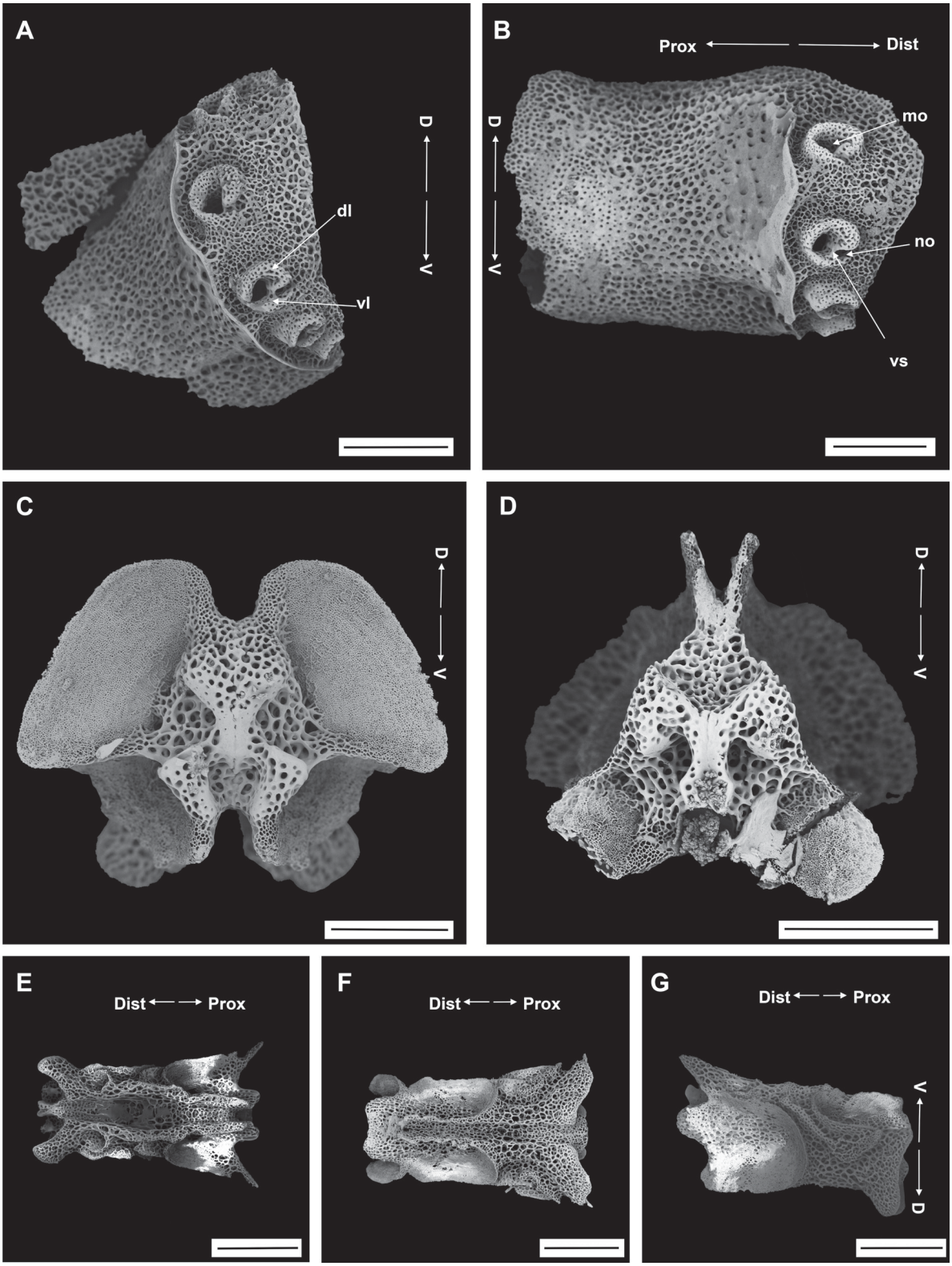

Fig. 16. *Ophiotreta eximia* (Koehler, 1904), SEM (IDSSE EEB-SW0030). **A–B**. Lateral arm plate. **C–G**. Vertebrae. **C**. Proximal view. **D**. Distal view. **E**. Ventral view. **F**. Dorsal view. **G**. Lateral view. Abbreviations: D = dorsal; Dist = distal; dl = dorsal lobe; mo = muscle opening; no = nerve opening; Prox = proximal; V = ventral; vl = ventral lobe; vs = volute-shaped. Scale bars: A–D = 300 μm; E–G = 500 μm.

segments slightly flattened with curved shape and straight, elongated thorns along tip of curved surface (Fig. 15H). One elongated, large tentacle scale with thorny apex, longer than ventral arm plate but becoming narrow and pointed distalwards on arm (Fig. 15K). First arm segment with two tentacle scales covering tentacle pore (Fig. 15F).

Color. When alive, grey to whitish on disc and arms, mouth region and spines light brown (Fig. 15A–B).

Ossicle morphology. Arm spine articulations well developed and placed at small angle in relation to distal edge of lateral arm plate, separated from proximal part of plate by wavy ridge. Ventral and dorsal articular lobes fused into a single volute-shaped articular structure (with sigmoidal fold, see Martynov 2010), dorsal lobe perforated by small holes, ventral lobe smooth and non-perforated (Fig. 16A). Large muscle opening and small nerve opening, but dorsalmost arm spine articulation without sigmoidal fold and ventral ones entire but connected to main part of lateral arm plate by short ridge (Fig. 16A–B). Vertebrae with long zygospondylous articulation, distally abruptly truncated, dorsal median furrow moderately expressed and podial basins long and large (Fig. 16C–G).

Remarks

The disc diameter of our specimen is within the range of the type specimens (11–21 mm). Koehler (1904) divided these specimens according to morphological variation of the arm plate and arm spines, but these variations fall within the morphological type series of *O. eximia*, and little morphological variation is expressed in the number of arm spines, height of the disc spines and number of oral papillae. The size of the specimens affects the morphological variation in *O. eximia* such as the number of oral papillae, the number of tentacle scales on the first arm segment and disc spine length. Due to these morphological variations, it is rather difficult to distinguish species of *Ophiotreta*. *Ophiotreta matura* Koehler, 1904 is quite similar to *O. eximia,* but differs in having stouter disc spines with flared terminal thorns, thornier upper arm spines and arm plates and hook-shaped thorny ventralmost arm spines (O'Hara & Stöhr 2006). The specimen in the present study showed a unique morphological feature in two small thorny spines located at the ventral margin of the oral shields directly proximal to the genital slits (Fig. 15F).

Distribution

724–1893 m depth. South China Sea, New Zealand, Makassar Strait, Sulu Sea, Molucca Sea, Flores Sea, Coral Sea and Tasman Sea (O'Hara & Stöhr 2006; OBIS 2021).

Genus *Ophiopristis* Verrill, 1899

Ophiopristis shenhaiyongshii sp. nov.
urn:lsid:zoobank.org:act:31D1CA52-EBB3-4BCB-9327-BF43B085AB6D
Figs 17–19

Diagnosis

Disc spines rugose with two to three small terminal thorns on truncated tip or minutely bifurcated tip. Radial shields with distal end exposed. Oral shield distal edge with series of thick, rugose thorny spines. Ventralmost arm spine with longer thorns at lateral edge, distally with some ventrally directed thorns. Tentacle scales oval and pointed, two on the first three segments, thereafter one large scale.

Etymology

The specific name is dedicated to the manned submersible vessel 'Shenhaiyongshi', which collected the specimen.

Material examined

Holotype

CHINA • South China Sea, SE of Zhongsha Islands, seamount; 13°23.98′ N, 114°51.50′ E; depth 1360 m; 23 Sep. 2020; collection event: stn SC012; MSV Shenhaiyongshi leg.; preserved in 95% ethanol; GenBank: MZ198776; IDSSE EEB-SW0022.

Description

Measurements. Disc diameter 6.3 mm, base of arm width 1.5 mm.

Disc. Pentagonal and covered with translucent, perforated, rounded, overlapping scales bearing one or two tall spines (Fig. 17A–C). Disc spines 0.4 to 0.8 mm high, glassy, hollow, rugose with two to three small terminal thorns on truncated tip or minutely bifurcated tip. Disc spine height and shape change from center to periphery of disc (Fig. 17C–G). Central disc spines short (0.3–0.4 mm high), smooth, with one to two terminal thorns. Peripheral disc spines and around radial shields taller (0.6–0.8 mm high), strongly rugose, with subterminal tooth and two to three terminal thorns on truncated or bifid tip (Fig. 17D–E). Edge of disc periphery and distal margin of radial shield with few short thorny stumps with crown of two spinelets (Fig. 17E). Proximal ends of radial shields largely covered by disc scales, distal ends exposed, triangular, pair of shields widely separated (Fig. 17G). Ventral disc covered by scales with spines, but shorter and less dense than a dorsal disc. Oral shield wider than long, triangular with obtuse proximal angle, curved lateral margins, rounded to truncated distal edge with series of short, thick, rugose, thorny-tipped spines (Figs 17H, 18A–B). Adoral shield long, with straight lateral margin, but near first ventral arm plate slightly curved, pair of shields meeting proximally (Fig. 18A). Adoral shields enclose proximal edges of oral shield, curving to lateral plate of first arm segment, separating oral shield from arm. Jaw slightly longer than wide, opening of second tentacle pore superficial (Fig. 18A). Mostly two (one jaw has three) small, pointed tooth papillae on apex of jaw, below large pointed single column of teeth. Up to five finger-like, tapering, pointed lateral oral papillae. Two enlarged and flattened, pointed oral papillae arising from adoral shield and separated from other oral papillae, probably adoral shield spines (Fig. 18A). Genital slits conspicuous and extending from oral shield to periphery of disc (Fig. 18B). Oral surface covered by transparent integument, partially obscuring oral frame beneath, but only visible in live wet condition (fresh) (Fig. 17H).

Arms. Five moniliform arms, with glassy plates (Fig. 18C–F). Dorsal arm plates separate, as long as wide, bell-shaped, with straight proximal end, slightly wavy distal margin covered with minute spines (Fig. 18C–D). Ventral arm plates as wide as long, with convex distal end, slightly obtuse proximal end, lateral edges concave, well separated along arm, axe head-shaped proximalmost arm plates (Fig. 18E–F). Lateral arm plates meeting above and below. Six arm spines. Three dorsal spines, three arm segments in length, laterally compressed, thorny, lateral margins with row of widely spaced, tall sharp thorns, apex truncated or bluntly rounded (Fig. 18H). Three ventral arm spines, one to two arm segments in length, laterally compressed, dense row of shorter, sharp thorns, apex truncated or blunt (Fig. 18H). Ventralmost arm spines with longer thorns at lateral edge, distally with some ventrally directed thorns, but without true hook-shape (Fig. 18H). Tentacle pores large, on up to three proximalmost segments with two scales, oval to pointed, one on lateral arm plate, other on ventral plate. Beyond third segment with single large tentacle scale on lateral plate, covering pore (Fig. 17A, E–F).

Color. In dried specimen glassy, darker in center but rest of specimen white and arm spines transparent (Fig. 17A–B). When alive, disc glassy dark brown, arms creamy white and arm spines transparent (Fig. 17G–H).

Ossicle morphology. Arm spine articulations well developed, volute-shaped, on protruding distal part of lateral plate with porous stereom, delimited from smooth middle part of lateral plate by thin

wavy edge. Proximal edge of spine articulation entire, but connected with main part of lateral arm plate by short ridge. Arm spine articulation with large muscle opening and small nerve opening (Fig. 19A–C). Dorsal arm spine laterally compressed, thorny, several longitudinal rows of perforations with widely spaced, tall thorns, apex truncated (Fig. 19D). Vertebrae with zygospondylous articulation, with moderately expressed narrow dorsal furrow, distally abruptly truncated, and podial basins moderate in size (Fig. 19E–I). Ambulacral furrow with greatly widened middle, without oral bridge (Fig. 19G).

Remarks

The genera *Ophiopristis* and *Ophiotreta* are at present poorly delimited from each other. On the phylogenetic tree in Christodoulou *et al.* (2019) they are both polyphyletic and several species may have to be reassigned to other genera in a future taxonomic revision. Assigning our new species to either of them is therefore difficult. We compared the new species to the type species of both genera,

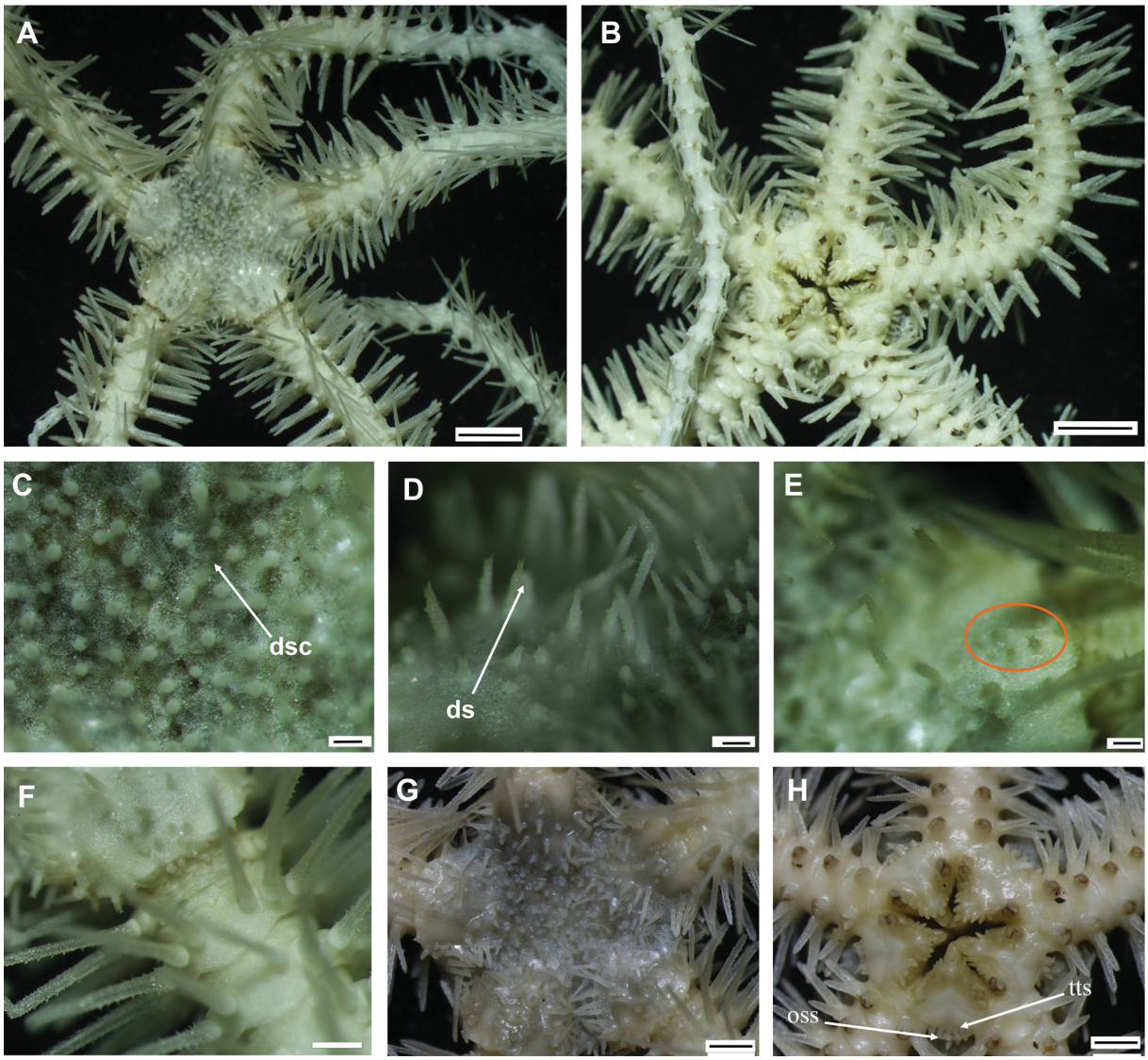

Fig. 17. *Ophiopristis shenhaiyongshii* sp. nov., holotype (IDSSE EEB-SW0022). **A**. Dorsal side of the specimen. **B**. Ventral side of the specimen. **C**. Overlapping disc scales. **D–F**. Various sizes of disc spines. **G–H**. Fresh specimen. **G**. Dorsal disc. **H**. Ventral disc. Abbreviations: ds = disc spine; dsc = disc scale; oss = oral shield spine; tts = thin transparent skin. Scale bars: A–B = 2 mm; C–E = 200 µm; F = 500 µm; G–H = 1 mm.

Ophiotreta lineolata (Lyman, 1883) and *Ophiopristis hirsuta* (Lyman, 1875). Both are present on the tree in Christodoulou *et al.* (2019), in different clades, suggesting that they indeed represent two different genera. According to the original description, *O. lineolata* has a cluster of tooth papillae, a dense dorsal disc cover of coarse grains intermingled with a few short spines, the radial shields are obscured by granules and there are 8–9 translucent, almost smooth arm spines and a single large tentacle scale on all but the first pore (Lyman 1883). *Ophiopristis hirsuta* has elongated jaws with seven spiniform lateral oral papillae and no tooth papillae (although the illustration seems to show two tooth papillae), the dorsal disc is covered by short, fine spines (which on the illustration look rather long), the distal ends of the radial shields are exposed and swollen, the six arm spines are flattened, glassy and strongly serrated,

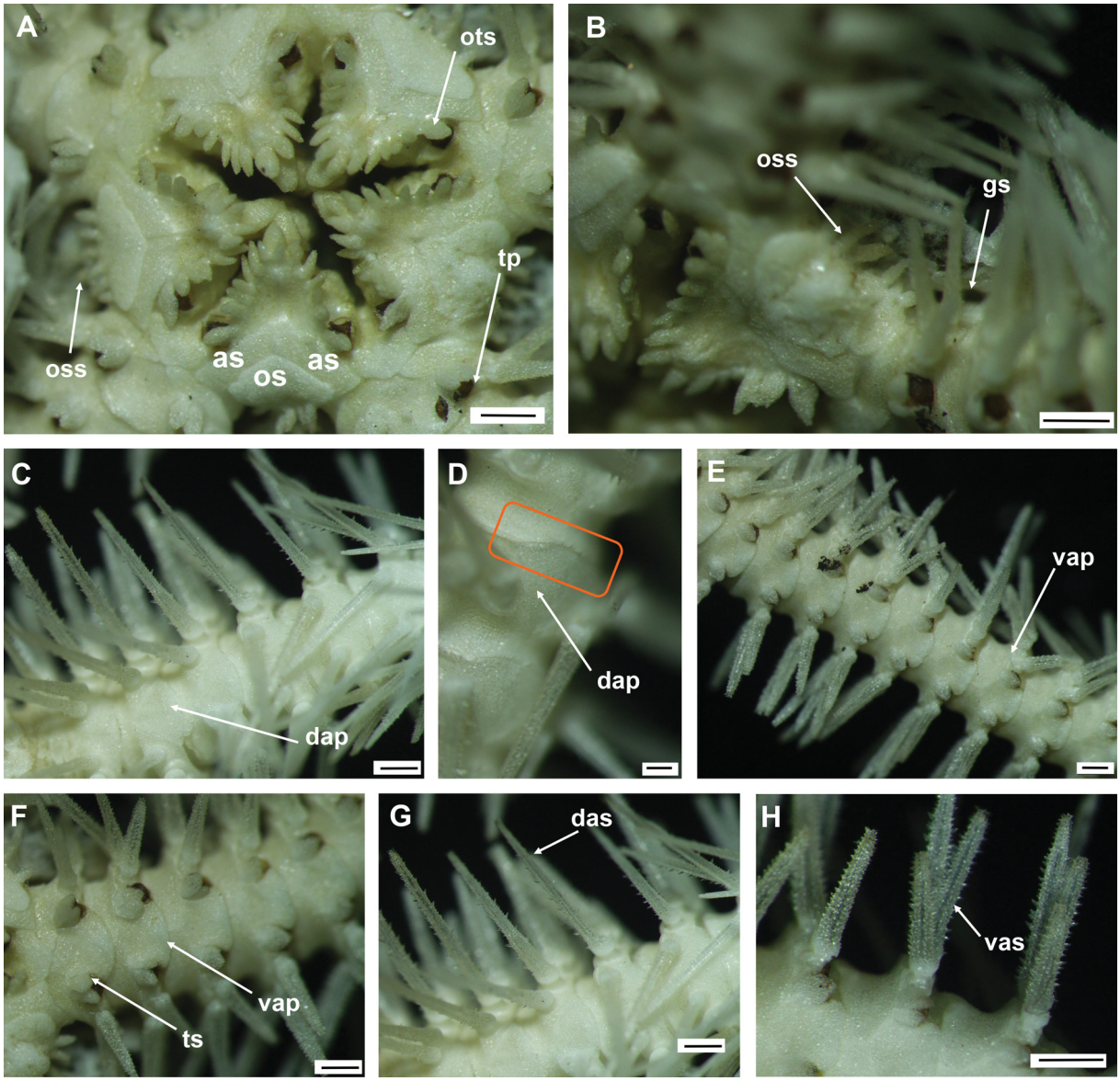

Fig. 18. *Ophiopristis shenhaiyongshii* sp. nov., holotype (IDSSE EEB-SW0022). **A**. Oral frame. **B**. Lateral disc. **C–D**. Dorsal arm (distal margin with minute spines highlighted on D). **E–F**. Ventral arm. **G**. Dorsal arm spines. **H**. Ventral arm spines. Abbreviations: as = adoral shield; dap = dorsal arm plate; das = dorsal arm spine; gs = genital slit; os = oral shield; oss = oral shield spine; ots = oral tentacle scale; tp = tentacle pore; ts = tentacle scale; vap = ventral arm plate; vas = ventral arm spine. Scale bars: A–C = 1 mm; D, G–H = 200 µm; E–F = 500 µm.

and there are two large tentacle scales (Lyman 1875). There was also a striking size difference, with *O. lineolata* having a disc diameter of 18 mm and *O. hirsuta* just 3.7 mm.

Ophiopristis shenhaiyongshii sp. nov. shares the disc spines, distally exposed radial shields, few or no tooth papillae, flat serrated arm spines and the small size with *Ophiopristis hirsuta* and differs from

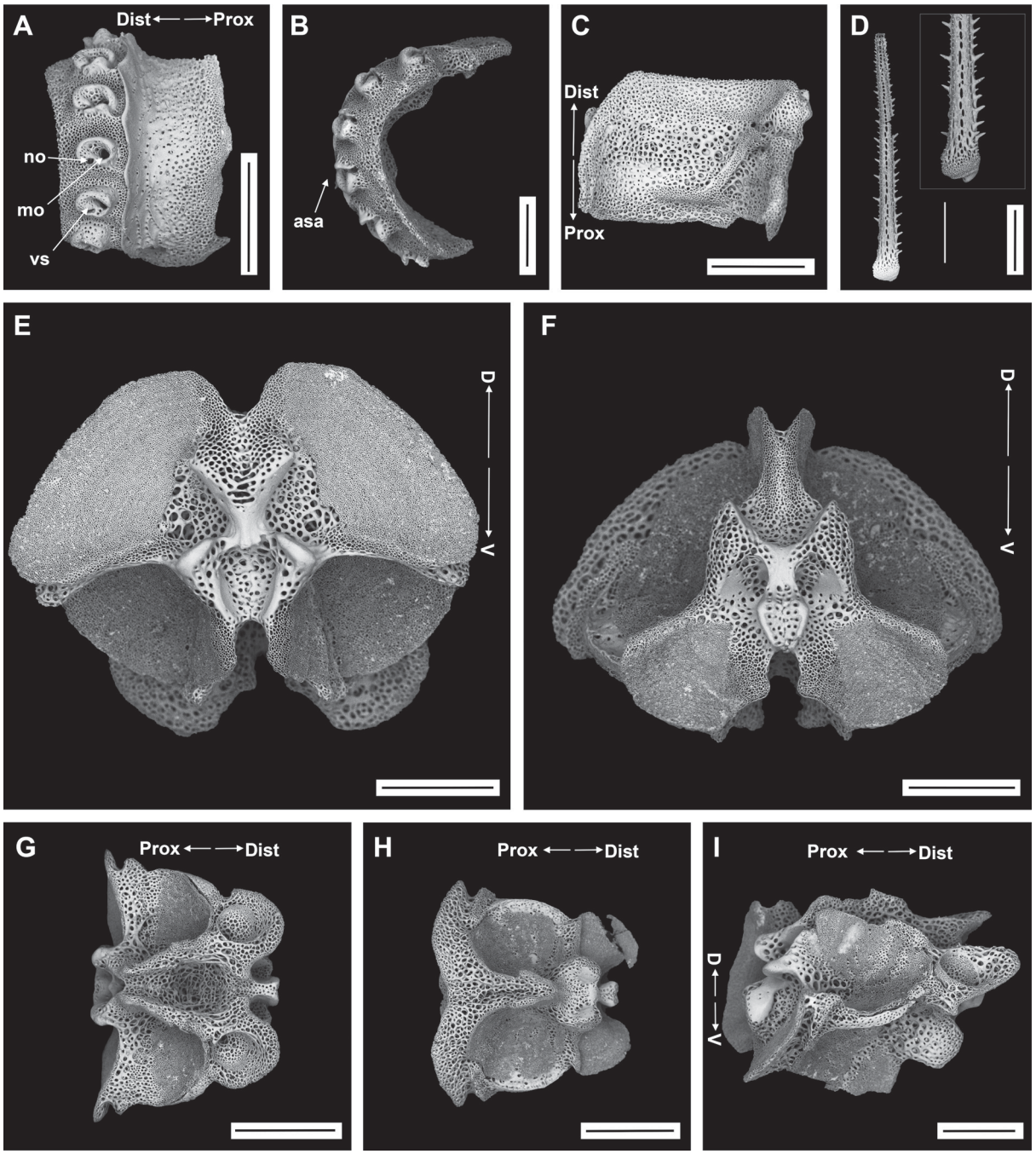

Fig. 19. *Ophiopristis shenhaiyongshii* sp. nov., SEM, holotype (IDSSE EEB-SW0022). **A–C**. Lateral arm plate. **D**. Dorsal arm spine. **E–I**. Vertebrae. **E**. Proximal view. **F**. Distal view. **G**. Ventral view. **H**. Dorsal view. **I**. Lateral view. Abbreviations: asa = arm spine articulation; D = dorsal; Dist = distal; mo = muscle opening; no = nerve opening; Prox = proximal; V = ventral; vs = volute-shaped. Scale bars: A, G–H = 500 µm; B–F, I = 300 µm.

Ophiotreta lineolata in all respects. Hence, we propose to assign it to the genus *Ophiopristis* due to its similarity to the generic type species. It can be delimited from other species currently assigned to *Ophiopristis* as follows:

Ophiopristis dissidens (Koehler, 1905) is similar to *O. shenhaiyongshii* sp. nov. by having exposed distal radial shields, the oral shield wider than long and widely separated ventral and dorsal arm plates, but differs by having smooth disc spines, two to three tentacle scales until the twelfth segment and a brown line running discontinuously along the dorsal surface of each arm (O'Hara & Stöhr 2006).

Ophiopristis gadensis Rodrigues *et al.*, 2011 is similar to *O. shenhaiyongshii* sp. nov. by having exposed radial shields, rugose disc spines with two or three thorns, the oral frame covered by a transparent integument and glassy arm plates and arm spines, but differs by having rounded pentagonal oral shields, contiguous dorsal and ventral arm plates, and two to three tentacle scales along the arm (Rodrigues *et al.* 2011).

Ophiopristis shenhaiyongshii sp. nov. differs from most species of *Ophiopristis* by having a series of thorny spines on the distal margin of the oral shield. This character is only shared by *O. luctosa* (Koehler, 1904) and *O. procera* (Koehler, 1904), and both species were first recorded from Indonesian waters. *Ophiopristis luctosa* differs from *O. shenhaiyongshii* sp. nov. by having long, thin, sharp, hollow, smooth disc spines, the radial shield largely obscured, small rounded oral papillae, ventral arm plates twice as long as wide, rectangular and contiguous, the ventralmost spine with a hook-like appearance and one oval tentacle scale, and a yellow color with a few broad brown bands on the arms (Koehler 1904; O'Hara & Stöhr 2006). *Ophiopristis procera* differs from *O. shenhaiyongshii* sp. nov. by having completely concealed radial shields, the ventral arm plate twice as long as wide, rectangular and contiguous, the first pair of tentacle pores covered by tentacle scales variable in size and overlapping, and the following pairs only covered by one large, elongated oval scale, equal to the length of an arm segment. *Ophiopristis shenhaiyongshii* sp. nov. shares similar disc spine and arm spine characteristics with *O. procera* (Koehler 1904).

Distribution

South China Sea (1360 m). Near Zhongsha Islands, found on a deep-sea seamount.

Family Ophiacanthidae Ljungman, 1867
Genus *Ophientrema* Verrill, 1899

Ophientrema scolopendrica (Lyman, 1883)
Figs 20–22

Ophiacantha scolopendrica Lyman, 1883: 259.
Ophiacantha leucosticta H.L. Clark, 1911: 235.

Ophientrema leucosticta – Matsumoto 1917: 111.
Ophientrema leucostictum – H.L. Clark 1911: 217. — Koehler 1922a: 85, pl. 8 figs 1–4, pl. 94 fig. 1.

Material examined

CHINA • 1 spec.; South China Sea, E of Hainan Island, seamount; 18°30.14′ N, 112°49.62′ E; depth 1400 m; 28 Jun. 2019; collection event: stn SC003; MSV Shenhaiyongshi leg.; preserved in -80°C; IDSSE EEB-SW0035 • 1 spec.; South China Sea, SE of Hainan Island, seamount; 17°27.00′ N, 111°15.00′ E; depth 1550 m; 24 Mar. 2018; collection event: stn SC018; MSV Shenhaiyongshi leg.; preserved in -80°C; GenBank: MZ198775, MZ203271; IDSSE EEB-SW0021 • 2 specs; same collection

data as for preceding; IDSSE EEB-SW0036, IDSSE EEB-SW0037 • 2 specs; South China Sea, SE of Hainan Island, seamount; 17°35.80′ N, 111°02.00′ E; depth 1750 m; 3 Apr. 2018; collection event: stn SC022; MSV Shenhaiyongshi leg.; preserved in -80°C; IDSSE EEB-SW0038, IDSSE EEB-SW0039 • 1 spec.; South China Sea, SE of Hainan Island, seamount; 17°17.81′ N, 110°31.92′ E; depth 1460 m; 4 Apr. 2018; collection event: stn SC023; MSV Shenhaiyongshi leg.; preserved in -80°C; IDSSE EEB-SW0040 • 1 spec.; South China Sea, Xisha Islands, seamount; 17°06.00′ N, 110°58.20′ E; depth 1500 m; 23 Mar. 2018; collection event: stn SC017; MSV Shenhaiyongshi leg.; preserved in -80°C; GenBank: MZ198774 , MZ203270; IDSSE EEB-SW0020 • 1 spec.; same collection data as for preceding; IDSSE EEB-SW0041.

Description (IDSSE EEB-SW0020)

Measurements. Disc diameter 13 mm, length of arms 80–100 mm.

Disc. Disc slightly pentagonal (Fig. 20A–B). Dorsal disc covered by thin, uncalcified, dark skin with surface of small projecting granules (Fig. 20A). Ventral disc smooth, with few or no smooth granules (Fig. 20B, E). Radial shields short, distally wider and widely separated (Fig. 21F). Distal half of radial shields uncovered, bearing few granules on outer margin but do not reach periphery of disc (Fig. 21F–G). Oral shields short, twice as wide as long and somewhat rhombic. Adoral shields short and wide, proximally meeting fully or some hardly meeting (Fig. 21A). Teeth significantly larger than oral papillae. Lateral oral papillae broad, flat, rounded, transparent, distal edges break easily (Fig. 21E). Number of lateral oral papillae varies among jaws, three per side, but some jaws have four oral papillae on one side (Fig. 21E). Genital slits conspicuous and extending from distal end of oral shield to periphery of disc (Fig. 21B).

Arms. Dorsal arm plate transversely oval with pointy corners, nearly twice as broad as long, covering only about half width of arm (Fig. 21C). First ventral arm plate transverse diamond-shaped, with rounded angles, next two plates square with convex outer margin. Beyond third ventral arm plate, arm segments nearly semicircular with slight peak, covering one third of width of arm segment (Fig. 21D–E). Tentacle scale absent on first arm segment and starts to appear from second or third arm segment (Fig. 21E). Lateral arm plates stout, forming well defined spine ridge and meeting on ventral side except on first two arm segments (Fig. 21D–F). Seven arm spines on an elevated ridge, four dorsal and three to four ventral. Dorsal arm spines often nearly two segments long, stout, nearly cylindrical and tapering to a blunt point (Fig. 21G). Ventral arm spines smaller, thorny with hook-shaped tip, with a few spiny points on their adoral or proximal side (Fig. 21H–I). Ventralmost arm spines on first few arm segments elongated and less hook-like, with rough surface but distalwards along arm developing into a short, little hyaline hook (Fig. 21I).

Color. Dark olivaceous green on dorsal disc, light brown color on radial shield, dorsal arm spine, and dorsal and ventral arm plate; dark reddish brown on oral papillae and ventral arm spine (Fig. 20A–B).

Ossicle morphology. Ventralmost arm spine short, thorny, with proximally oriented tip (Fig. 22A). Arm spine articulation well developed, with volute-shaped perforated lobe except in dorsal- and ventralmost articulations (Fig. 22B–C), with large muscle opening and small nerve opening (Fig. 22B–C). Vertebrae with short zygospondylous articulation with a broad dorsal extension of lateral muscle flanges, distally abruptly truncated, dorsal median furrow moderately expressed, and podial basins short and large (Fig. 22D–G). Middle segment of ventral vertebrae with deeply expressed furrow without oral bridge (Fig. 22F).

Remarks

The genus *Ophientrema* includes only two species, *O. euphylactea* (H.L. Clark, 1911) and *O. scolopendrica* (Lyman 1883). H.L. Clark (1911) mentioned a band of black spots on the dorsal disc of

O. scolopendrica caused by tissue on the inner surface of the skin. In the present study, we examined nine specimens and all of them concurred with the description of the holotype of *O. scolopendrica*. However, there are some slightly different features in the color of the dorsal disc and number of lateral oral papillae, but the color of the present specimens matched the description by Koehler (1922a).

Among the specimens from this study, we identified two different color patterns: 1) dark olivaceous green on the dorsal disc, light brown on radial shield, dorsal arm spine, and dorsal and ventral arm plate; 2) dark reddish brown on oral papillae and ventral arm spine, dark olivaceous green and brown

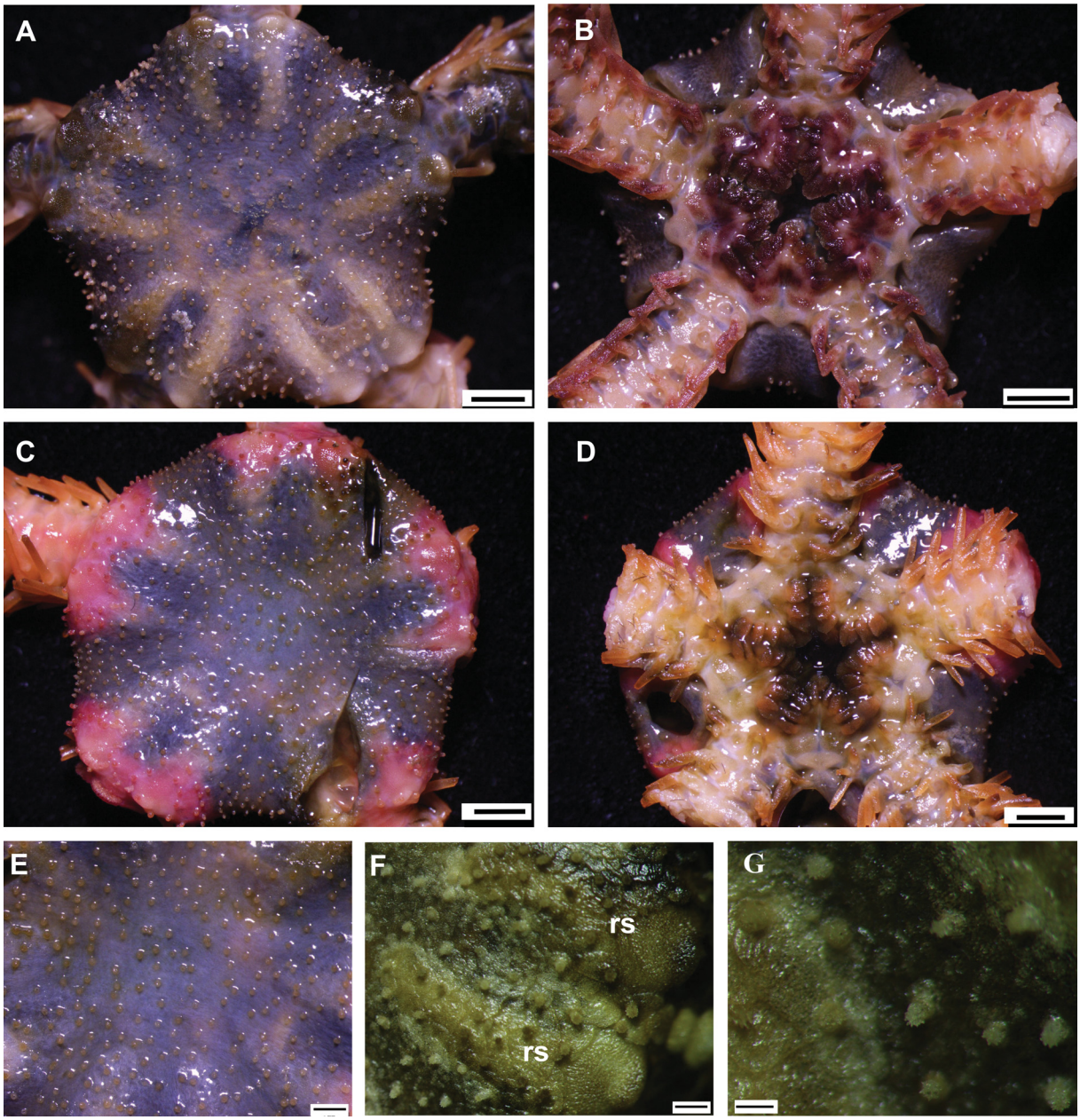

Fig. 20. *Ophientrema scolopendrica* (Lyman, 1883) (A–B, E–G = IDSSE EEB-SW0020; C–D = IDSSE EEB-SW0021). **A, C**. Dorsal disc. **B, D**. Ventral disc. **E**. Center of dorsal disc. **F**. Lateral disc. **G**. Granules on the disc. Abbreviation: rs = radial shield. Scale bars: A–D = 2 mm; E = 1 mm; F–G = 500 µm. (F and G taken of well-dried specimen)

on dorsal disc and bright red pink on radial shield, light brown on oral papillae, dorsal and ventral arm plate, and arm spine (Fig. 20A–D). Some specimens possessed seven oral papillae on one jaw, but when we examined our specimens and previous records, we considered this as intraspecific variation. *Ophientrema euphylactea* is distinguished from *O. scolopendrica* by the scale density on the dorsal disc and by having spiniform oral papillae (H.L. Clark 1911).

Distribution

1000–2000 m depth. South China Sea, Eastern Japan, Indonesia (Gulf of Tomoni), Eastern China Sea, Tasman Sea, Madagascar (OBIS 2021).

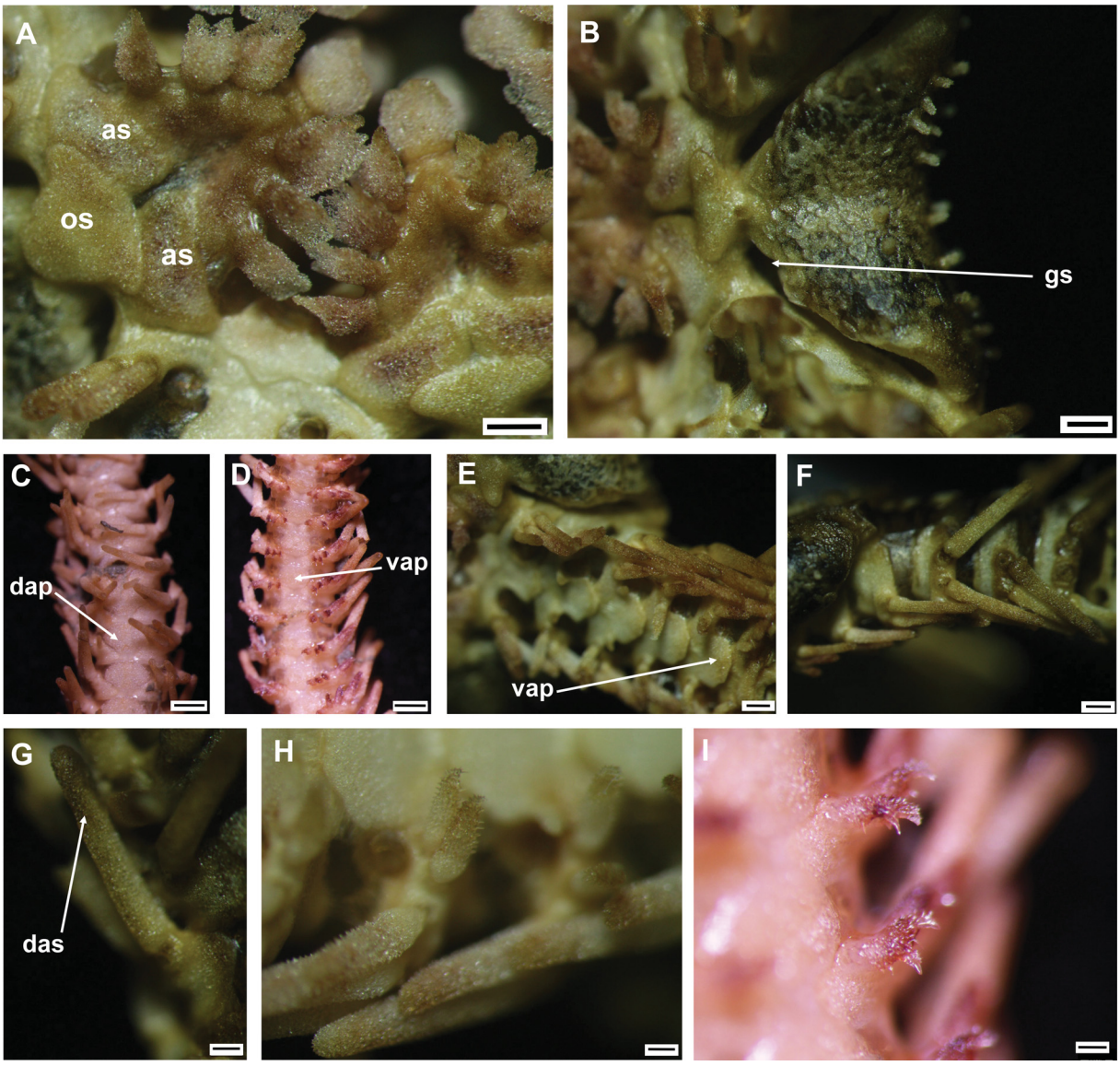

Fig. 21. *Ophientrema scolopendrica* (Lyman, 1883) (IDSSE EEB-SW0020). **A**. Oral frame. **B**. Lateral disc. **C**. Dorsal arm. **D–E**. Ventral arm. **F**. Lateral arm. **G**. Dorsal arm spine. **H–I**. Ventralmost arm spines on the arm. Abbreviations: as = adoral shield; dap = dorsal arm plate; das = dorsal arm spine; gs = genital slit; os = oral shield; vap = ventral arm plate. Scale bars: A–B, E–F = 500 µm; C–D = 1 mm; G–I = 200 µm. (A–B, E–H taken after thoroughly drying the specimen)

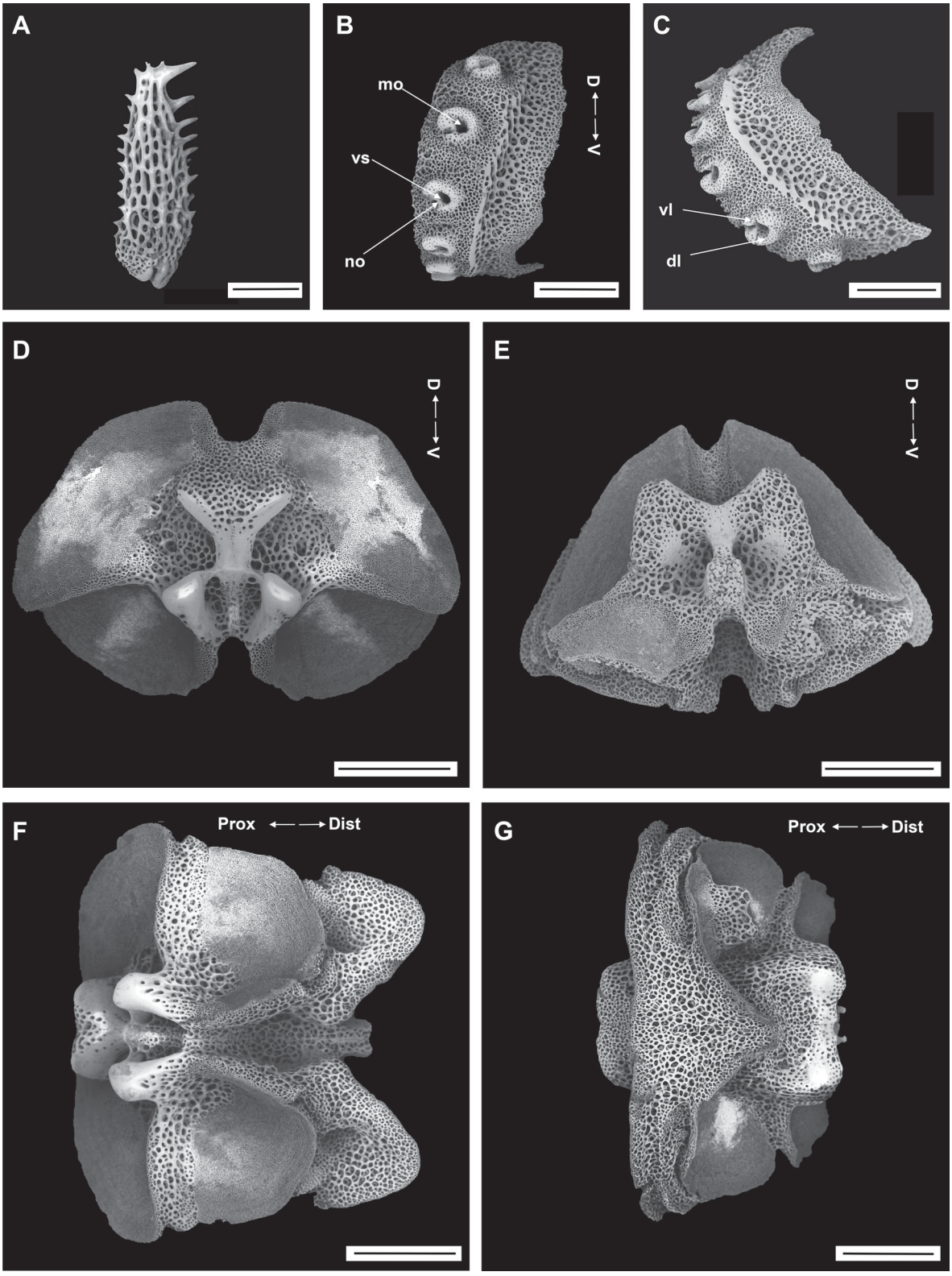

Fig. 22. *Ophientrema scolopendrica* (Lyman, 1883), SEM (IDSSE EEB-SW0020). **A**. Ventral arm spine. **B–C**. Lateral arm plate. **D–G**. Vertebrae. **D**. Proximal view. **E**. Distal view. **F**. Ventral view. **G**. Dorsal view. Abbreviations: D = dorsal; Dist = distal; dl = dorsal lobe; mo = muscle opening; no = nerve opening; Prox = proximal; V = ventral; vl = ventral lobe; vs = volute-shaped. Scale bars: A = 200 μm; B = 300 μm; C–G = 500 μm.

Genus *Ophiurothamnus* Matsumoto, 1917

Ophiurothamnus clausa (Lyman, 1878)
Figs 23–24

Ophioceramis clausa Lyman, 1878: 124, pl. 6 figs 161–163.
Ophiothamnus stultus Koehler, 1904: 141–142, pl. 25 figs 9–10, pl. 26 fig. 1.
Ophiurothamnus musorstomae Guille, 1981: 427, fig. 1g–j, pl. 3 figs 20–21.

Ophioceramis clausa – Lyman 1882: 26, pl. 11 figs 4–6.
Ophiurothamnus stultus – Matsumoto 1917: 130. — Koehler 1922a: 104–105, pl. 22 fig. 1–4. — Liao 2004: 149, fig. 78.
Ophiurothamnus clausa – O'Hara & Stöhr 2006: 105, fig. 14 (a–j). — Chen *et al.* 2020: 651–652, figs 1–2.

Material examined

CHINA • 1 spec.; South China Sea, SE of Hainan Island, seamount; 17°17.60′ N, 111°34.17′ E; depth 1500 m; 2 Apr. 2018; collection event: stn SC021; MSV Shenhaiyongshi leg.; preserved in 95% ethanol; GenBank: MZ198777; IDSSE EEB-SW0023 • 2 specs; South China Sea, SE of Hainan Island, seamount; 17°59.21′ N, 111°01.17′ E; depth 1500 m; 1 Apr. 2018; collection event: stn SC020; MSV Shenhaiyongshi leg.; preserved in -80°C; IDSSE EEB-SW0042, IDSSE EEB-SW0043.

Remarks

The disc diameter (4.5–5.0 mm), the circular disc and the morphology are similar to the description of *Ophiurothamnus clausa* in O'Hara & Stöhr (2006) and to the description from the South China Sea in Chen *et al.* (2020), but we identified some variability in the number of scales on the dorsal disc and in the shape of the radial shields (Fig. 23). The arm skeleton characters of *O. clausa* differ from those of other species in the family Ophiacanthidae.

The dorsal arm plate is triangular and well developed (Fig. 24A). The arm spine articulation is well developed and has a large muscle opening and a small nerve opening. A volute-shaped perforated lobe is present in most articulations, but is lacking in the dorsalmost one (Fig. 24B). A perforation is present on the inner side of each lateral arm plate (Fig. 24C). The vertebrae have a long streptospondylous articulation, with broad proximal and distal ends and a narrow middle segment. The proximal end of a vertebra has two clearly separated openings and the distal end of the podial basin becomes short and small. The dorsal side of the vertebrae is distally triangular and proximally flattened, without a keel. The ventral side of the vertebrae has a narrow and straight ambulacral furrow without an oral bridge (Fig. 24D–G).

Ophiurothamnus clausa has variable morphological features according to O'Hara & Stöhr (2006), especially regarding the characters of the disc, and the variation in disc covering is very striking, ranging from smooth naked plates to plates with granules, the number and shape of the scales covering the disc, the shape and position of the radial shields and the shape of the arm spines. These character differences cannot be explained by biogeographic distribution or size of the animal (O'Hara & Stöhr 2006) and may instead be evidence of cryptic speciation.

Distribution

480–3202 m depth. East China Sea, South China Sea, Indonesia, Australia, New Zealand, Kermadec Islands, Philippines, New Caledonia, Papua New Guinea, Mozambique Channel (O'Hara & Stöhr 2006; OBIS 2021).

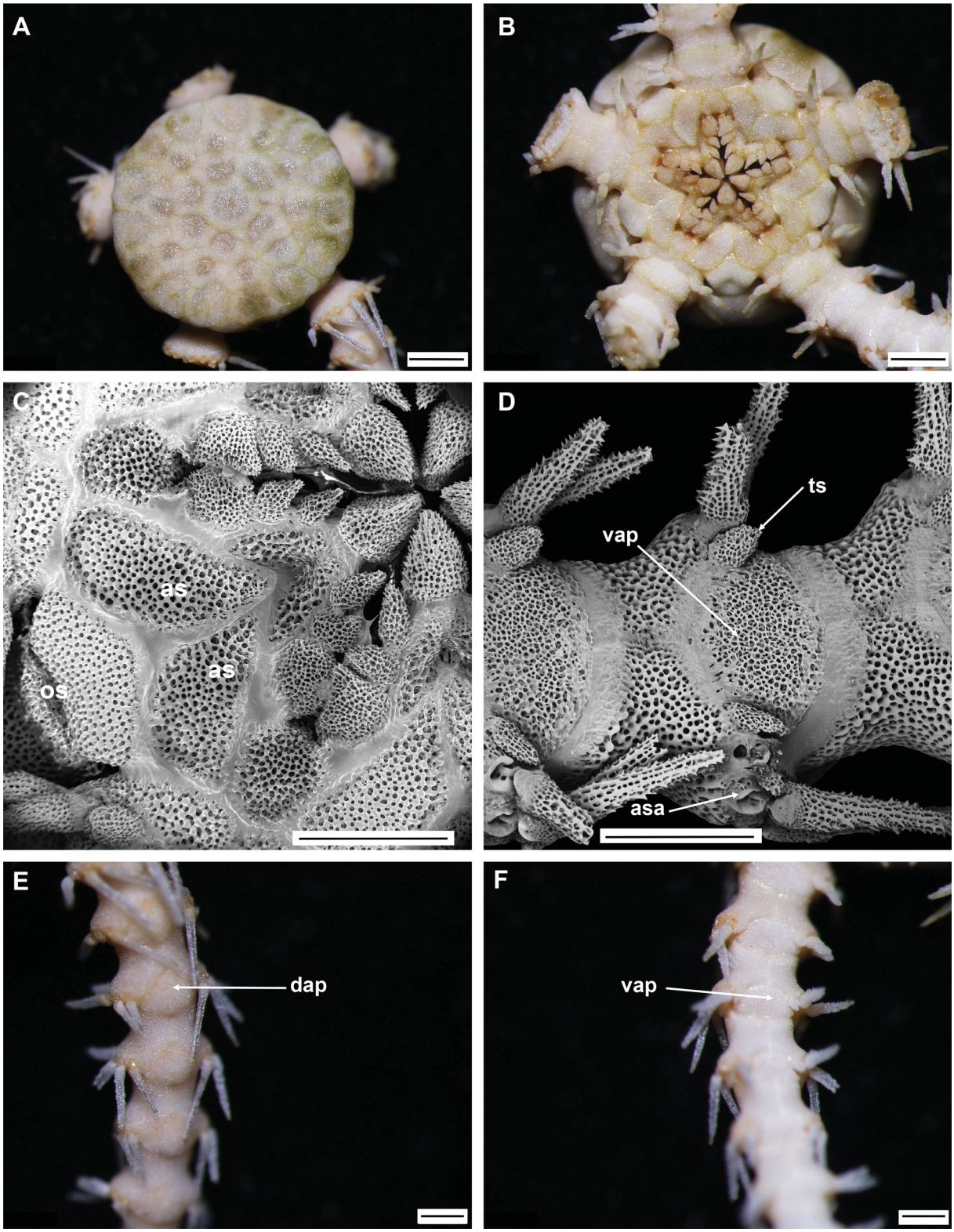

Fig. 23. *Ophiurothamnus clausa* (Lyman, 1878) (IDSSE EEB-SW0023). **A**. Dorsal disc. **B**. Ventral disc. **C**. Oral frame (SEM). **D**. Ventral arm (SEM). **E**. Dorsal arm. **F**. Ventral arm. Abbreviations: as = adoral shield; asa = arm spine articulation; dap = dorsal arm plate; os = oral shield; ts = tentacle scale; vap = ventral arm plate. Scale bars: A–B = 1 mm; C–F = 500 μm.

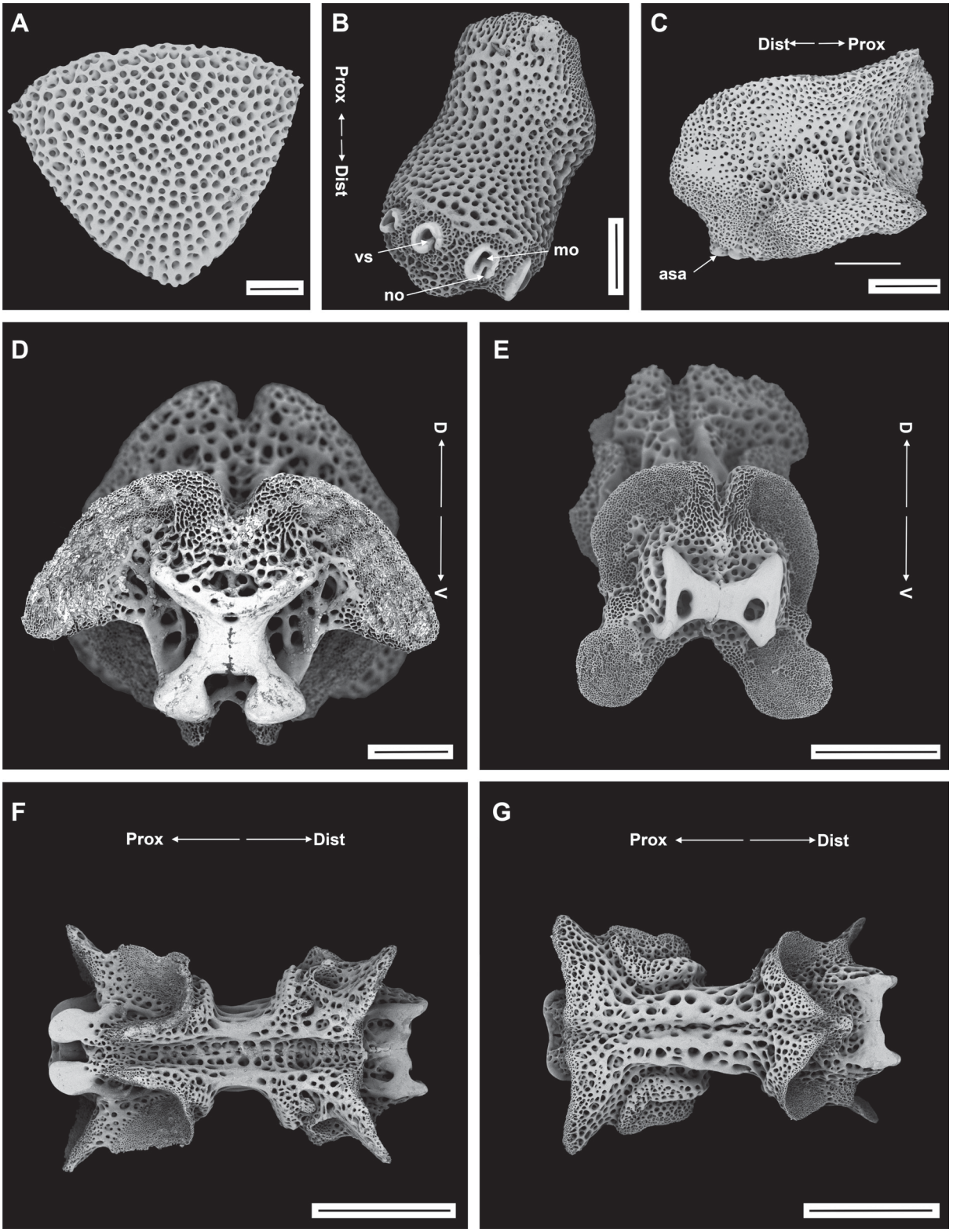

Fig. 24. *Ophiurothamnus clausa* (Lyman, 1878), SEM (IDSSE EEB-SW0023). **A**. Dorsal arm plate. **B–C**. Lateral arm plate. **B**. External view. **C**. Internal view. **D–G**. Vertebrae. **D**. Proximal view. **E**. Distal view. **F**. Ventral view. **G**. Dorsal view. Abbreviations: asa = arm spine articulation; D = dorsal; Dist = distal; mo = muscle opening; no = nerve opening; Prox = proximal; V = ventral; vs = volute-shaped. Scale bars: A, D = 100 µm; B, F–G = 300 µm; C, E = 200 µm.

Genus *Ophioplinthaca* Verrill, 1899

Ophioplinthaca plicata (Lyman, 1878)
Figs 25–26

Ophiomitra plicata Lyman, 1878: 150, pl. 8 figs 209–212, pl. 9 figs 233–235.
Ophioplinthaca vicina Koehler, 1904: 129-130, pl. 25 figs 1–3.

Ophiomitra plicata – Lyman 1882: 203–204, pl. 10 figs 7–9. — Li 1987: 143–145, pl. 1 fig. 2. — Liao 2004: 139–140, fig. 70.
Ophioplinthaca plicata – O'Hara & Stöhr 2006: 84–85, fig. 8g, m–p.

Material examined

CHINA • 1 spec.; South China Sea, Zhongsha Islands, seamount; 15°36.20′ N, 113°33.74′ E; depth 1820 m; 27 Sep. 2019; collection event: stn SC014; MSV Shenhaiyongshi leg.; preserved in 95% ethanol; GenBank: MZ198773, MZ203269; IDSSE EEB-SW0019.

Remarks

The present study found only one specimen of *O. plicata,* with 12.5 mm in disc diameter (Fig. 25). Within Chinese waters, this species has previously been recorded only from the South China Sea.

The arm spine articulation is well developed and placed at a slight angle to the distal edge of the lateral arm plate. A volute-shaped perforated lobe is present in most articulations, but is reduced in the dorsalmost one (Fig. 26A–B). The arm spine articulation has a large muscle opening and a small nerve opening (Fig. 26A–B), and it decreases significantly in size ventralwards (Fig. 26A). The vertebrae have a streptospondylous articulation, with a short, broad podial basin at the proximal end and a narrow, small distal end. The dorsal end of the vertebrae is distally triangular and proximally flattened with a longitudinal groove along the midline (Fig. 26C–G). The ventral end of the vertebrae has a broad ambulacral groove without an oral bridge (Fig. 26E).

The genus *Ophioplinthaca* is clearly distinguishable from other genera within the family Ophiacanthidae by the deep interradial incisions into the disc, which are lined distally by enlarged disc scales. *Ophioplinthaca plicata* is morphologically variable among individuals and is difficult to distinguish from other species of *Ophioplinthaca*, especially from *O. pulchra* Koehler, 1904. The morphological features of the specimen of *O. plicata* from our collection and previous descriptions show complex morphological variation among individuals, and more specimens need to be analyzed from neighboring seas and the Indo-Pacific region to understand their morphological variation with respect to geographic distribution (O'Hara & Stöhr 2006). A molecular analysis using specimens from many localities is required to understand the genetic variation in this species and its impact on morphological variation.

Distribution

480–2003 m depth. South China Sea, Philippines, Indonesia, New Caledonia, Kermadec Island, New Zealand, SE Australia (O'Hara & Stöhr 2006; OBIS 2021).

Genus *Ophiacantha* Müller & Troschel, 1842

Ophiacantha bathybia H.L. Clark, 1911
Figs 27–28

Ophiacantha bathybia H.L. Clark, 1911: 233–234.

Material examined

CHINA • 1 spec.; South China Sea, E of Hainan Island, seamount; 18°11.96′ N, 114°21.01′ E; depth 3536 m; 11 Sep. 2017; collection event: stn SC016; MSV Shenhaiyongshi leg.; GenBank: MZ203273; IDSSE EEB-SW0024 • 1 spec.; South China Sea, E of Hainan Island, seamount; 18°11.93′N, 114°21.01′E; depth 1550 m; 9 Sep. 2017; collection event: stn SC016; MSV Shenhaiyongshi leg.; GenBank: MZ203274; IDSSE EEB-SW0025 • 1 spec.; South China Sea, E of Hainan Island; 18°12.03′ N,

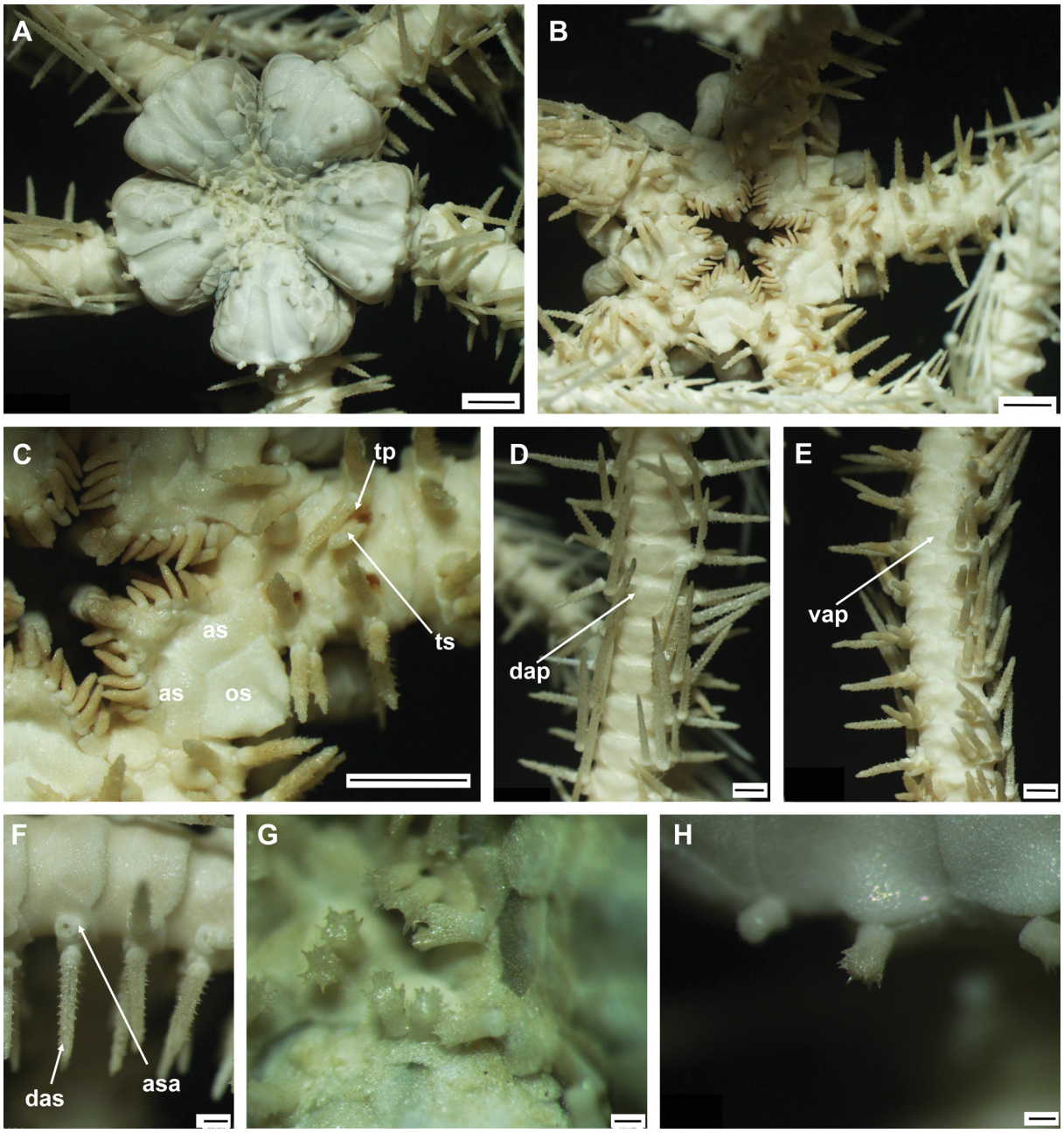

Fig. 25. *Ophioplinthaca plicata* (Lyman, 1878) (IDSSE EEB-SW0019). **A**. Dorsal disc. **B**. Ventral disc. **C**. Oral frame. **D**. Dorsal arm. **E**. Ventral arm. **F**. Lateral arm. **G–H**. Disc spine on the dorsal disc and distal end of the radial shields. Abbreviations: as = adoral shield; asa = arm spine articulation; dap = dorsal arm plate; das = dorsal arm spine; os = oral shield; tp = tentacle pore; ts = tentacle scale; vap = ventral arm plate. Scale bars: A–C = 2 mm; D–E = 1 mm; F = 500 µm; G–H = 200 µm.

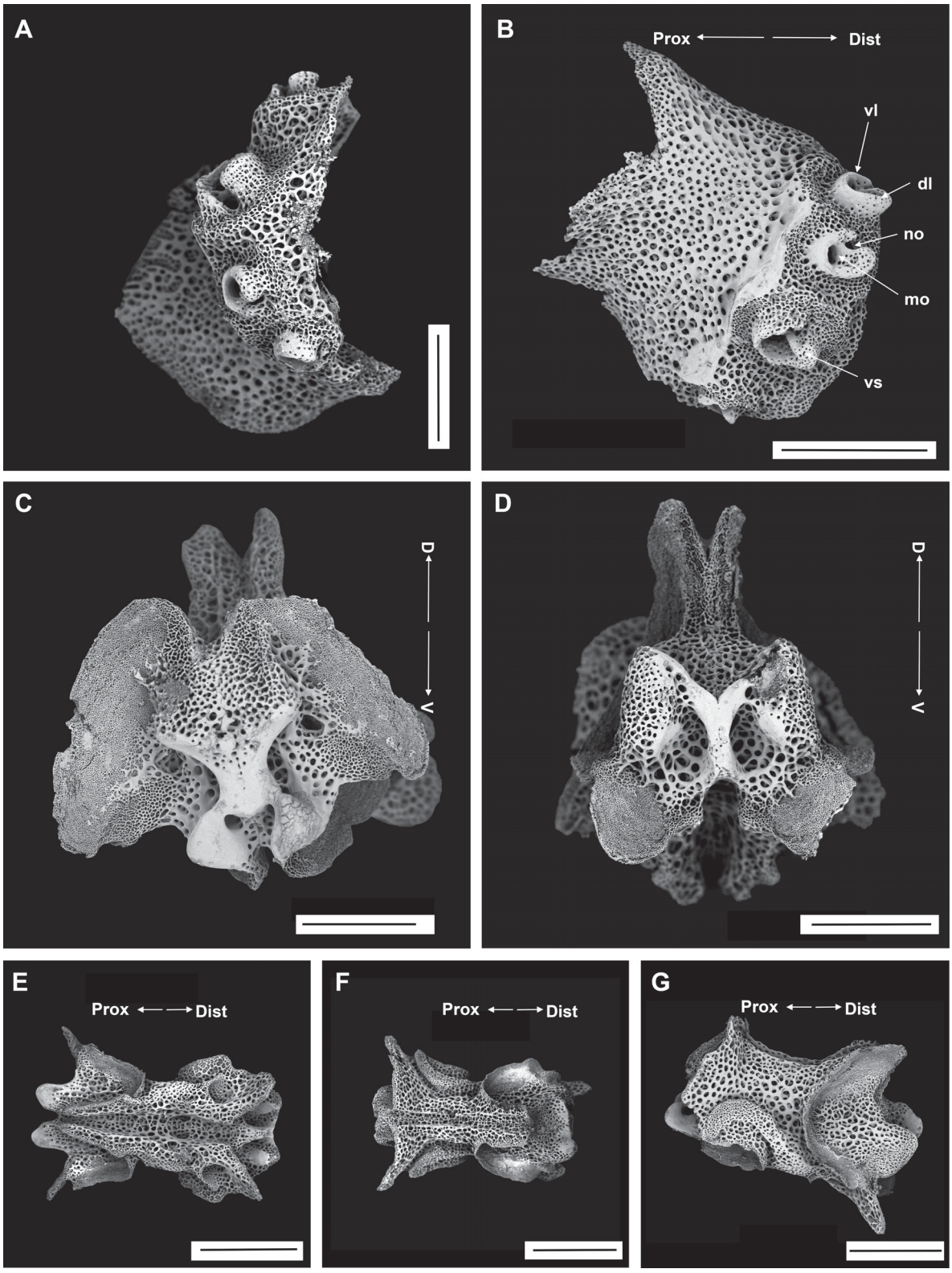

Fig. 26. *Ophioplinthaca plicata* (Lyman, 1878), SEM (IDSSE EEB-SW0019). **A–B**. Lateral arm plate. **C–G**. Vertebrae. **C**. Proximal view. **D**. Distal view. **E**. Ventral view. **F**. Dorsal view. **G**. Lateral view. Abbreviations: D = dorsal; Dist = distal; dl = dorsal lobe; mo = muscle opening; no = nerve opening; Prox = proximal; V = ventral; vl = ventral lobe; vs = volute-shaped. Scale bars: A, C–D = 300 μm; B, E–G = 500 μm.

114°21.25′ E; depth 3500 m; 6 Sep. 2017; collection event: stn SC016; MSV Shenhaiyongshi leg.; preserved in -80°C; IDSSE EEB-SW0044.

Description (IDSSE EEB-SW0025)

Measurements. Disc diameter 17.5 mm.

Disc. Flat, pentagonal, covered by thin skin, underlying scales with short disc spines (Fig. 27A–B), 0.3–0.4 mm high, rough, with two to three sharp terminal thorns, similar on both dorsal and ventral disc (Fig. 27C–E). Radial shields long, narrow, well separated, parallel to each other, concealed by thin skin, their form and position clearly visible through skin, with thorny stumps (Fig. 27A, E). Ventral disc near oral shields with scales without thorny stumps (Fig. 27B). Oral shield much wider than long, broadly triangular, with wide, pointed proximal angle and a straight or convex distal edge (Fig. 27F). Madreporite larger, with central depression, pentagonal. Adoral shields large, three times as long as wide, narrow, not separated (Fig. 27B, F). Adoral shields enclose proximal oral shield edges and extend around it, separating it from first lateral arm plate (Fig. 27C, F). Jaws wider than long, ventralmost tooth with large, blunt, pointed or flat edge, and three pointed, spiniform lateral oral papillae with thick and rounded base (Fig. 27F). Genital slits conspicuous and extending from oral shield to periphery of disc (Fig. 27I).

Arms. Dorsal arm plate on first few arm segments triangular, somewhat fan-shaped and distal margin more convex, but along arm becoming straighter, towards rhombic, somewhat swollen, two times as wide as long, barely separated (Fig. 27G). Ventral arm plate widely triangular, two times as wide as long, distal margin convex, proximally with low, wide angle, lateral side weakly concave and widely separated, but along arm ventral arm plate decreasing in size, as wide as long, with convex distal margin (Fig. 27H). Lateral arm plates meeting above and below, but along arm becoming separated ventrally (Fig. 27H). Six sharp and thorny arm spines (Fig. 27J). Three uppermost spines longest, two to three arm segments in length, one to two dorsal arm spines smooth but others thorny (Fig. 27K). Two to three tapering ventral arm spines with rough tip (Fig. 24L). One tentacle scale, elongated, half as long as ventral arm plate, pointed (Fig. 27I).

Color. When alive, entire specimen light red, light brown when dry (Fig. 27A–B).

Ossicle morphology. Arm spine articulation well developed and placed at small angle to distal edge of lateral arm plate (Fig. 28A–B). Volute-shaped perforated lobe forms most articulations, but reduced in dorsalmost articulation (Fig. 28A–B). Arm spine articulation with large muscle opening (Fig. 28B). Ventral arm spine smooth, but with rough tip (Fig. 28C). Vertebrae with a well-developed zygospondylous articulation, with a broad dorsal surface, distally abruptly truncated, with a shallow dorsal medial furrow, podial basins slightly wider than long (Fig. 28D–H). Ambulacral groove widened in middle, without oral bridge (Fig. 28G).

Remarks

Ophiacantha bathybia was described by H.L. Clark (1911); additional specimens have been collected in 1980, 1981 and 2015 (OBIS 2021). *Ophiacantha bathybia* from the present study is quite similar to the holotype description, but it differs in the arm spine and arm plate characters. Our specimens were larger than the holotype (12 mm disc diameter) and some of the morphological differences may be caused by this size difference. The lateral arm plates in the holotype description are connected at both the dorsal and ventral edges, but in our specimens they were only connected by a ligament. Another morphological variation was the number of thorny spines, which differs from segment to segment and arm to arm.

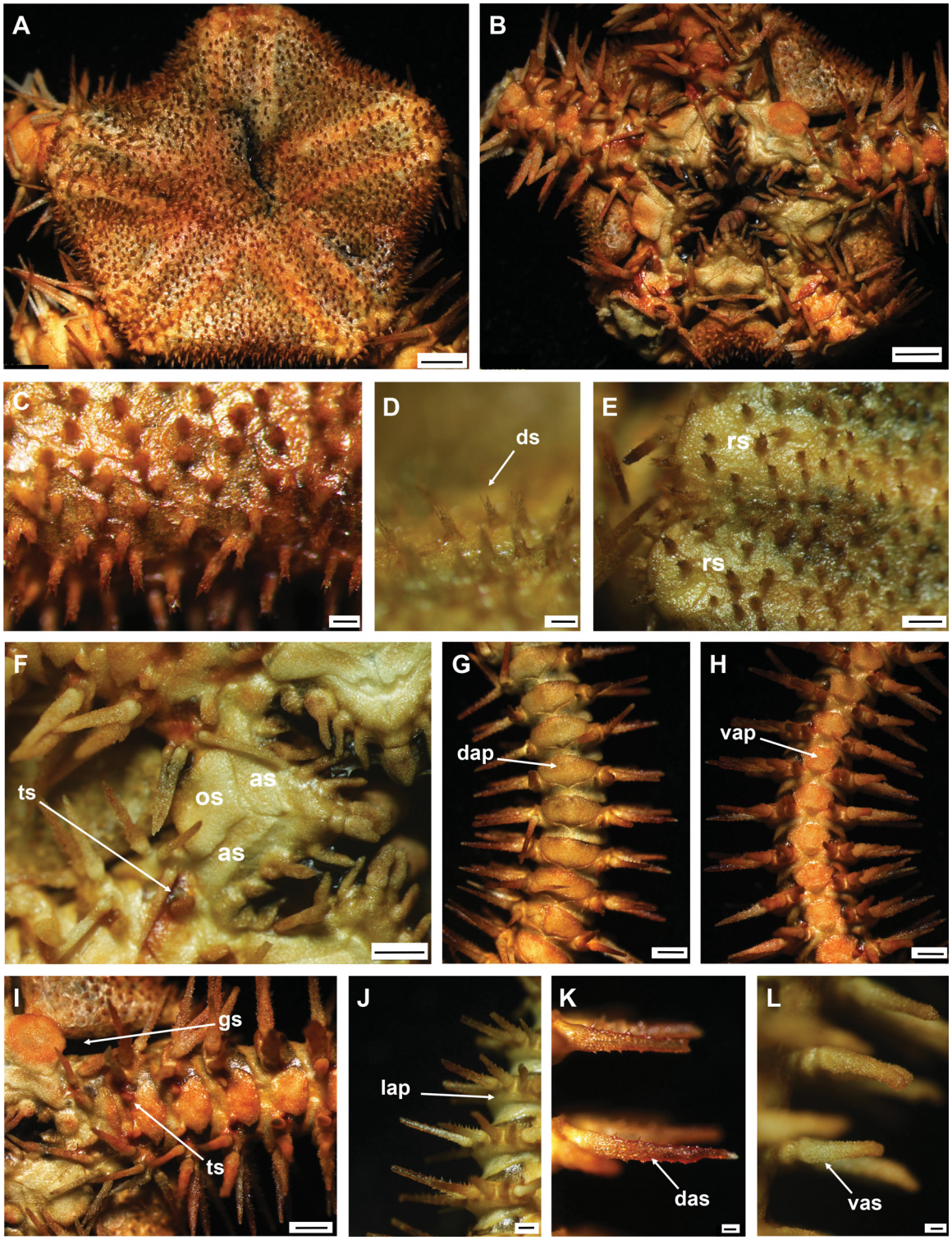

Fig. 27. *Ophiacantha bathybia* H.L. Clark, 1911 (IDSSE EEB-SW0025). **A**. Dorsal disc. **B**. Ventral disc. **C–E**. Different angles of disc spines on dorsal and ventral disc. **F**. Oral frame. **G**. Dorsal arm. **H**. Ventral arm. **I**. Ventral arm base. **J**. Arm spine structure in lateral plate. **K**. Dorsal arm spine. **L**. Ventralmost arm spine. Abbreviations: as = adoral shield; dap = dorsal arm plate; das = dorsal arm spine; ds = disc spine; gs = genital slit; lap = lateral arm plate; os = oral shield; rs = radial shield; ts = tentacle scale; vap = ventral arm plate; vas = ventral arm spine. Scale bars: A–B = 2 mm; C–F = 1 mm; G, L = 500 μm; H–K = 200 μm.

Ophiacantha bathybia has no uniquely distinguishing characters, but appears to be different from other species of *Ophiacantha* by the size of the disc and characters of the disc covering, dorsal arm plates, arm spines and tentacle scale. Mature specimens have narrow, long radial shields and thorny disc stumps, but differ in arm spine and dorsal arm plate shape.

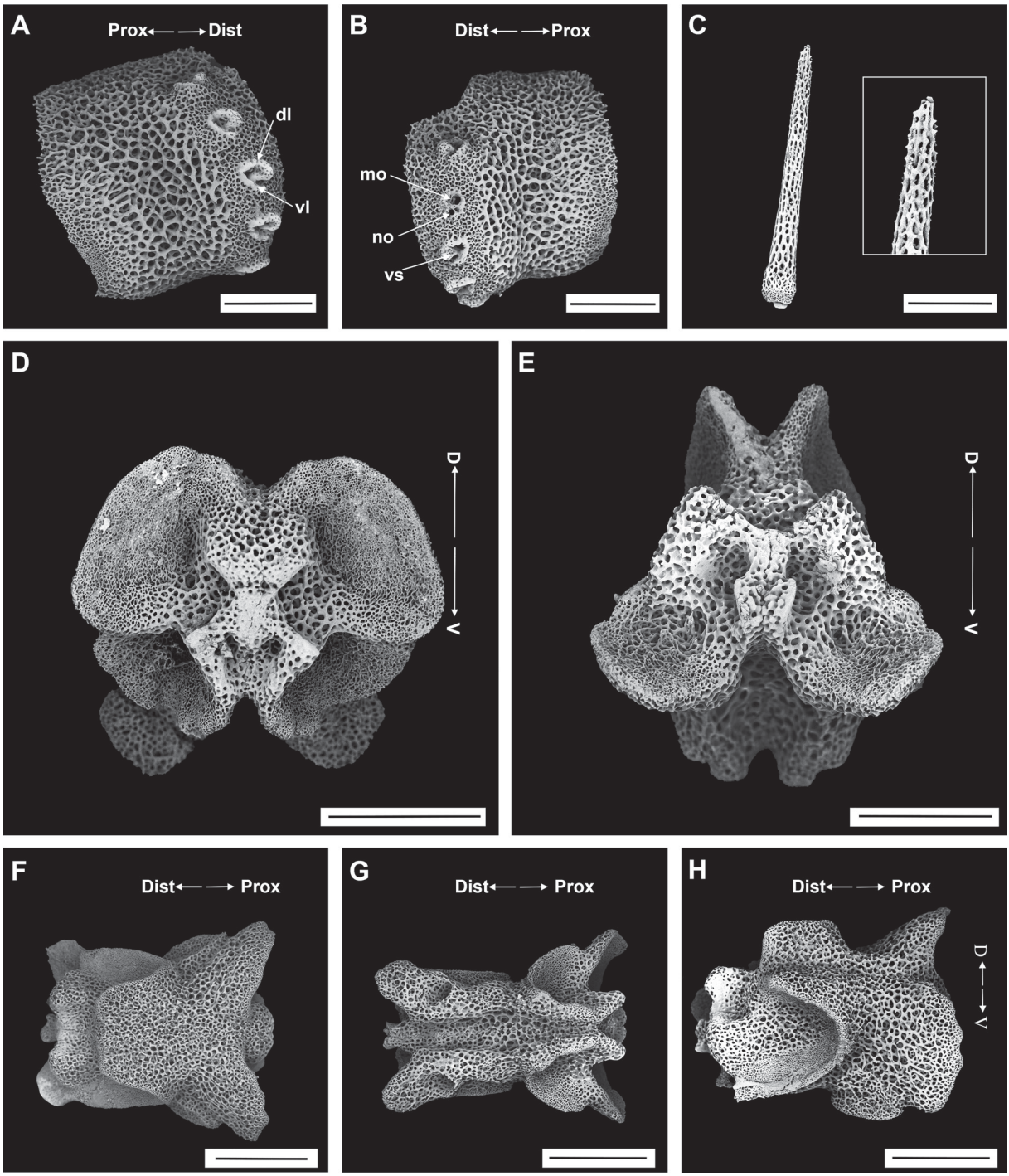

Fig. 28. *Ophiacantha bathybia* H.L. Clark, 1911, SEM (IDSSE EEB-SW0025). **A–B**. Lateral arm plate. **C**. Ventral arm spine. **D–H**. Vertebrae. **D**. Proximal view. **E**. Distal view. **F**. Dorsal view. **G**. Ventral view. **H**. Lateral view. Abbreviations: D = dorsal; Dist = distal; dl = dorsal lobe; mo = muscle opening; no = nerve opening; Prox = proximal; V = ventral; vl = ventral lobe; vs = volute-shaped. Scale bars: A–D, F–H = 500 µm; E = 300 µm.

It has been recorded from abyssal depths, and its morphological characters are similar to those of other abyssal species of *Ophiacantha*, namely *O. pacifica* Lütken & Mortensen, 1899, *O. sollicita* Koehler, 1922, *O. cosmica* Lyman, 1878, *O. frigida* Koehler, 1907 and *O. sociabilis* Koehler, 1897, but these species have been recorded from Panama, the Southern Ocean and the Atlantic Ocean. *Ophiacantha bathybia* may be considered as a sister species to these abyssal species of *Ophiacantha* based on their morphological features.

Ophiacantha cosmica differs from *O. bathybia* by having up to eight arm spines, slender lateral oral papillae without a thick base and a blunt ventralmost tooth (Lütken & Mortensen 1889; Stöhr & O'Hara 2021). *Ophiacantha sociabilis* differs from *O. bathybia* by having four to five lateral oral papillae, a less enlarged distalmost papilla and wider jaws (Koehler 1897; Stöhr & O'Hara 2021). *Ophiacantha sollicita* differs from *O. bathybia* by having up to eight arm spines, conical disc spines, a notably thickened distal oral papilla and non-moniliform arms (Koehler 1922b). *Ophiacantha frigida* differs from *O. bathybia* by having a larger distalmost lateral oral papilla and usually two tentacle scales on the first tentacle pore (Koehler 1922b). *Ophiacantha pacifica* is highly similar to *O. bathybia* in morphological features of the oral frame, as well as the number and length of arm spines, but the ventralmost arm spines of *O. bathybia* have a rough tip (Lütken & Mortensen 1889) (Fig. 28C). However, these morphological differences vary and overlap among individuals between species of the genus *Ophiacantha*. Therefore, a molecular analysis from a wider range of localities is needed to understand the species boundaries.

Distribution

1602–3656 m depth. South China Sea, Alaska, British Colombia, Bering Sea, Shumagin Island, Makassar Strait and Northwest Pacific (OBIS 2021).

Ophiacantha vorax Koehler, 1897
Figs 29–30

Ophiacantha vorax Koehler, 1897: 353–356, pl. 8 figs 68–69.
Ophiacantha anchilabra H.L. Clark, 1911: 204–206, fig. 95.

Ophiacantha vorax – Koehler 1899: 62, pl. 7 figs 52–54; 1922a: 63, pl. 15 figs 4–5. — Liao 2004: 122–123, fig. 59.
Ophiacantha anchilabra – H.L. Clark 1915: 196. — Matsumoto 1917: 117.

Material examined

CHINA • 1 spec.; South China Sea, SE of Hainan Island, seamount; 17°59.21′ N, 111°01.17′ E; depth 1500 m; 1 Apr. 2018; collection event: stn SC020; MSV Shenhaiyongshi leg.; preserved in -95°C ethanol; GenBank: MZ198765, MZ203267; IDSSE EEB-SW0011 • 1 spec.; South China Sea, SE of Hainan Island, sea plain; 18°26.13′ N, 111°49.09′ E; depth 1576 m; 26 Jun. 2019; collection event: stn SC001; MSV Shenhaiyongshi leg.; preserved in -80°C; GenBank: MZ198766, MZ203268; IDSSE EEB-SW0012 • 1 spec.; South China Sea, SE of Hainan Island, seamount; 17°17.60′ N, 110°34.18′ E; depth 1500 m; 2 Apr. 2018; collection event: stn SC021; MSV Shenhaiyongshi leg.; preserved in -80°C; IDSSE EEB-SW0045.

Description (IDSSE EEB-SW0011)

Mesurements. Disc diameter 6.2 mm.

Disc. Sub-pentagonal, covered by skin with underlying scales, bearing four to six short, stump-like spines with crown of sharp, straight thorns and a few elongated thick, thorny stumps in the center

(Fig. 29A–F). Radial shields long, narrow, widely separated, slightly convex, distal end thickened and exposed (Fig. 29A). Radial shields concealed by thin skin and thorny stumps, but clearly visible through skin when specimen dried (Fig. 29A). Dorsal arm plate on first arm segment covered by thorny stumps (Fig. 29D). Ventral disc also covered by thorny stumps, but less dense than on dorsal disc, scales clearly visible, genital slits short (Fig. 29F). Oral shield triangular, much wider than long, distal end slightly convex, proximal edges concave or straight (Fig. 29B), madreporite larger, as long as wide, distal edge strongly convex (Fig. 29G). Adoral shields narrow, curved, three times as long as wide and not separated, bordering proximal edges of oral shield, not separating it from arm (Fig. 29G). Jaws elongated, with one large pointed ventralmost tooth and three long, spiniform, pointed lateral oral papillae on each side, distalmost papilla wider than other two (Fig. 29G).

Arms. Dorsal arm plates triangular, distal edge convex, separated (Fig. 29I). Ventral arm plate on first arm segment small, wider than long, slightly triangular with concave distal edge. Second ventral arm plate pentagonal, wider than long, with obtuse proximal angle, excavated lateral edges and slightly convex distal edge. Following plates as wide as long, distalwards becoming wider than long, slightly hexagonal, with curved distal edge and angular proximal edges, separated except on second arm segment (Fig. 29H, J). Lateral arm plates meeting above and below. Six smooth arm spines, three dorsal and three ventral. Dorsalmost arm spine one and a half to two arm segments in length, second dorsalmost arm spine longest and meeting across dorsal midline (Fig. 29I–J). Ventral arm spines similar in length, with finely thorny surface (Fig. 29K). One elongated tentacle scale, large, often as long as ventral arm plate (Fig. 29H).

Color. When alive, entire specimen light brown, darker brown when dry (Fig. 29).

Ossicle morphology. Arm spine articulations well-developed, placed at an angle on separate, protruding distal part of lateral plate, bordered by a wavy ridge, middle articulations largest (Fig. 30A–B). Arm spine with thorny surface (Fig. 30C). Volute-shaped perforated lobe in most articulations, reduced in dorsalmost articulation, with large muscle opening and small nerve opening (Fig. 30A–B). Vertebrae with short, well-developed zygospondylous articulation with a broad, shallow dorsal furrow, distally abruptly truncated, podial basins wider than long (Fig. 30D–H). Ambulacral groove widely diverging distally, without oral bridge (Fig. 30H).

Remarks

The holotype description of the dorsal disc of *Ophiacantha vorax* (5 mm disc diameter) is slightly different from conditions in our specimen, which has no elongated disc stumps. However, this morphological feature was only found here on one of the 3 specimens collected. Variability in morphological characters (arm spines, extent of thorny stumps on radial shields, tentacle scale) is low in *O. vorax* (Koehler 1922a). Koehler (1897) considered one of the distinguishing features of *O. vorax* to be the presence of only six arm spines, but H.L. Clark (1911) and Liao (2004) documented eight to nine arm spines in their specimens. Therefore, the number of arm spines is not a suitable character to distinguish *O. vorax* from other species of *Ophiacantha*.

Ophiacantha pentagona Koehler, 1897 is related to *O. vorax*, but differs in having long and thicker oral papillae, strongly moniliform arms and longer ventral arm plates in the middle region of the arm. *Ophiacantha vorax* closely resembles *O. longidens* Lyman, 1878 in the shape of the oral papillae and oral shields, as well as in the disc shape, but differs in the arrangement of arm spines, and the shape of the arm plates and tentacle scales. *Ophiacantha longidens* has flattened arm spines, blunt with a thorny surface. Another species resembling *O. vorax* is *O. duplex* Koehler, 1897, recorded from deep waters

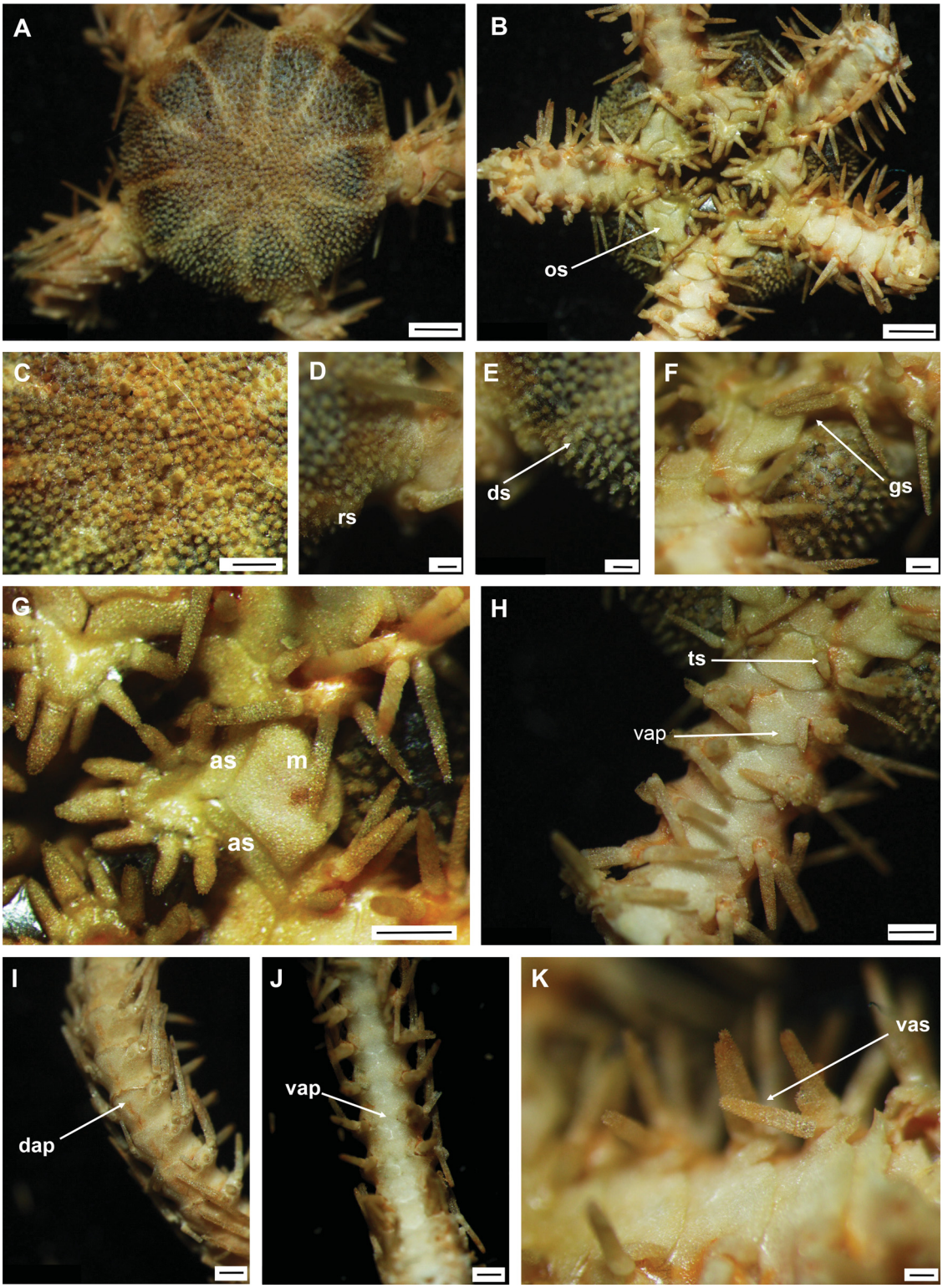

Fig. 29. *Ophiacantha vorax* Koehler, 1897 (IDSSE EEB-SW0011). **A**. Dorsal disc. **B**. Ventral disc. **C**. Center of disc with tall disc stump. **D**. Distal area of the radial shield. **E**. Thorny stumps. **F**. Lateral disc. **G**. Oral frame. **H**. Ventral arm base. **I**. Dorsal arm. **J**. Ventral arm. **K**. Ventralmost arm spine. Abbreviations: as = adoral shield; dap = dorsal arm plate; ds = disc spine; gs = genital slit; m = madreporite; os = oral shield; rs = radial shield; ts = tentacle scale; vap = ventral arm plate; vas = ventral arm spine. Scale bars: A–B = 1 mm; C, F–J = 500 μm; D–E, K = 200 μm.

in Japan, Philippines, Indonesia, Australia and Madagascar. It can clearly be distinguished by its large tentacle scale, less thorny, long, thin arm spines, large dorsal arm plate and the presence of large disc spines, as well as the smaller thorned spines.

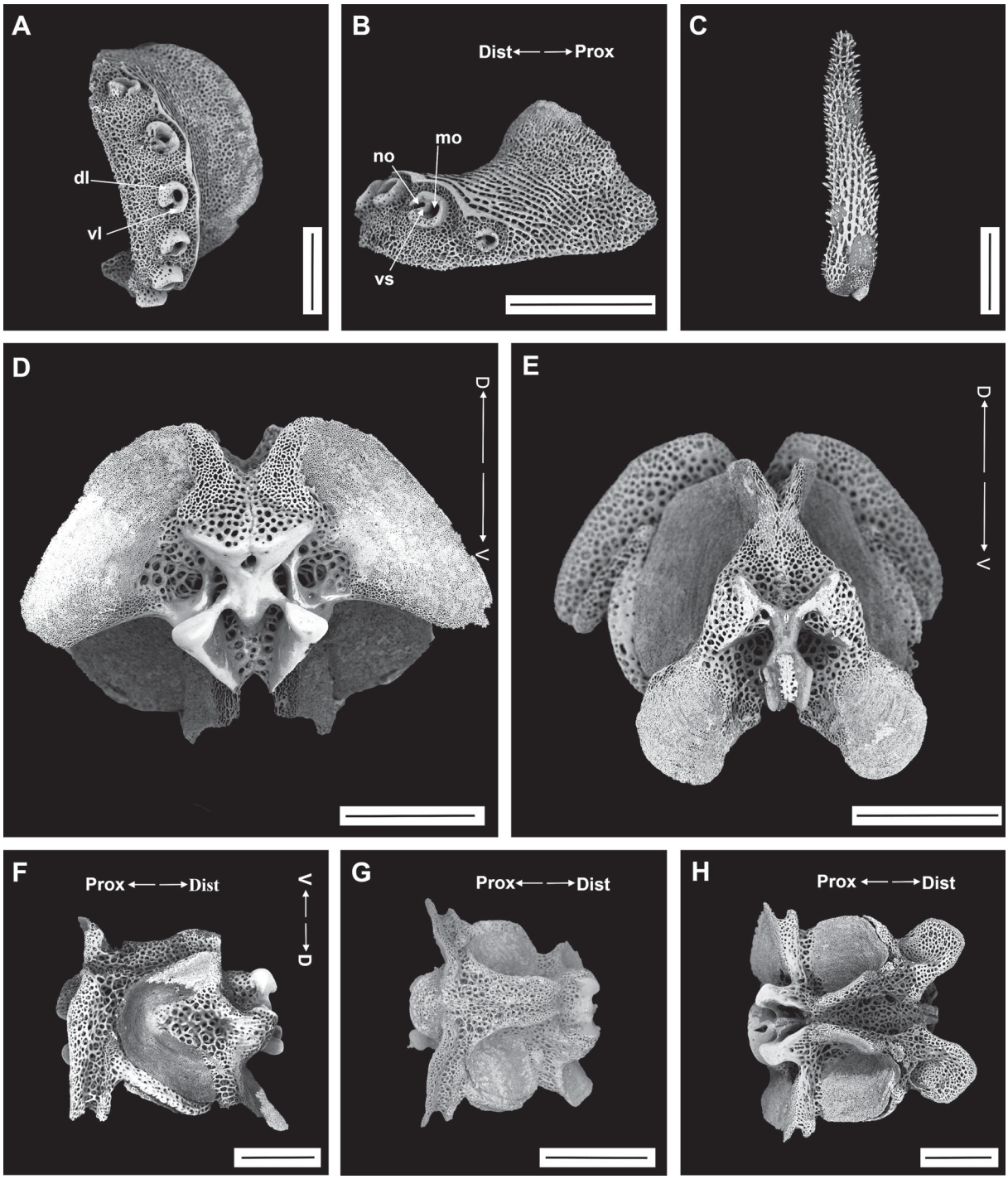

Fig. 30. *Ophiacantha vorax* Koehler, 1897, SEM (IDSSE EEB-SW0011). **A–B**. Lateral arm plate. **C**. Ventral arm spine. **D–H**. Vertebrae. **D**. Proximal view. **E**. Distal view. **F**. Lateral view. **G**. Dorsal view. **H**. Ventral view. Abbreviations: D = dorsal; Dist = distal; dl = dorsal lobe; mo = muscle opening; no = nerve opening; Prox = proximal; V = ventral; vl = ventral lobe; vs = volute-shaped. Scale bars: A, C–F, H = 300 µm; B, G = 500 µm.

Distribution

550–1908 m depth. South China Sea, East China Sea, off East Japan, India, Philippines, Indonesia, Makassar Strait and Molucca Sea, Coral Sea and New Zealand (OBIS 2021).

Ophiacantha aster sp. nov.
urn:lsid:zoobank.org:act:6AB8A891-700D-4BF2-8873-5CD18178795E
Figs 31–33

Diagnosis

Disc slightly pentagonal, interradially excavated and covered by conical pointed granules with wide, round base. Single small, broad, triangular, pointed tentacle scale. Adoral shields larger than oral shield. Jaw with one large, blunt, wide ventralmost tooth and four to five lateral oral papillae. Top of radial shields and center of disc creamy white, dark brown lines radiate from disc center to arms.

Etymology

The specific name is derived from the Greek word for 'star', alluding to the shape and color of the dorsal disc.

Material examined

Holotype

CHINA • South China Sea, SE of Zhongsha Islands, seamount; 13°59.70′ N, 115°24.81′ E; depth 516 m; 20 Sep. 2020; collection event: stn SC011; MSV Shenhaiyongshi leg.; preserved in 95% ethanol; GenBank: MZ203275; IDSSE EEB-SW0026.

Paratypes

CHINA • 1 spec.; same collection data as for holotype; GenBank: MZ203276; IDSSE EEB-SW0027 • 12 specs; same collection data as for holotype; IDSSE EEB-SW0046 to EEB-SW0057.

Description (holotype)

Measurements. Disc diameter 8.5 mm.

Disc. Disc slightly pentagonal, interradially excavated, covered by oval disc scales, each bearing a conical pointed granule with wide, round base (Fig. 31A–B). At disc periphery and lateral disc, granules lower and less pointed, near oral shields no granules on scales (Fig. 31C–F). In disc center, granules spine-like (Fig. 31C). Ventral disc reduced to oral frame (Fig. 31B). Radial shields long, narrow, parallel to each other, but well separated, distal ends exposed (Fig. 31A, E). Genital slits conspicuous, short, extending from oral shield to periphery of disc (Fig. 31E). Oral shield broadly triangular, with acute proximal angle, with straight, convex or wavy distal edge. Adoral shields larger than oral shield, trapezoid extending along concave proximal edges of oral shield, not separating it from arm (Fig. 31F). Jaw with one large, blunt, wide ventralmost tooth, four to five lateral oral papillae, first three elongated, spiniform, first possibly infradental papilla, distal two papillae larger, distalmost one scale-like (possibly adoral shield spine) (Fig. 31F). Dorsal teeth square, with straight proximal edge (Fig. 31F).

Arms. Moniliform. Dorsal arm plates fan-shaped, distal edge convex, acute proximal angle, straight to slightly concave proximolateral edges, completely separated (Fig. 31G). Ventral arm plates pentagonal to broadly rectangular, wider than long, concave lateral edges around tentacle pore, distal edge straight with small inward curve, separated (Fig. 31H). Lateral arm plates with a high spine-bearing ridge, meeting dorsally and ventrally (Fig. 31I–K). Eight transparent, rounded arm spines, more or less thorny (Fig. 31J–K). Four dorsalmost spines longest, with rough surface, as long as three arm segments, meeting

at dorsal midline, length gradually decreasing ventralwards. Ventral arm spines tapering, rougher than dorsal arm spines, one to two arm segments in length (Fig. 31I–K). Tentacle pore on proximalmost and

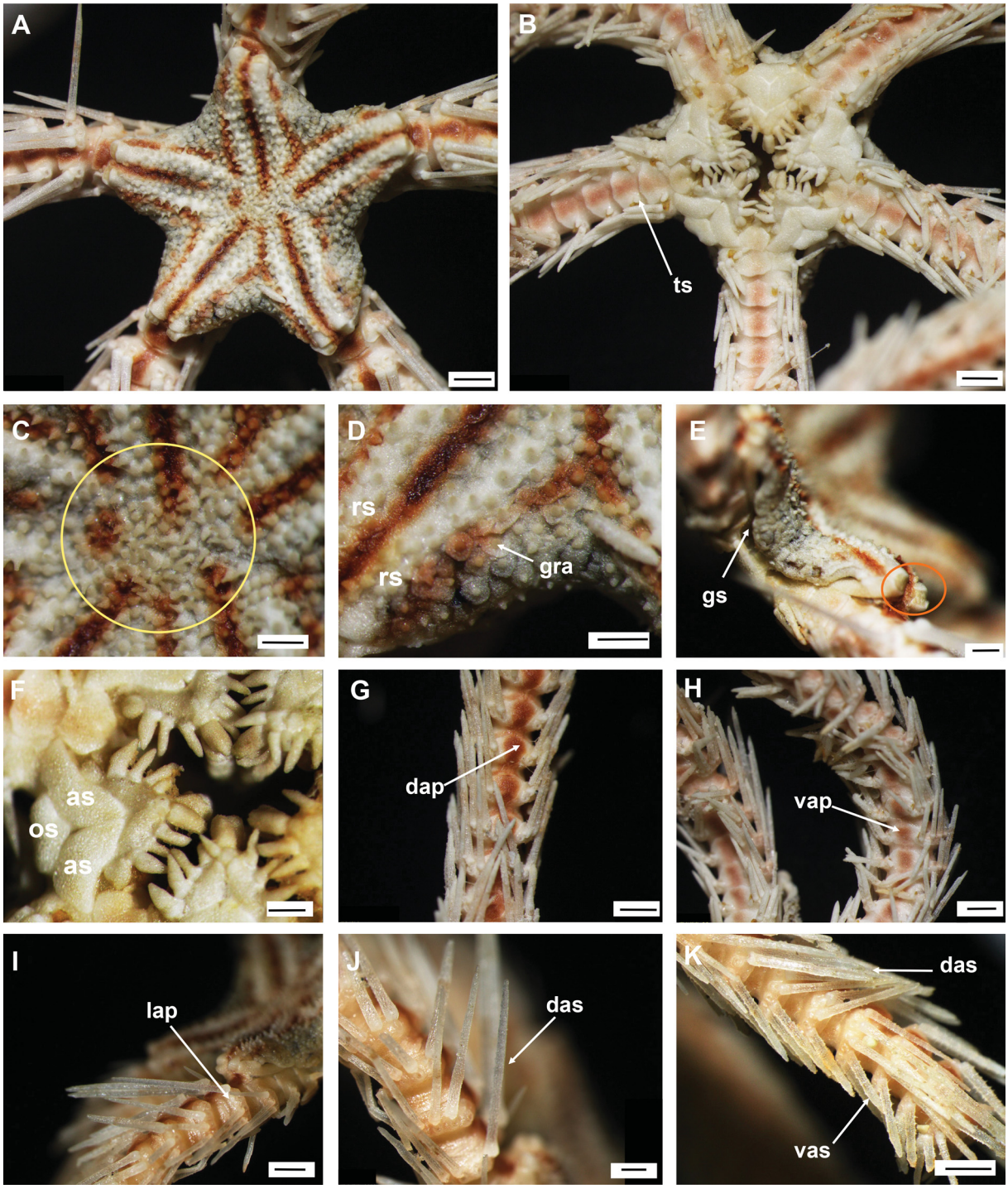

Fig. 31. *Ophiacantha aster* sp. nov., holotype (IDSSE EEB-SW0026). **A**. Dorsal disc. **B**. Ventral disc. **C**. Center of disc (elongated conical granules highlighted). **D**. Distal edges of radial shield. **E**. Lateral disc. **F**. Oral frame. **G**. Dorsal arm. **H**. Ventral arm. **I–K**. Lateral arm. Abbreviations: as = adoral shield; dap = dorsal arm plate; das = dorsal arm spine; gra = granule; gs = genital slit; lap = lateral arm plate; os = oral shield; rs = radial shield; ts = tentacle scale; vap = ventral arm plate; vas = ventral arm spine. Scale bars: A–B, G–K = 1 mm; C–F = 500 µm.

second arm segments half to two-thirds arm segment in length (Fig. 31B). One to three arm segments covered by disc and only possessing ventral arm spines (Fig. 31I). Arm spines on fourth to sixth arm segments longer than those on middle or dorsal arm segments (Fig. 31I–J). Arm spines on first six arm

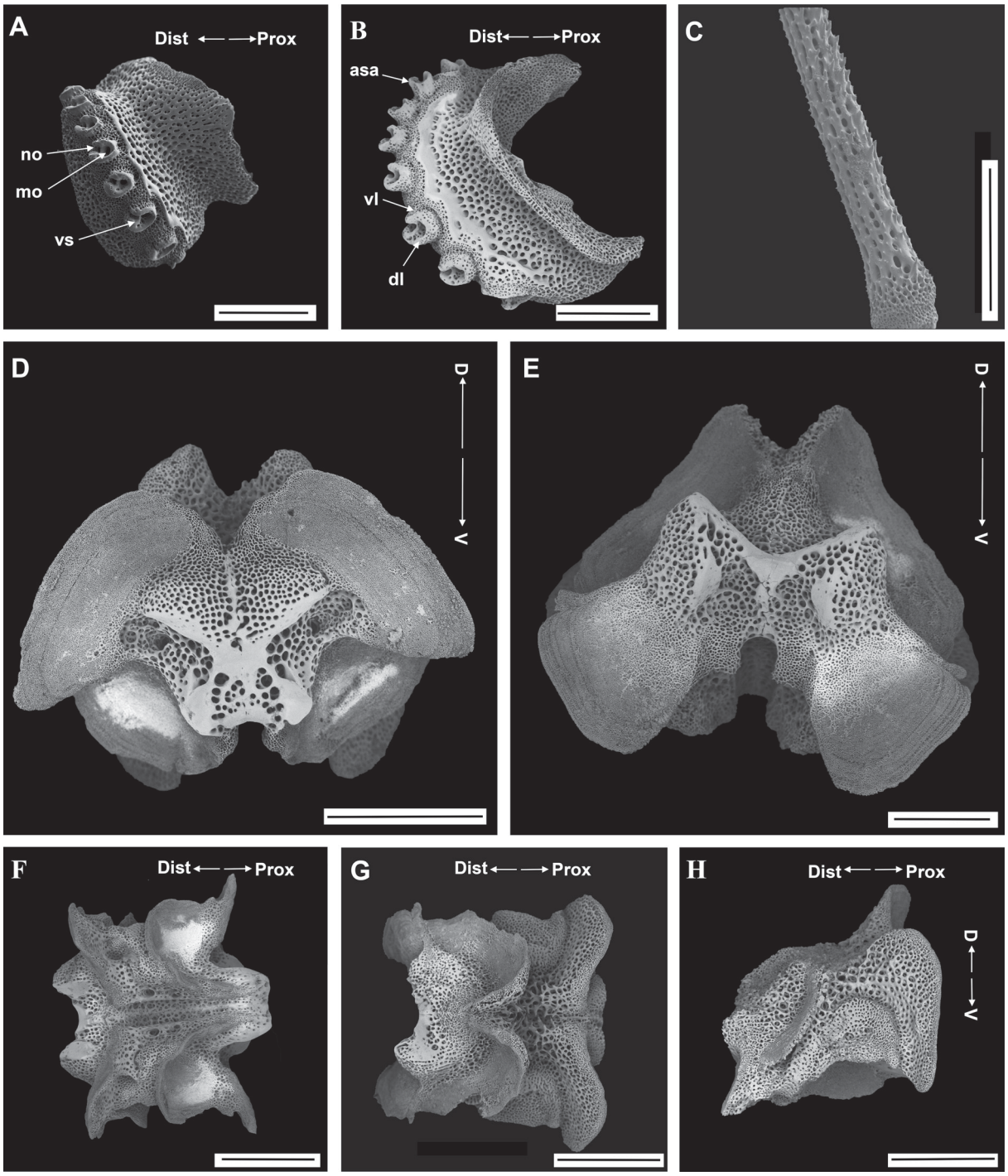

Fig. 32. *Ophiacantha aster* sp. nov., SEM, paratype (IDSSE EEB-SW0027). **A–B**. Lateral arm plate. **C**. Base of dorsal arm spine. **D–H**. Vertebrae. **D**. Proximal view. **E**. Distal view. **F**. Ventral view. **G**. Dorsal view. **H**. Lateral view (broken distal end). Abbreviations: asa = arm spine articulation; D = dorsal; Dist = distal; dl = dorsal lobe; mo = muscle opening; no = nerve opening; Prox = proximal; V = ventral; vl = ventral lobe; vs = volute-shaped. Scale bars: A–D, F–H = 500 μm; E = 300 μm.

segments tapered, smooth, but distal to sixth segment spines rough or thorny (Fig. 31K). One small, broad, triangular, pointed tentacle scale, one third as long as ventral arm plate (Fig. 31B).

Color. Top of radial shields and center of disc creamy white, but dark brown lines radiate from disc center to arms, outside radial shields, a third line between each pair of radial shields continues along center of each arm. Similar longitudinal, lighter brown line on ventral arms (Fig. 31).

Ossicle morphology. Proximal lateral arm plate short, strongly curved and arm spine articulations well developed, with large muscle opening and small nerve opening (Fig. 32A). Spine articulations volute-shaped perforated lobe (Fig. 32A–B). Arm spines with sparse thorns (Fig. 32C). Vertebrae

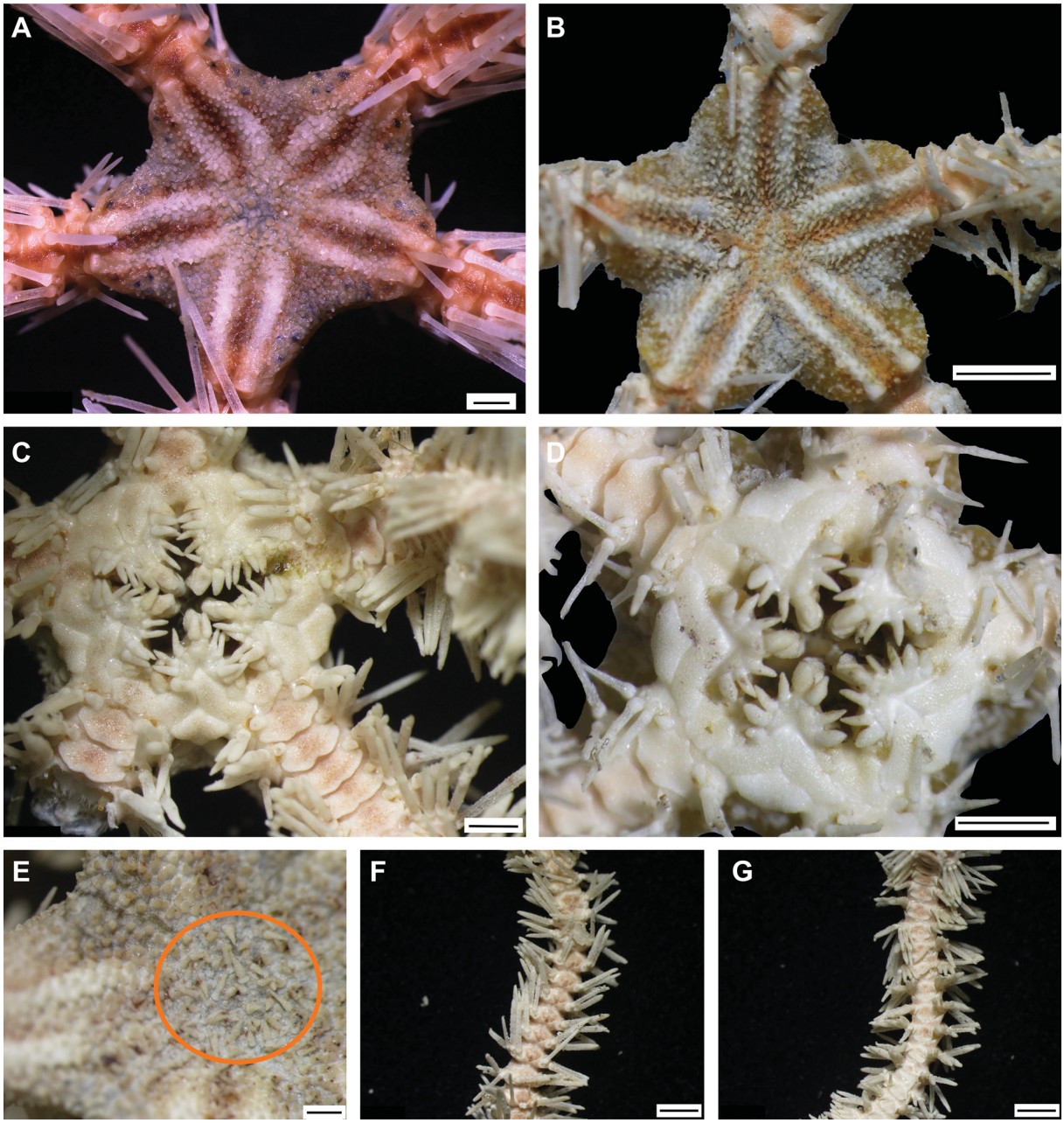

Fig. 33. *Ophiacantha aster* sp. nov., paratypes. **A–B**. Dorsal disc. **C–D**. Ventral disc. **E**. Center of disc (elongated conical granules highlighted). **F**. Dorsal arm. **G**. Ventral arm. Scale bars A, C = 1 mm; B, D, F–G = 2 mm; E = 500 µm.

with a short streptospondylous articulation, as wide as long, proximal end with podial basins. Dorsal end of vertebrae distally triangular, proximally slightly curved inwards, with shallow dorsal furrow (Fig. 32D–H). Ambulacral groove without oral bridge (Fig. 32F–G).

Variations in paratypes

Paratypes generally similar to holotype, disc diameters 3.9–9.0 mm, but some morphological variations were observed. Only dorsal arm spines tapered or thorny in some specimens (Fig. 33). One paratype had black dots scattered near periphery of disc (Fig. 33A). Disc color of some paratypes slightly lighter than in holotype and interradials not as strongly excavated as in holotype, radial shields more widely separated (Fig. 33B). Smallest paratype with 3.9 mm disc diameter and similar to holotype, except fifth arm segments with thorny spines. Lateral oral papillae four to six, distalmost one varies from scale-like, flat to narrower and pointed, ventralmost tooth much larger than oral papillae (Fig. 33C–D). Disc granules varied in shape; some specimens with taller spines in disc center (Fig. 33E).

Remarks

The arm spine articulation is here interpreted as a variation of the zygospondylous type, not uncommon in the family Ophiacanthidae, typical of epizoic species. The deeply interradially excavated disc is a character used by Paterson (1985) to distinguish the no longer valid subfamily Ophioplinthacinae Paterson, 1985 (Martynov 2010), but the narrow, long radial shields and the oral frame fit with the genus *Ophiacantha*. *Ophiacantha aster* sp. nov. differs from most species of the genus by having deep incisions in the disc along with five (more or less) lateral oral papillae. *Ophiacantha antarctica* Koehler, 1900 resembles *O. aster* sp. nov. by having long narrow radial shields with a more or less excavated interradial disc, four elongated lateral oral papillae and tapering long uppermost arm spines, but it differs in having a thickened integument that covers the disc scales, conical granules on the scales with two to five fine spinules, and near the periphery of the disc the granules are less elongated and more cylindrical. *Ophiacantha antarctica* has seven arm spines with a thin pointed tip (Koehler 1900), frequently has disc spines on the dorsal arm plates and transversely split dorsal arm plates dividing them into a small proximal and larger distal section (observation from anonymous reviewer).

Another species that resembles *Ophiacantha aster* sp. nov. is *O. veterna* Koehler, 1907, known from the Atlantic Ocean (2200 m), which has similar morphological characteristics in its disc shape, oral shield, adoral shield, oral papillae and arm spines, but differs mainly in having dense small granules on both ventral and dorsal disc and in the shape of the ventral arm plate along the arm (Koehler 1907a). The new species is unusually colorful among deep-water species.

Distribution and habitat

Found on a seamount near the Zhongsha Islands, South China Sea (516 m) as a colony attached to a dead coral branch. The vertebrae of *Ophiacantha aster* sp. nov. are almost streptospondylous and suggest an epizoic life-style, typical of suspension feeders.

Genus *Ophiomoeris* Koehler, 1904

Ophiomoeris petalis sp. nov.
urn:lsid:zoobank.org:act:656A30A3-A81A-4A87-9C19-4007F194788A
Figs 34–35

Diagnosis

Disc with deep interradial incisions with seven lobes and ring of irregular scales bearing a few granules around centrodorsal plate and overlapping with radial shields. Seven thin arms curled under disc.

Etymology

The specific name is derived from the Latin word for flower petals, alluding to the shape of the disc.

Material examined

Holotype

CHINA • South China Sea, SE of Zhongsha Islands, seamount; 13°58.65′ N, 114°52.09′ E; depth 1550 m; 25 Sep. 2020; collection event: stn SC013; MSV Shenhaiyongshi leg.; preserved in 95% ethanol; GenBank: MZ203278; IDSSE EEB-SW0029.

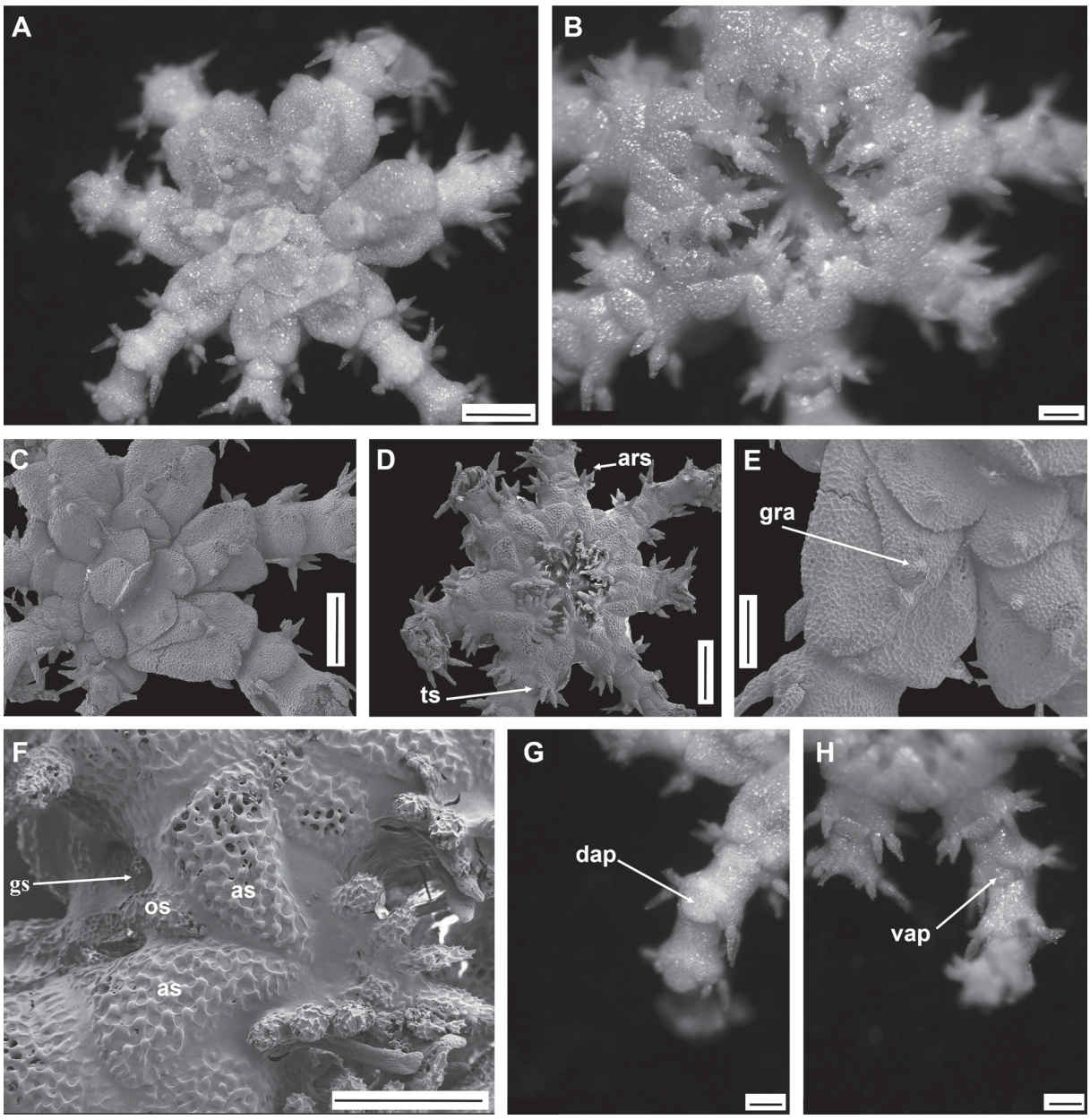

Fig. 34. *Ophiomoeris petalis* sp. nov., holotype (IDSSE EEB-SW0029). **A**. Dorsal disc. **B**. Ventral disc. **C**. Dorsal disc (SEM). **D**. Ventral disc (SEM). **E**. Dorsal disc lobe (SEM). **F**. Oral frame (SEM). **G**. Dorsal arm. **H**. Ventral arm. Abbreviations: ars = arm spine; as = adoral shield; dap = dorsal arm plate; gra = granula; gs = genital slit; os = oral shield; ts = tentacle scale; vap = ventral arm plate. Scale bars: A, C = 500 µm; B, G–H = 200 µm; D = 1 mm; E = 250 µm; F = 300 µm.

Paratypes

CHINA • 5 specs; same collection data as for holotype; IDSSE EEB-SW0058 to EEB-SW0062.

Description (holotype)

Measurements. Disc diameter 2.2 mm, heptamerous specimen.

Disc. Disc heptamerous with deep interradial incisions and a lobe above each arm, four large lobes, three smallest lobes and one intermediate lobe (signs of regeneration after fission). Arms differ in width in groups of 3, 3, 1 arms. Lobes formed by large drop-shaped radial shields, largest one a third of disc diameter in length and two to three times as long as wide (Fig. 34A–C). Radial shields distally connected, separated proximally by large triangular scales, covered by small conical granules (Fig. 34E). Center of disc sunken and covered by large, round centrodorsal plate without granules (Fig. 34A, C). Ring of irregular plates bearing a few conical granules around centrodorsal plate and overlapping with radial shields (Fig. 34A, C). Genital slits small, half as long as interradial ventral disc (Fig. 34F). Oral shields swollen, much smaller than adoral shields, as wide as long, fan-shaped with pointed proximal angle, slightly concave lateral edges and convex distal edge; size varies among radials (Fig. 34B, D, F). Adoral shields swollen, twice as wide as long, with angled, concave proximal edges of oral shield, not separating it from arm (Fig. 34F). Jaw as wide as long bearing one pointed ventralmost tooth and three spiniform lateral oral papillae, proximalmost one spine-like, other two shorter and rounded (Fig. 34F). All teeth spiniform like ventralmost tooth (Fig. 35B, D, F).

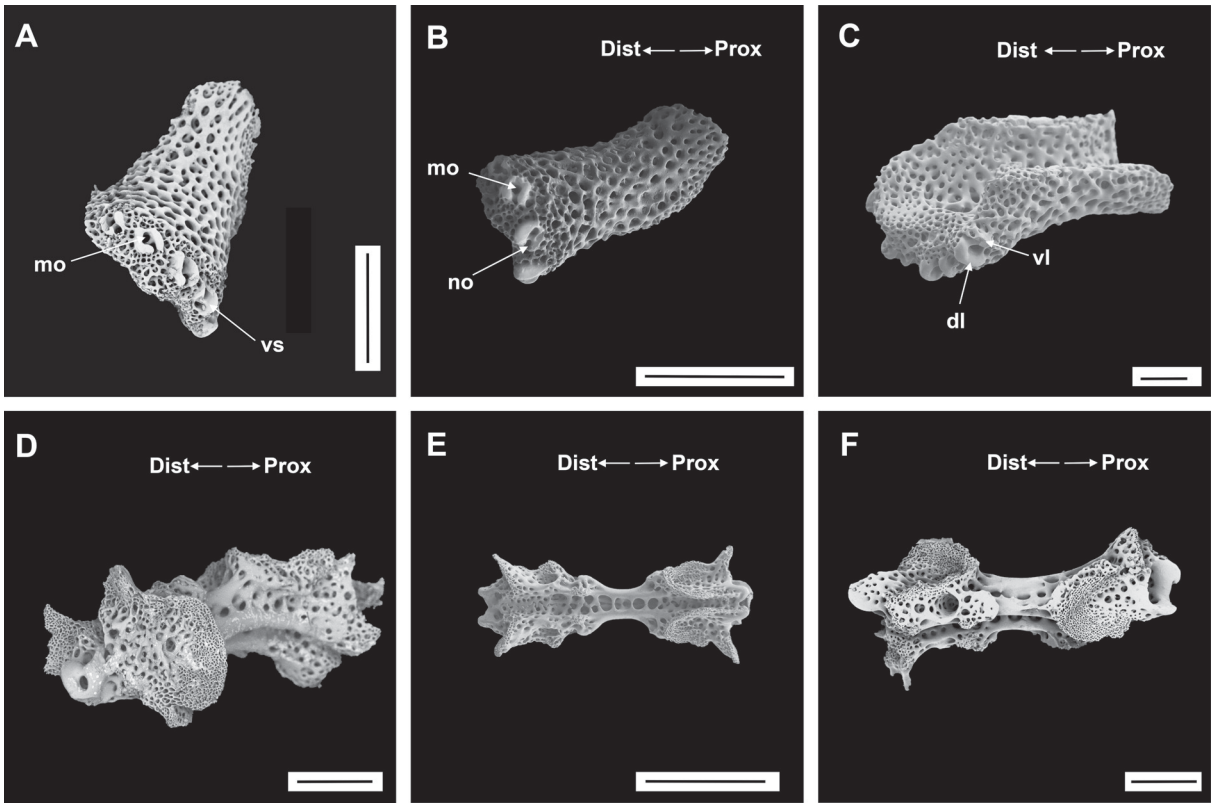

Fig. 35. *Ophiomoeris petalis* sp. nov., SEM, paratype (IDSSE EEB-SW0031). **A–C**. Lateral arm plate. **D–F**. Vertebrae. **D**. Dorsolateral view. **E**. Ventral view. **F**. Lateral view. Abbreviations: Dist = distal; dl = dorsal lobe; mo = muscle opening; no = nerve opening; Prox = proximal; vl = ventral lobe; vs = volute-shaped. Scale bars: A–B, E = 200 µm; C–D, F = 100 µm.

Arms. Seven thin arms, curled under disc. Dorsal arm plates fan-shaped, two times as wide as long, with convex distal edge and always separated (Fig. 34G). Ventral arm plate much wider than long on proximal segments, but reduced to small, round, thin scales, embedded in a strand of thick skin running along entire arm distally, always present along arm and always separated (Fig. 34H). Four thick, conical, smooth arm spines, two thirds arm segment in length (Fig. 34D, H). One minute tentacle scale clearly visible on proximal arm segments (Fig. 34D).

Color. In alcohol, entire specimen creamy white.

Ossicle morphology. Arm spine articulation formed by two thick, smooth, curved lobes, ventral lobe smaller than dorsal lobe, positioned at angle to distal edge of lateral plate, with large muscle opening and small nerve opening, the latter large in dorsalmost articulation. Volute-shape not well defined, absent in dorsalmost articulation, dorsal and ventral articular lobes connected but separating in ventral articulations (Fig. 35A–C). Vertebrae elongated, with streptospondylous articulation, dorsal and lateral furrows absent, middle section much lower than proximal part and distal muscle flanges, with straight ambulacral groove. Podial basins at distal end, tongue-like with round hole (Fig. 35D–F).

Variations in paratypes

Five heptamerous paratypes, with disc diameter ranging from 1.45 mm to 1.87 mm. All with similar morphological features as holotype, having conical granules on disc plates/scales and large, drop-shaped radial shields. Most paratypes with arms curled under disc.

Remarks

The oral frame arrangement and the lobe-like shape of the disc concur with the genus *Ophiomoeris*, which was recently transferred to Ophiacanthidae (O'Hara *et al.* 2018). The arm spine articulation of this genus is interpreted as a variation of the volute-shape typical of the family Ophiacanthidae. Previously only four species of *Ophiomoeris* were recognized and all of them are pentamerous: *O. obstricta* (Lyman, 1878), *O. exuta* Stöhr, 2011, *O. nodosa* (Koehler, 1905) and *O. tenera* (Koehler, 1897). The seven-fold symmetry is consistent in all our specimens. This is the first record of a seven-armed (or indeed non-pentamerous) species in the genus *Ophiomoeris*, and this distinguishes it from all congeners. The size differences among the seven sections of the animals suggests that it is a fissiparous species. Morphological characters to differentiate species in the genus *Ophiomoeris* are otherwise difficult to interpret due to their high morphological variation among individuals. Taking geographic distribution into account, there may be several cryptic species complexes in the genus *Ophiomoeris* that can only be resolved by a molecular study (O'Hara & Stöhr 2006; Stöhr 2011).

Distribution and habitat

South China Sea (1550 m), found on a deep-sea seamount near the Zhongsha Islands.

Order Amphilephidida O'Hara, Hugall, Thuy, Stöhr & Martynov, 2017
Suborder Gnathophiurina Matsumoto, 1915
Superfamily Ophiactoidea Ljungman, 1867
Family Ophiactidae Matsumoto, 1915
Genus *Ophiactis* Lütken, 1856

Ophiactis cf. ***perplexa*** Koehler, 1897
Figs 36–37

Ophiactis perplexa Koehler, 1897: 327–328, pl. 7 figs 40–41.

Material examined

CHINA • 1 spec.; South China Sea, SE of Zhongsha Islands, seamount; 13°23.97′ N, 114°51.15′ E; depth 1618 m; 22 Sep. 2020; collection event: stn SC012; MSV Shenhaiyongshi leg.; preserved in 95% ethanol; GenBank: MZ198767; IDSSE EEB-SW0013 • 1 spec.; same collection data as for preceding; GenBank: MZ198768; IDSSE EEB-SW0014 • 1 spec.; same collection data as for preceding; IDSSE EEB-SW0063.

Description (IDSSE EEB-SW0013)

Measurements. Disc diameter 7.2 mm.

Disc. Sub-pentagonal or circular, pentamerous. Dorsal disc covered by large, coarse, irregular, polygonal overlapping scales, increasing in size arranged as a rosette in disc center (Fig. 36A–B). Radial shields longer than wide, completely separated mostly by a single series of two scales but sometimes three scales (Fig. 36A). Radial shield length less than half disc radius, distal edge with two smooth and pointed spines (one on each radial shield) (Fig. 36C). Ventral disc covered by small, irregular, overlapping scales (Fig. 36D–E). Oral shield lozenge-shaped with widely angular proximal end, wider than long (Fig. 36F). Adoral shields as large as oral shield, curved around lateral edges of oral shield, three times as long as wide (Fig. 36F). Wide tricuspid teeth. Single large, broad (wider than teeth), operculiform lateral oral papilla at proximal edge of adoral shield (probably adoral shield spine), covering second tentacle pore inside mouth angle (Fig. 36F). Genital slits conspicuous and extending from oral shield to disc periphery (Fig. 36G).

Arms. Dorsal arm plates large, triangular, with straight distal edge, truncated proximal edge, twice as wide as long and contiguous (Fig. 36H). Ventral arm plates pentagonal, wider than long, completely separated (Fig. 36I). Lateral arm plate bears three arm spines with thick base, rounded, blunt tip, 1–1½ arm segment in length and middle one longest (Fig. 36J). Ventralmost spine thicker than others for first few arm segments. One large, broad, rounded tentacle scale, two thirds as long as ventral arm plate (Fig. 36I–J).

Color. Dorsal disc white with a few brown patches on scales. Disc periphery and distal part of radial shields light brown. Arms and ventral disc also light brown, but arm spines dark brown (Fig. 36A–B).

Ossicle morphology. Lateral arm plate with three well developed arm spine articulations, consisting of two unequal, subparallel, curved lobes (not volute-shaped). Arm spine articulation with two similar openings for muscle and nerve, but in some articulations nerve opening slightly larger than muscle opening (Fig. 37A–C). Vertebrae with well-developed zygospondylous articulation, narrow, shallow dorsal furrow, truncated far from distal articulation (Fig. 37D–H). Ambulacral groove deep, with hole in middle, without oral bridge (Fig. 37F).

Remarks

All specimens in the present study were found attached to a glass sponge species from a deep-sea seamount. *Ophiactis perplexa* was first described by Koehler (1897) and has not been redescribed since, but specimens were recorded in 2000, 2003 and 2007 (OBIS 2021). Our specimens are similar to the holotype description, but we noticed variations in some morphological characters that prevent us from fully associating these specimens with *O. perplexa*. In particular, the spines on the periphery of the ventral disc only appear in two of our specimens, and most specimens have disc spines at the base of the radial shields (Fig. 35C–E), but most of the species in the genus *Ophiactis* show this morphological variation among individuals. *Ophiactis flexuosa* Lyman, 1879 is related to *O. perplexa*, but is distinguished by the presence of spines on the disc, the shape of the radial shield and the pentagonal shape of the ventral arm plate. Another similar species is *O. definita* Koehler, 1922, recorded in deep waters from the South China Sea, Celebes Sea, Molucca Sea, Banda Sea, Solomon Sea, Coral Sea, Bismarck Sea and Australia.

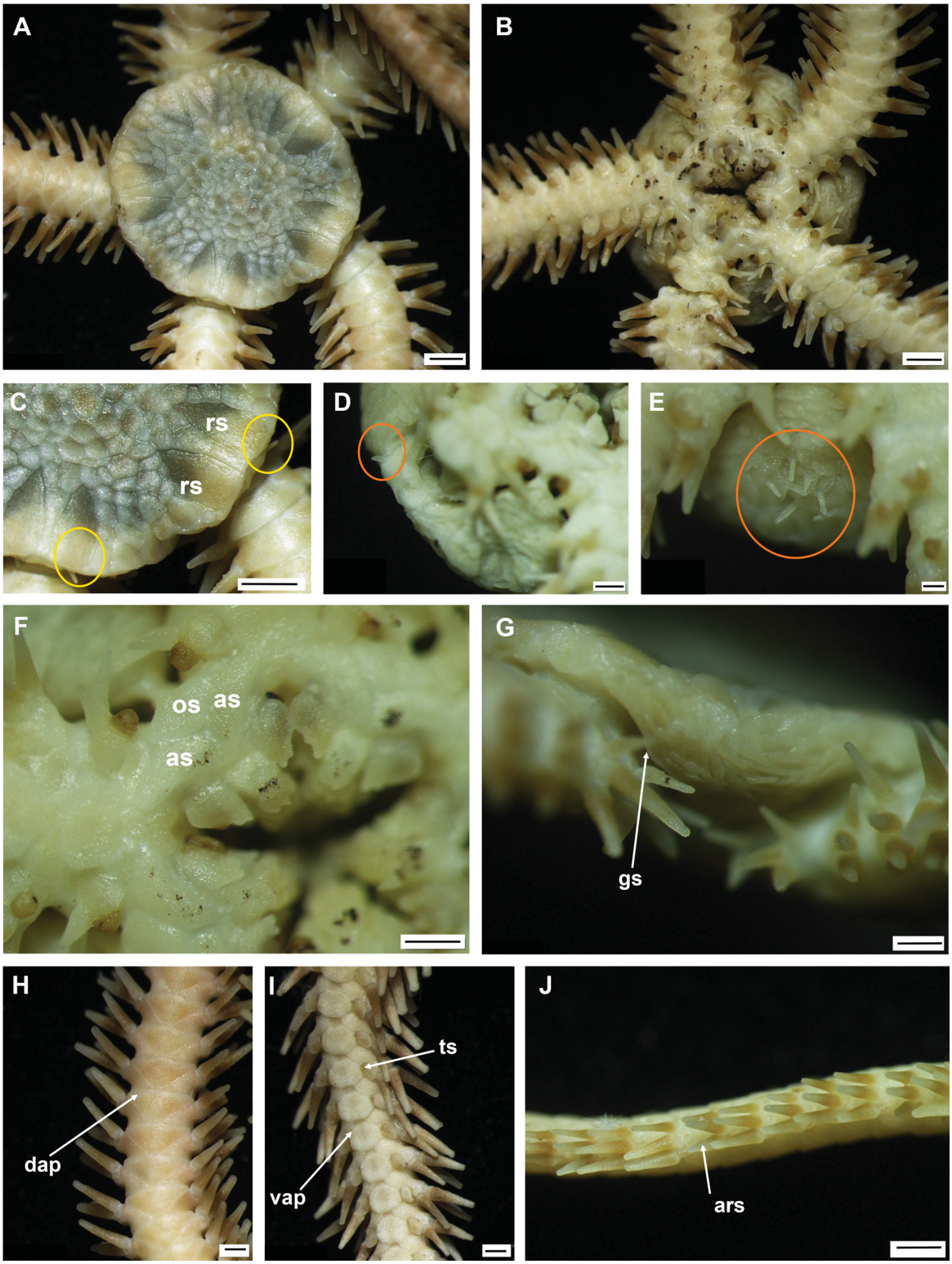

Fig. 36. *Ophiactis* cf. *perplexa* Koehler, 1897 (A–D, F–J = IDSSE EEB-SW0013; E = IDSSE EEB-SW0014). **A**. Dorsal disc. **B**. Ventral disc. **C**. Radial shields (disc spines below radial shields highlighted). **D–E**. Disc spines on ventral disc. **F**. Oral frame. **G**. Lateral disc. **H**. Dorsal arm. **I**. Ventral arm. **J**. Lateral arm. Abbreviations: ars = arm spine; as = adoral shield; dap = dorsal arm plate; gs = genital slit; os = oral shield; rs = radial shield; ts = tentacle scale; vap = ventral arm plate. Scale bars: A–C, E, J = 1 mm; D = 200 µm; F–I = 500 µm.

Ophiactis definita (currently accepted as *O. brachygenys*, see below) is clearly distinguished from *O. perplexa* by the absence of spines on the disc, a longer oral shield with a much smaller border and a pointed distalmost oral papilla. *Ophiactis brachygenys* H.L. Clark, 1911 has separated dorsal arm plates and a smaller disc border than *O. perplexa*, but rarely has a few spines on the disc (Fig. 38M).

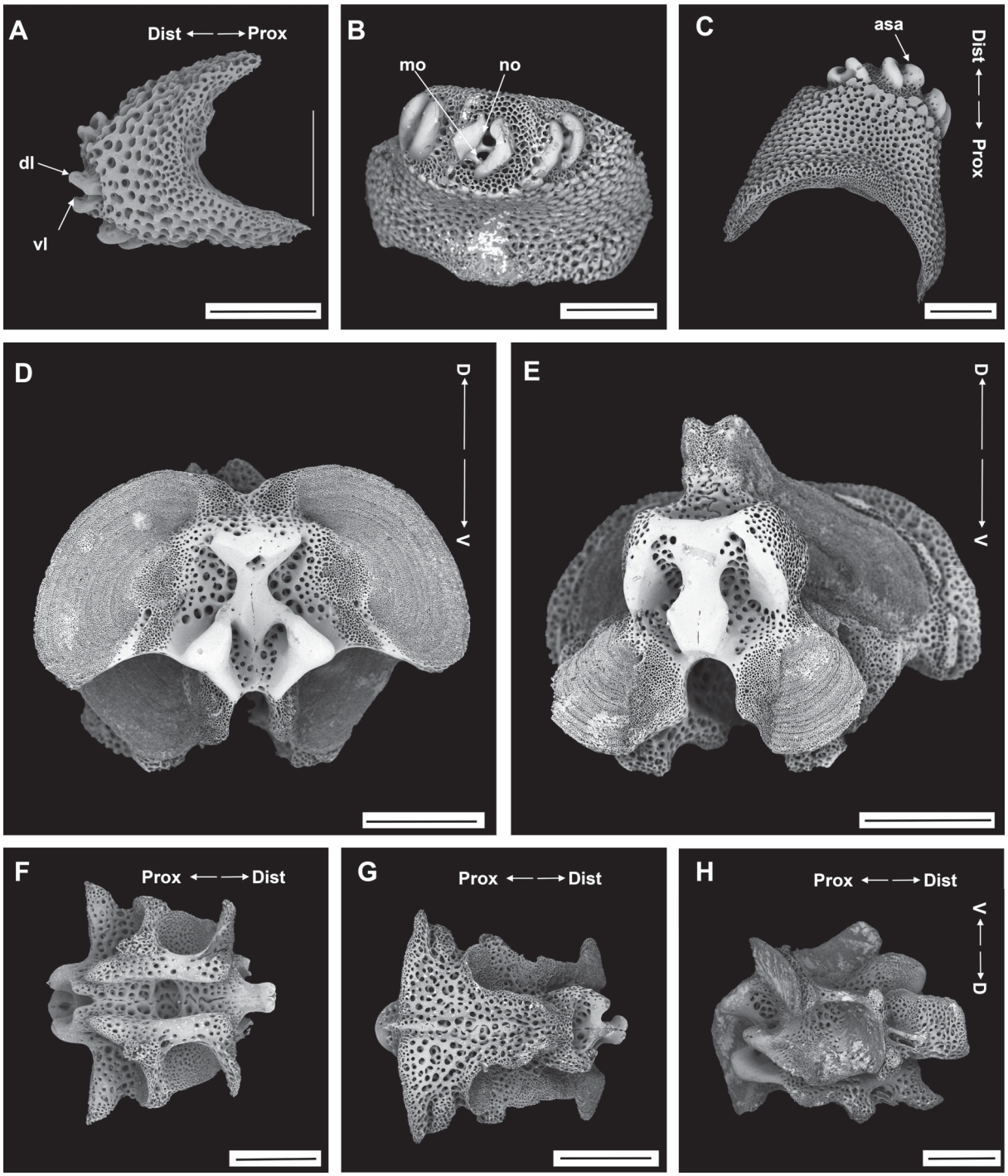

Fig. 37. *Ophiactis* cf. *perplexa* Koehler, 1897, SEM (IDSSE EEB-SW0013). **A–C**. Lateral arm plate. **D–H**. Vertebrae. **D**. Proximal view. **E**. Distal view. **F**. Ventral view. **G**. Dorsal view. **H**. Lateral view. Abbreviations: asa = arm spine articulation; D = dorsal; Dist = distal; dl = dorsal lobe; mo = muscle opening; no = nerve opening; Prox = proximal; V = ventral; vl = ventral lobe. Scale bars: A, G = 200 µm; B–F, H = 300 µm.

Distribution

600–2000 m depth. East China Sea, Indian Ocean, Timor Sea, Tasman Sea (OBIS 2021).

Ophiactis profundi Lütken & Mortensen, 1889
Figs 38–39

Ophiactis profundi Lütken & Mortensen, 1889: 140–142, pl. 6 figs 4–6.
Ophiactis pteropoma H.L. Clark, 1911: 134, fig. 50.

Ophiactis pteropoma – H.L. Clark 1915: 264. — Matsumoto 1917: 154.
Ophiactis profundi – Koehler 1922a: 192, pl. 63 fig. 8. — Guille 1981: 439. — Liao 2004: 235–236, fig. 139.

Material examined

CHINA • 1 spec.; South China Sea, SE of Zhongsha Islands, seamount; 13°58.65′ N, 114°52.09′ E; depth 1550 m; 25 Sep. 2020; collection event: stn SC013; MSV Shenhaiyongshi leg.; preserved in 95% ethanol; GenBank: MZ198771; IDSSE EEB-SW0017 • 1 spec.; same collection data as for preceding; GenBank: MZ198772; IDSSE EEB-SW0018 • 5 specs; same collection data as for preceding; IDSSE EEB-SW0064 to EEB-SW0068.

Remarks

Ophiactis profundi is a hexamerous, fissiparous species. The disc diameter ranged from 4 mm to 6 mm and all the specimens were found at one station on a deep-sea seamount in the South China Sea. Morphological descriptions of the holotype of *Ophiactis profundi* (Lütken & Mortensen 1889) from the eastern Pacific Ocean and of other specimens from the Philippine Sea (Koehler 1922a) were similar to our specimens (Fig. 38).

The dorsal arm plates are well-developed, widely triangular (Fig. 39A). The lateral arm plate has three well-developed arm spine articulations, formed by two subparallel bent lobes, not connected to each other, placed at an angle to the distal edge and equal in size, with two similar openings for muscle and nerve (Fig. 39B–C). The vertebrae have a well-developed zygospondylous articulation, with a narrow, shallow dorsal furrow, not extending beyond the distal articulation, and the ambulacral groove is distalwards widened (Fig. 39D–F).

Ophiactis profundi is closely related to *Ophiactis flexuosa* Lyman, 1879, but it differs in the shape of the oral shield and ventral arm plate, the shape of the oral papillae and the number of arms (*O. flexuosa* is pentamerous). *Ophiactis flexuosa* has distinct scales all around the radial shields (Lütken & Mortensen 1889). *Ophiactis plana* Lyman, 1869 is related to *O. profundi*, but it differs in the shape of the adoral shields and oral shield, and in the smaller oral papillae.

Distribution

231–1644 m. From the South China Sea recorded from the Lubang Islands near the Philippines (this part of the South China Sea is sometimes called the West Philippine Sea), East China Sea, Bohol Sea, Gulf of Tomini, Bismarck Sea, Coral Sea, Australia and New Zealand (OBIS 2021).

Ophiactis cf. ***brachygenys*** H. L. Clark, 1911
Figs 40–42

Ophiactis brachygenys H.L. Clark, 1911: 135–137, fig. 51.

Ophiactis definita Koehler, 1922a: 187–189, pl. 64 figs 1–2, 7.

Ophiactis definita – Koehler 1930: 121. — Guille 1981: 439.
Ophiactis brachygenys – Irimura 1991: 80. — Liao 2004: 228–229, fig. 134.

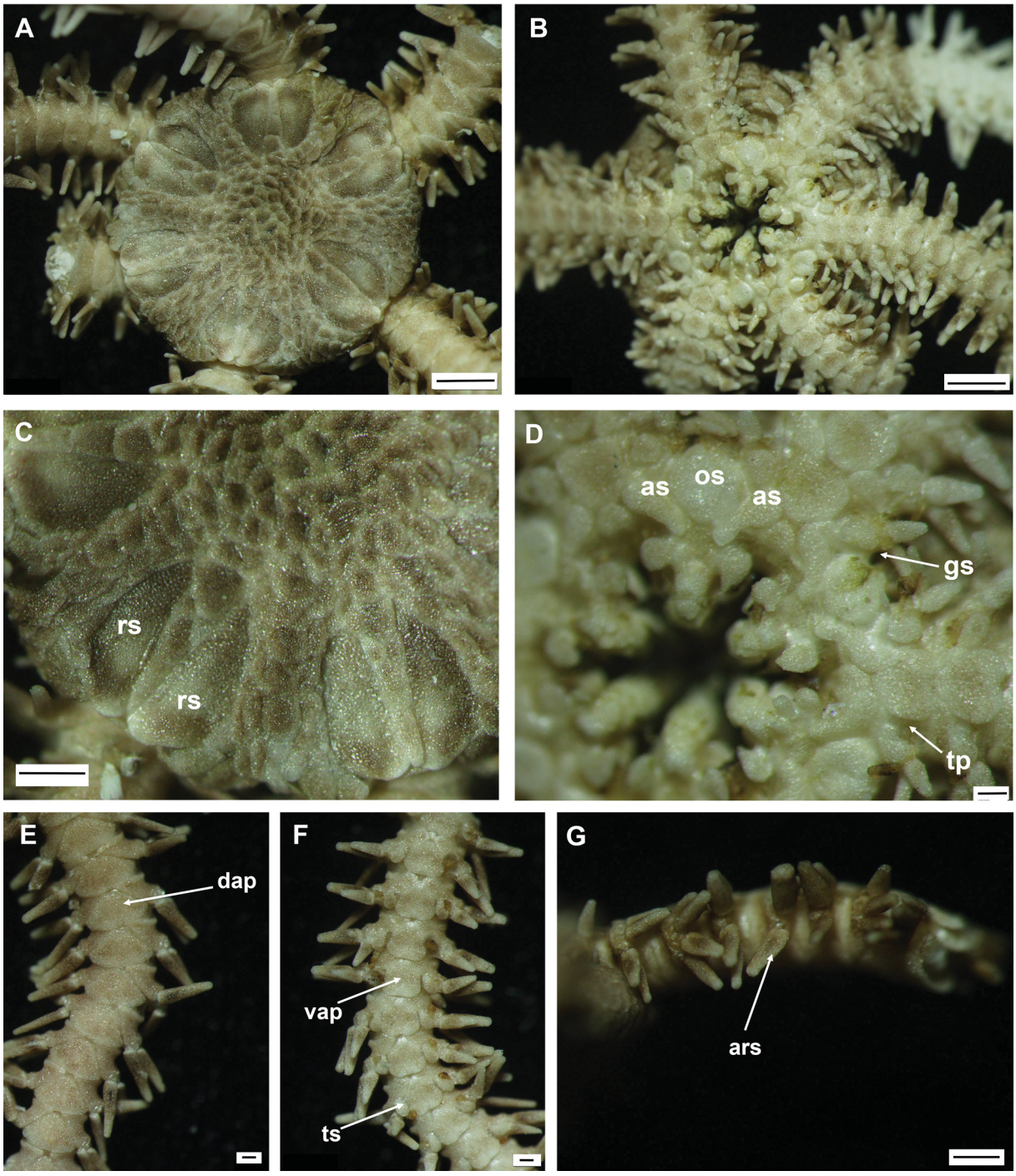

Fig. 38. *Ophiactis profundi* Lütken & Mortensen, 1889 (IDSSE EEB-SW0017). **A**. Dorsal disc. **B**. Ventral disc. **C**. Radial shields. **D**. Oral frame. **E**. Dorsal arm. **F**. Ventral arm. **G**. Lateral arm. Abbreviations: ars = arm spine; as = adoral shield; dap = dorsal arm plate; gs = genital slit; os = oral shield; rs = radial shield; tp = tentacle pore; ts = tentacle scale; vap = ventral arm plate. Scale bars: A–B = 1 mm; C, G = 500 µm; D–F = 200 µm.

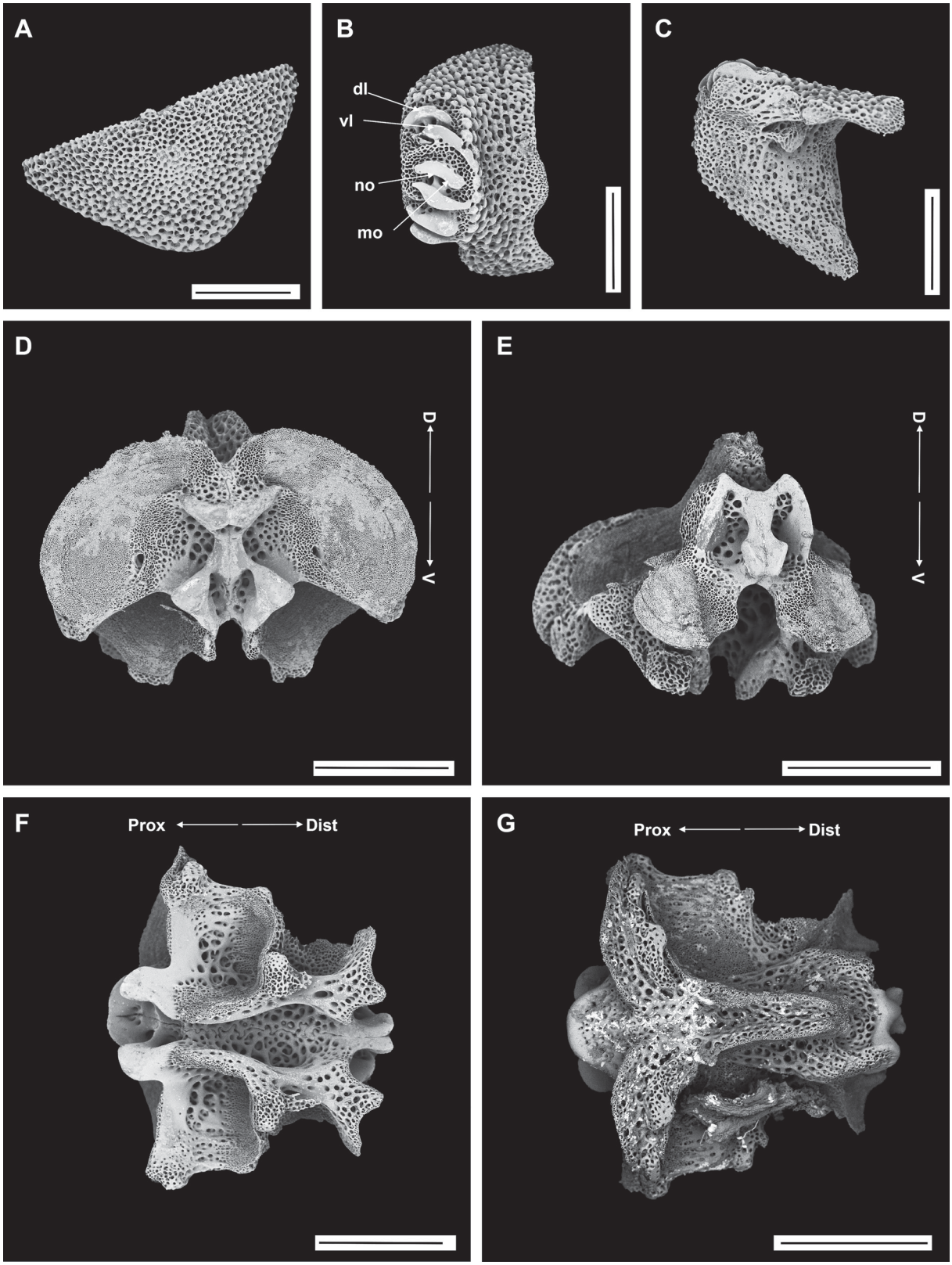

Fig. 39. *Ophiactis profundi* Lütken & Mortensen, 1889, SEM (IDSSE EEB-SW0017). **A**. Dorsal arm plate. **B–C**. Lateral arm plate (external, internal). **D–G**. Vertebrae. **D**. Proximal view. **E**. Distal view. **F**. Ventral view. **G**. Dorsal view. Abbreviations: D = dorsal; Dist = distal; dl = dorsal lobe; mo = muscle opening; no = nerve opening; Prox = proximal; V = ventral; vl = ventral lobe. Scale bars = 300 µm.

Material examined

CHINA • 1 spec.; South China Sea, SE of Zhongsha Islands, seamount; 13°58.65′ N, 114°52.09′ E; depth 1550 m; 25 Sep. 2020; collection event: stn SC013; MSV Shenhaiyongshi leg.; preserved in 95% ethanol; GenBank: MZ198769; IDSSE EEB-SW0015 • 1 spec.; same collection data as for preceding; GenBank: MZ198770; IDSSE EEB-SW0016.

Description (IDSSE EEB-SW0015)

Measurements. Disc diameter 5.8 mm, heptamerous specimen.

Disc. Robust and sub-pentagonal, heptamerous (Fig. 40A–B). Dorsal disc covered by large, coarse, irregular, polygonal overlapping scales, denser in disc center (Fig. 40A). Radial shields large, broad, internal margin straight, external margin convex, pointed proximal angle, longer than wide, half disc radius long, completely separated by a single series of two or three plates (Fig. 40D). Ventral disc also covered by small, irregular, overlapping scales. Genital slits conspicuous and extending from oral shield to disc periphery (Fig. 40C). Oral shield spearhead-shaped, with wide proximal angle, wider than long (Fig. 40F). Adoral shield larger than oral shield, pair proximally connected, proximal edge concave, three times as long as than wide, slightly narrowing distally, bordering proximal edges of oral shield, not separating oral shield from arm (Fig. 40F). One large, wide, rectangular ventralmost tooth with tricuspid edge. Single large, broad (wider than teeth), axe-shaped, operculiform lateral oral papilla, covering second tentacle pore inside mouth angle (Fig. 40F). Some oral papillae more pointed laterally or tricuspid (Fig. 40B, F).

Arms. Dorsal arm plate slightly fan-shaped, large, slightly convex distally, wide proximal angle, as long as wide and mostly separated (Fig. 40G). First ventral arm plate small, triangular with truncated distal end. Second ventral arm plate tetragonal or pentagonal, wider than long, connected to first ventral arm plate, then pentagonal with straight to concave distal edge, round proximal angle along arm and mostly separated (Fig. 40B, H). Three arm spines on most segments, with thickened base, rounded, blunt tip, 1–1½ arm segment in length, middle one longest (Fig. 40G–H). One large, broad, oval tentacle scale, half as long as ventral arm plate, covering pore completely (Fig. 40H).

Color. Wet specimen light brown, dry disc light grey and dorsal arm light brown or pink (Fig. 40).

Ossicle morphology. Extracted from heptamerous specimen, lateral arm plate with three well-developed spine articulations formed by two subparallel, bent, separated lobes, unequal in size. Two similarly sized openings for muscle and nerve (Fig. 41A–C). Vertebrae with well-developed zygospondylous articulation, narrow, shallow dorsal furrow, not extending beyond distal articulating structures, deep ambulacral groove, widened distally, large podial basins (Fig. 41D–H).

Remarks

According to our specimens, *Ophiactis* cf. *brachygenys* is a fissiparous species and these are the first records of specimens with more than five arms (confirmed by molecular data, see below). Six- and seven-armed specimens had similar morphological features. However, the hexamerous specimen (2.8 mm disc diameter) differs slightly from the heptamerous specimen in the number of arms, the widely separated radial shield, the first one to two arm segments having four arm spines but only on one or two arms, and a smooth, pointed disc spine near the periphery of the disc (Fig. 42).

The holotype description of *O. brachygenys* is similar to both specimens from the present study, except for the number of arms and completely separated radial shields.

H.L. Clark (1911) mentioned that one of his specimens (9 mm disc diameter) had distally separated radial shields, the dorsal arm plate was shorter and wider, and both dorsal and ventral arm plates were more closely together. Also, it had a few short disc spines at the periphery of the ventral disc

(H.L. Clark 1911). These variations concur with the specimens from the present study (Figs 40–42). *Ophiactis definita* was synonymized with *O. brachygenys* by Liao (2004). The description of *O. definita* is similar to that of *O. brachygenys*, but Koehler (1922a) described some morphological differences between the two species. *Ophiactis brachygenys* from the present study and the description of its holotype (H.L. Clark 1911) are morphologically distinguished from the type of *O. definita* by having separated dorsal arm plates along the arm, wider than long and not as broad radial shields, and wide as

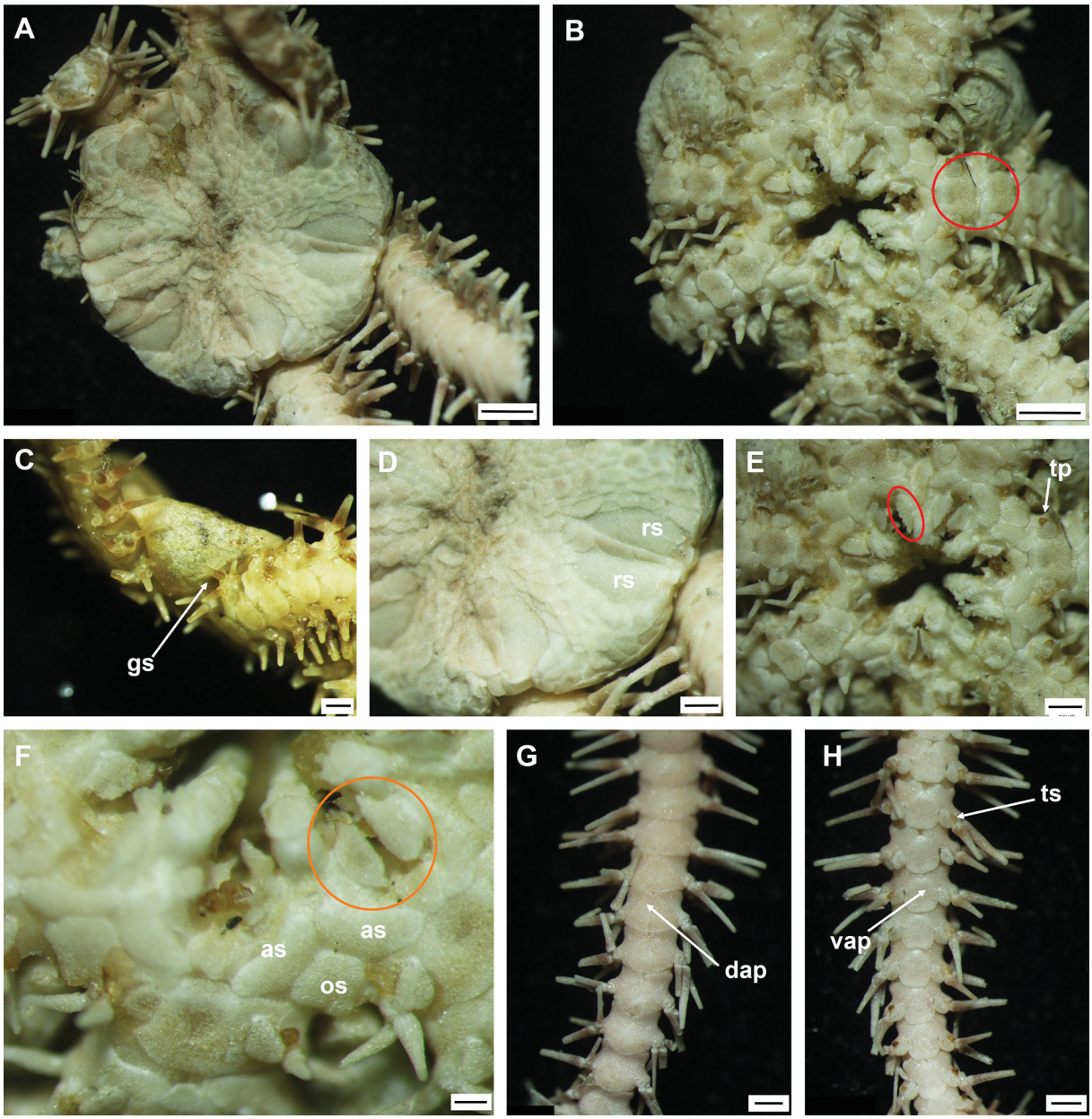

Fig. 40. *Ophiactis* cf. *brachygenys* H.L. Clark, 1911 (IDSSE EEB-SW0015 = heptamerous specimen). **A**. Dorsal disc. **B**. Ventral disc (first and second ventral arm plates highlighted). **C**. Lateral disc. **D**. Radial shields. **E–F**. Oral frame (operculiform lateral oral papillae highlighted). **G**. Dorsal arm. **H**. Ventral arm. Abbreviations: as = adoral shield; dap = dorsal arm plate; gs = genital slit; os = oral shield; rs = radial shield; tp = tentacle pore; ts = tentacle scale; vap = ventral arm plate. Scale bars: A–B = 1 mm; C–E, G–H = 500 µm; F = 200 µm.

long oral shields. In addition, the radial shields are proximally and distally separated, and disc spines are present on the ventral disc (Figs 40A, 42K, M). Molecular analysis of both species from different localities suggests that these morphological variations may be species specific (see below).

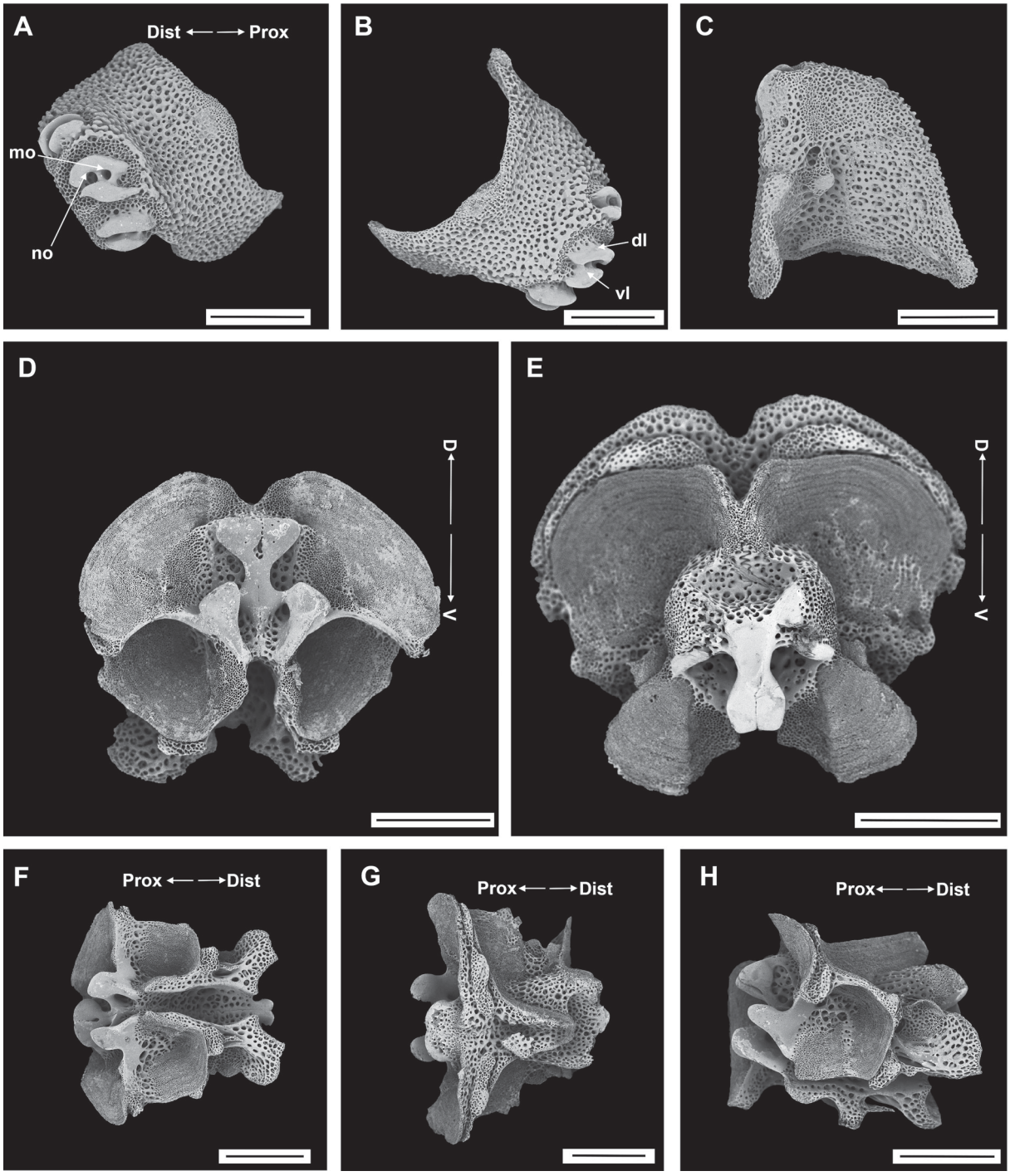

Fig. 41. *Ophiactis* cf. *brachygenys* H.L. Clark, 1911, SEM (IDSSE EEB-SW0015 = heptamerous specimen). **A–C**. Lateral arm plate (internal, external). **D–H**. Vertebrae. **D**. Proximal view. **E**. Distal view. **F**. Ventral view. **G**. Dorsal view. **H**. Lateral view. Abbreviations: D = dorsal; Dist = distal; dl = dorsal lobe; mo = muscle opening; no = nerve opening; Prox = proximal; V = ventral; vl = ventral lobe. Scale bars = 300 μm.

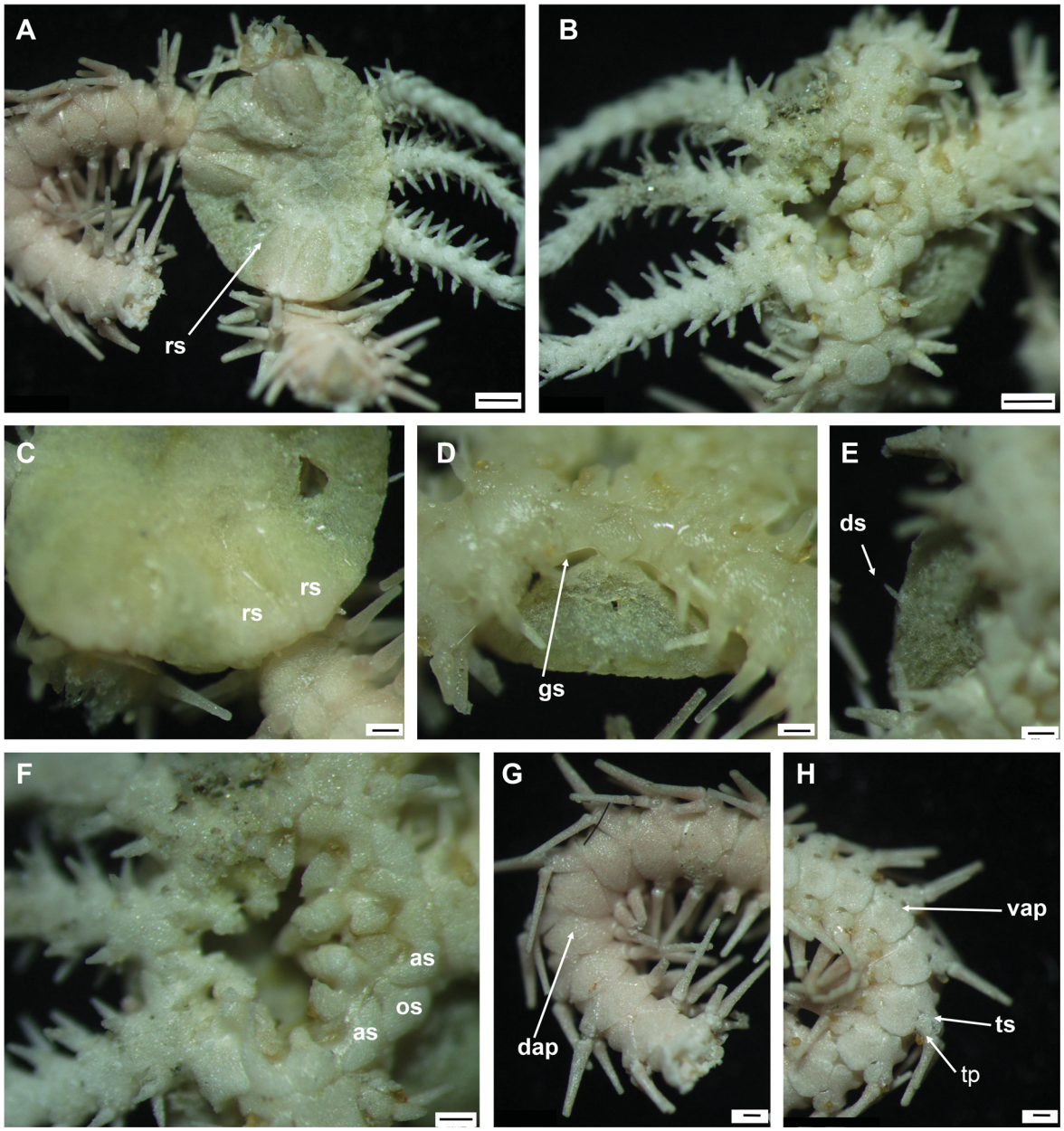

Fig. 42. *Ophiactis* cf. *brachygenys* H.L. Clark, 1911 (IDSSE EEB-SW0016 = hexamerous specimen). **A**. Dorsal disc. **B**. Ventral disc. **C**. Radial shields. **D**. Lateral disc. **E**. Disc spine. **F**. Oral frame. **G**. Dorsal arm. **H**. Ventral arm. Abbreviations: as = adoral shield; dap = dorsal arm plate; ds = disc spine; gs = genital slit; os = oral shield; rs = radial shield; tp = tentacle pore; ts = tentacle scale; vap = ventral arm plate. Scale bars: A–B = 500 µm; C–H = 200 µm.

Distribution

216–1550 m depth. Recorded from the Lubang Islands near the Philippines, East China Sea, southeast Japan, Indonesian seas, Coral Sea, Solomon Sea, Bismarck Sea and Timor Sea (OBIS 2021).

Molecular phylogenetic analysis

Family Asteronychidae

Final 581 bp partial COI and 443 bp partial 16S sequences were obtained after removing ambiguous aligned sites and successfully used in reconstructing a Maximum Likelihood (ML) tree from 16S

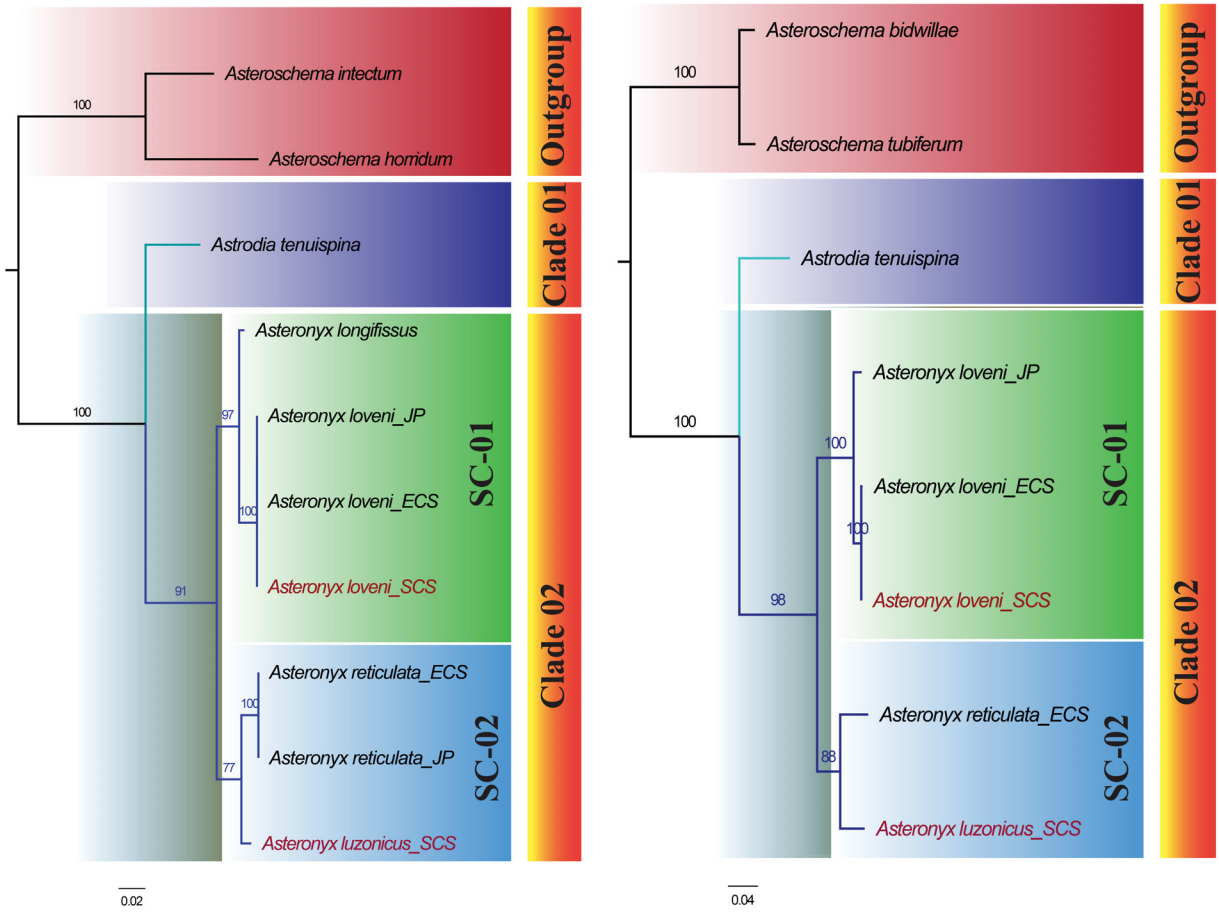

Fig. 43. Family Asteronychidae Ljungman, 1867, Maximum likelihood (ML) trees based on partial 16S and COI sequences (bootstrap support values were generated with rapid bootstrapping algorithm for 1000 replicates). **A**. 16S ML. **B**. COI ML. Abbreviations: ECS = East China Sea; JP = Japan; SC = Sub-Clade; SCS = South China Sea.

(8 specimens) and COI (7 specimens), respectively (Fig. 43). In the 16S ML tree, species of *Asteronyx* were divided into two subclades (Sub-Clades 01 and 02). Sub-Clade 01 consists of *A. loveni* (Japan, East China Sea and South China Sea) and *A. longifissus* Döderlein, 1927 (California). Sub-Clade 02 consists of *A. reticulata* (East China Sea and Japan) and *A. luzonicus* (South China Sea) (Fig. 43A). Similar results were found in the COI ML tree (Fig. 43B). Genetic distance values are provided in Suppl. file 1 and Suppl. file 2. Two samples of *A. reticulata* from Japan and the East China Sea had identical sequences and three samples of *A. loveni* from Japan, the East China Sea and the South China Sea also showed no sequence variation (Suppl. file 1).

Families Euryalidae and Gorgonocephalidae

A total of 26 COI sequences trimmed to 608 bp were obtained after removing ambiguous aligned sites and successfully used in reconstructing an ML tree (Fig. 44). Two main clades were detected, with the family Euryalidae belonging to Clade 01 and family Gorgonocephalidae belonging to Clade 02. The genus *Asteroschema* was detected as a sub-clade within family Euryalidae (Sub-Clade 01) and the genus *Gorgonocephalus* was detected as a sub-clade within family Gorgonocephalidae (Sub-Clade 02). Two inter-clades were detected among species of *Asteroschema* (Sub-Clade 01). Inter-Clade 1A consisted of *A. bidwillae* and *A. tubiferum* from New Zealand (depth 1126–1444 m). Inter-Clade 1B consisted of *A. edmondsoni* A.H. Clark, 1949 from New Caledonia and *A. horridum* from the South China Sea and Reunion Island (depth 498–1550 m). Two inter-clades were detected among species of

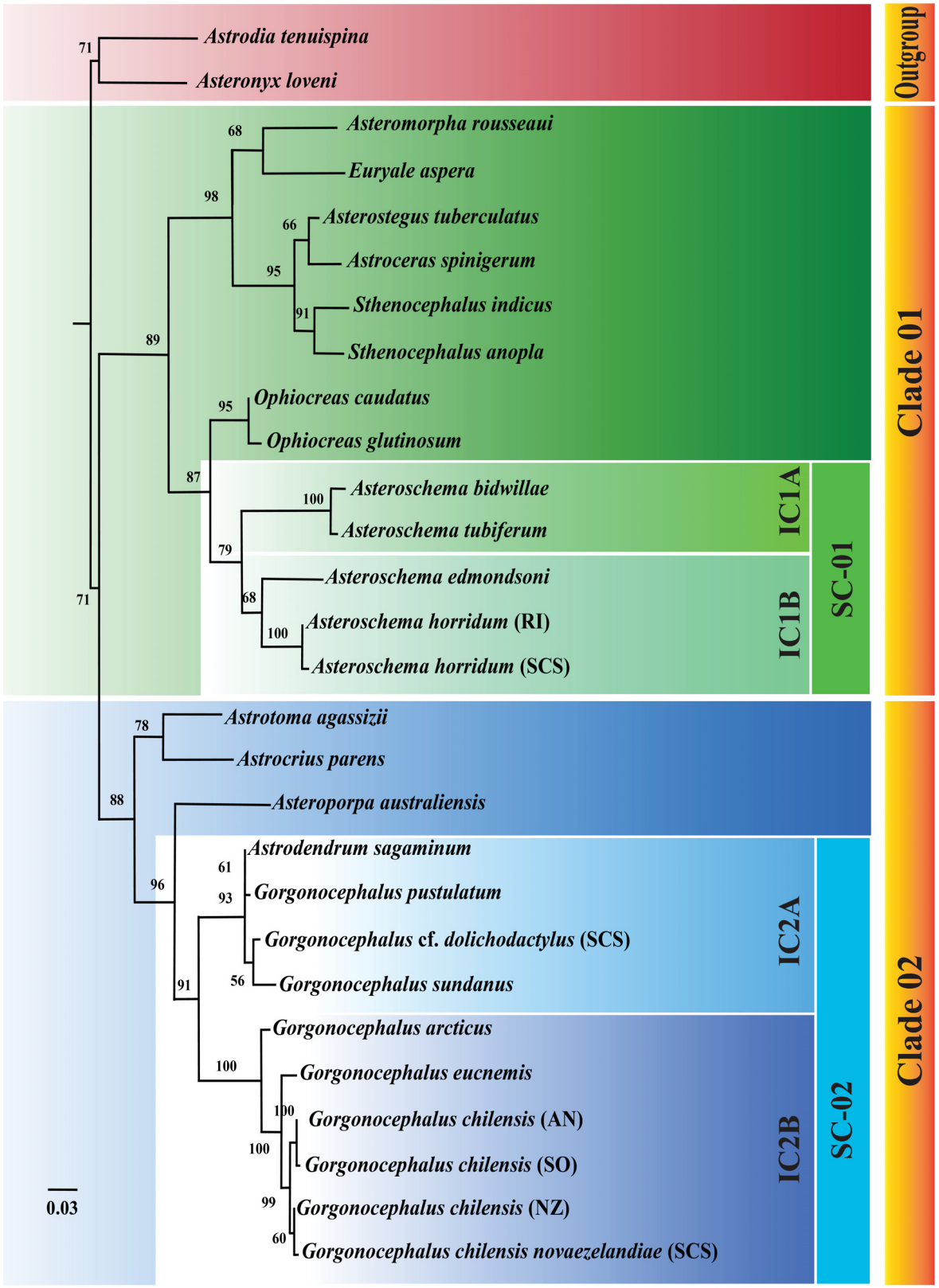

Fig. 44. Families Euryalidae Gray, 1840 and Gorgonocephalidae Ljungman, 1867, Maximum likelihood (ML) tree based on partial COI sequences (bootstrap support values were generated with rapid bootstrapping algorithm for 1000 replicates). Abbreviations: AN = Antarctica; IC = Inter-Clade; NZ = New Zealand; RI = Reunion Island; SC = Sub-Clade; SCS = South China Sea; SO = Sothern Ocean.

Gorgonocephalus (Sub-Clade 02). Inter-Clade 2A consists of *Astrodendrum sagaminum* (Döderlein, 1902) from Japan, *Gorgonocephalus pustulatum* (H. L. Clark, 1916) from New Zealand, *G. sundanus* Döderlein, 1927 from Australia and *G.* cf. *dolichodactylus* from the South China Sea (depth 400–1114 m). Inter-Clade 2B consists of *G. arcticus* Leach, 1819 from Cornwallis Island, *G. eucnemis* (Müller & Troschel, 1842) from Japan, *G. chilensis* from the Antarctic, the Southern Ocean, New Zealand and the South China Sea (depth 398–1550 m) (Fig. 44). Genetic distance values are provided in Suppl. file 3 and Suppl. file 4.

Family Ophiomusaidae

A 568 bp sequence of the COI gene was obtained after removing ambiguous aligned sites and successfully used in reconstructing the ML tree for 13 specimens from the family Ophiomusaidae (Fig. 45). Two main clades were detected within the family. Sub-Clade 01 represnts *Ophiomusa scalare* (Lyman, 1878),

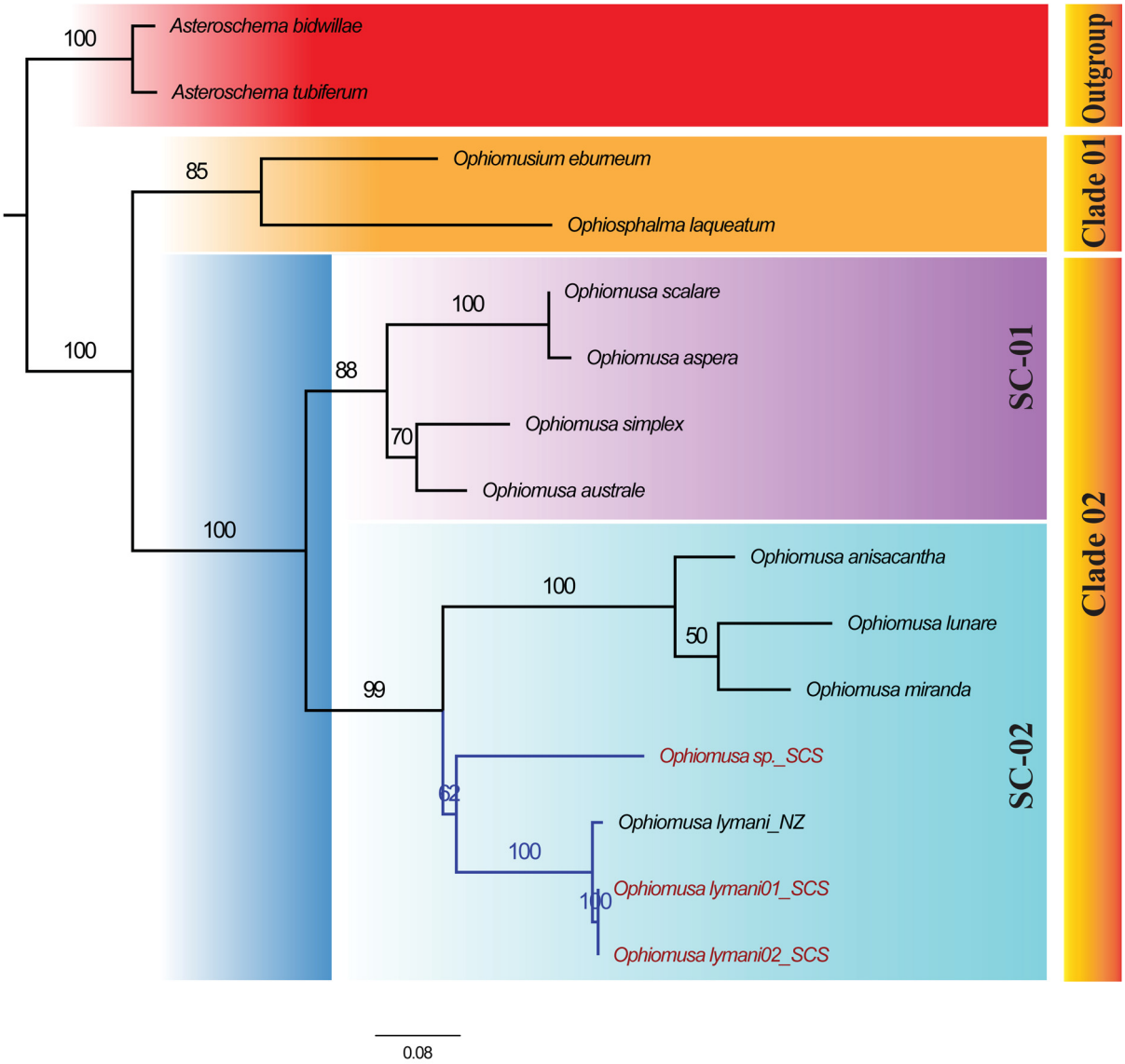

Fig. 45. Family Ophiomusaidae O'Hara *et al.*, 2018, Maximum likelihood (ML) tree based on partial COI sequences (bootstrap support values were generated with rapid bootstrapping algorithm for 1000 replicates). Abbreviations: NZ = New Zealand; SC = Sub-Clade; SCS = South China Sea.

O. aspera (Koehler, 1930), *O. simplex* (Lyman, 1878) and *O. australe* (H.L. Clark, 1928). Sub-Clade 02 represents *O. lymani*, *Ophiomusa* sp., *O. miranda* (Koehler, 1930), *O. lunare* (Lyman, 1878) and *O. anisacantha* (H.L. Clark, 1928) (Fig. 45). Genetic distance values are provided in Suppl. file 5.

Family Ophiotomidae

A 623 bp sequence of the COI gene was obtained after removing ambiguous aligned sites and used to reconstruct the ML tree from ten specimens for the family Ophiotomidae (Fig. 46). We failed to get COI or 16S gene sequences from *Ophiotreta eximia*. Therefore, only *Ophiopristis shenhaiyongshii* sp. nov. was added to this phylogenetic tree from our collection. Two main clades were detected within Ophiotomidae. Inter-Clade 2A represents *Ophiotreta matura*, *O. eximia*, *Ophiopristis shenhaiyongshii* sp. nov., *O. luctosa*, *O. procera* and *Ophiacantha spectabilis* G.O. Sars, 1872 (Fig. 46). Genetic distance values are provided in Suppl. file 6.

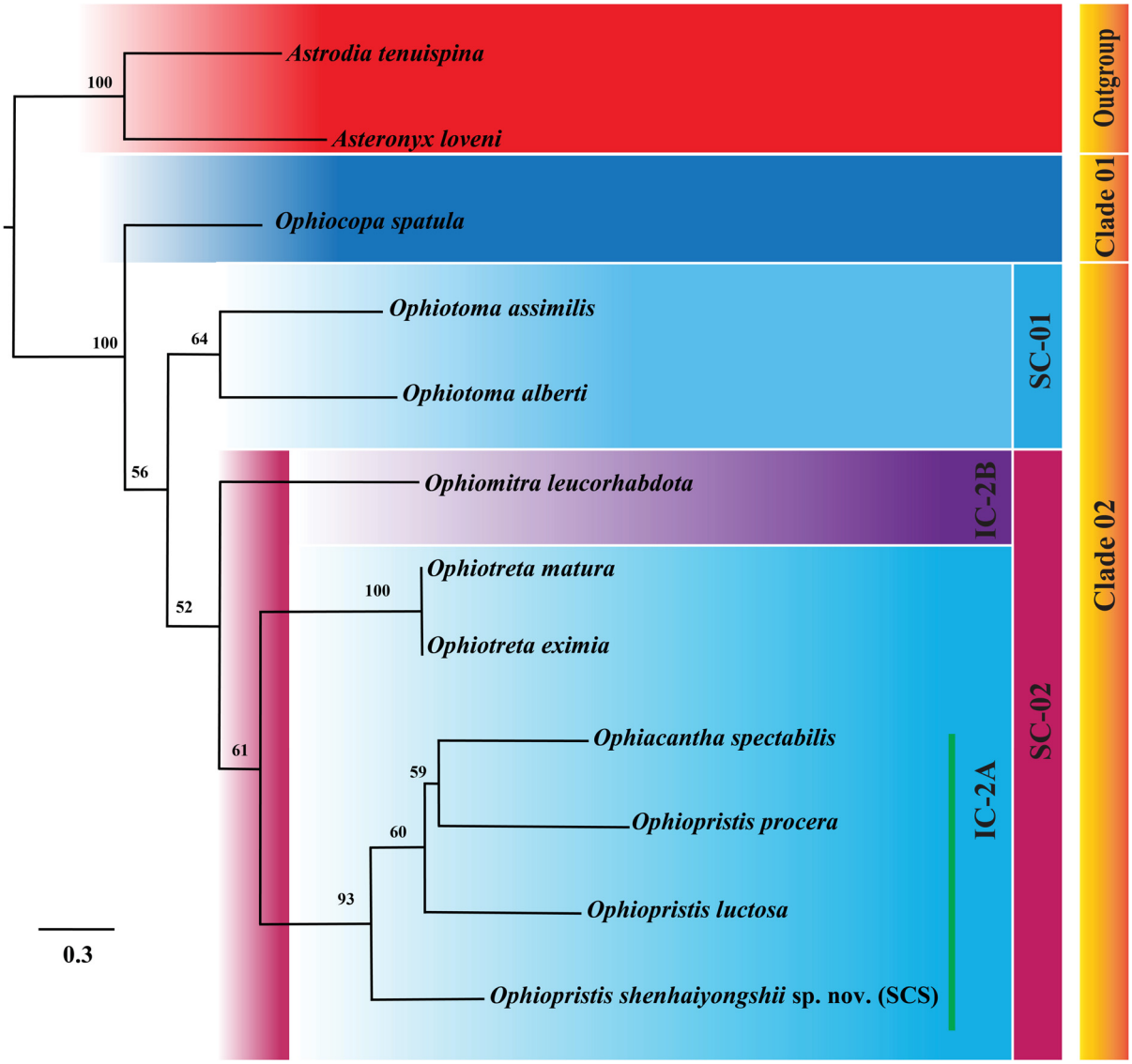

Fig. 46. Family Ophiotomidae Paterson, 1985, Maximum likelihood (ML) tree based on partial COI sequences (bootstrap support values were generated with rapid bootstrapping algorithm for 1000 replicates). Abbreviations: IC = Inter Clade; SC = Sub-Clade; SCS = South China Sea.

Family Ophiacanthidae

Final 449 bp COI and 487 bp 16S sequences were obtained after removing ambiguous aligned sites and successfully used in reconstructing Maximum Likelihood (ML) trees of 16S (8 specimens) and COI (7 specimens), respectively (Fig. 47). In the 16S ML tree, species from the South China Sea divided into two subclades (Sub-Clades 01 and 02). *Ophiurothamnus clausa*, *Ophiomoeris petalis* sp. nov., *Ophiomoeris* sp., *Ophiacantha aster* sp. nov. and *Ophioplinthaca plicata* from the present study fell into Sub-Clade 01. *Ophiacantha vorax*, *O. bathybia* and *Ophientrema scolopendrica* from the present study fell into Sub-Clade 02. The genus *Ophioplinthaca* fell into a new interclade within Sub-Clade 01 (Inter-Clade 1B). Inter-Clade 1A consists of three different genera: *Ophiacantha*, *Ophiomoeris* and *Ophiurothamnus*. *Ophientrema scolopendrica*, *Ophiacantha bathybia* and *O. vorax* also fell into two interclades within Sub-Clade 02 (Inter-Clades 2A and 2B) (Fig. 47A).

The clades in the COI ML tree were grouped corresponding to the 16S ML tree. Therefore, all the species represented in the COI ML belong to the main Clade 02. *Ophiurothamnus clausa* and *Ophioplinthaca plicata* from the South China Sea fell into Sub-Clade 01. *Ophiacantha vorax* and *Ophientrema scolopendrica* from the South China Sea fell into Sub-Clade 02. The genus *Ophioplinthaca* fell into

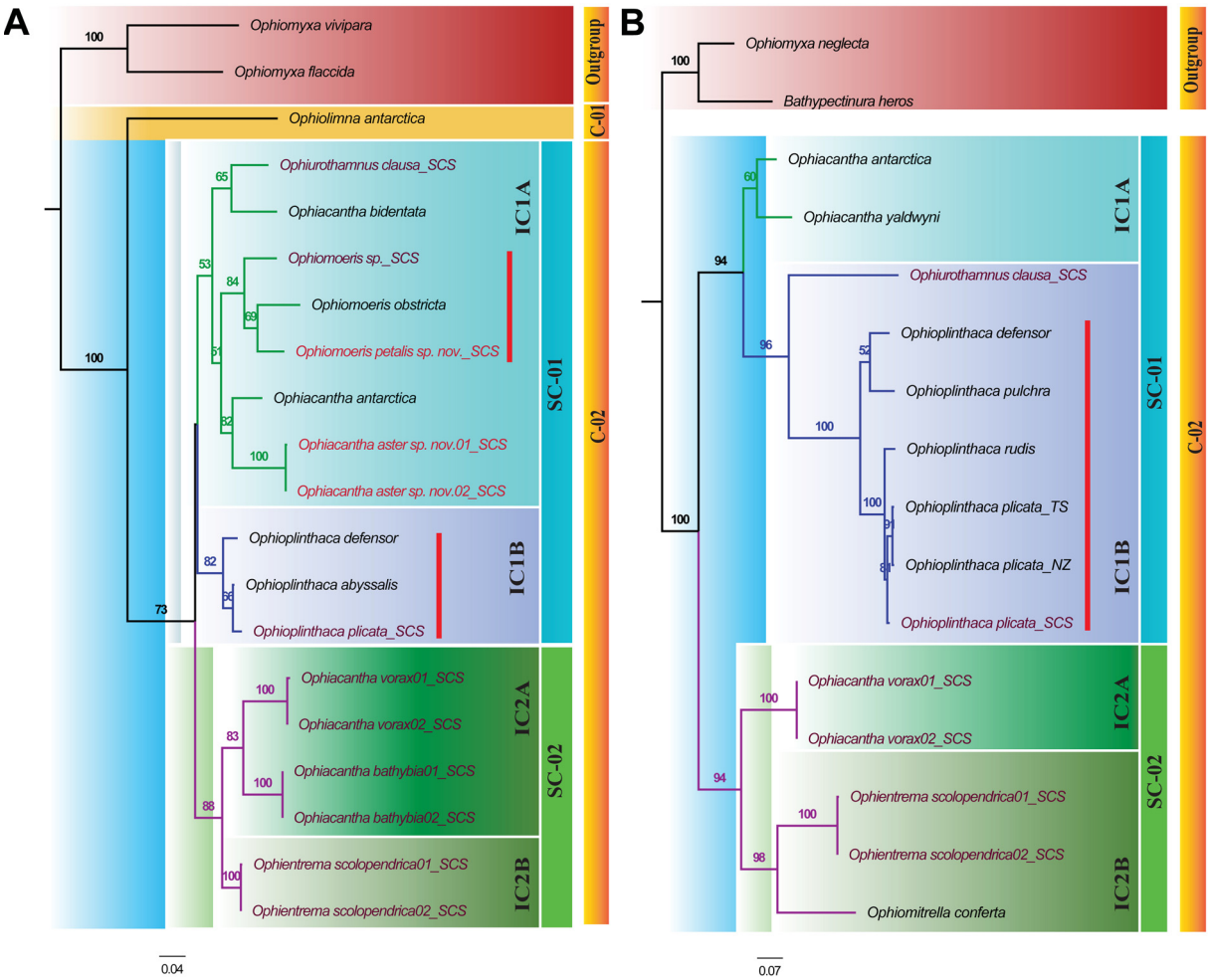

Fig. 47. Family Ophiacanthidae Ljungman, 1867, Maximum likelihood (ML) trees based on partial 16S and COI sequences (bootstrap support values were generated with rapid bootstrapping algorithm for 1000 replicates). **A**. 16S ML. **B**. COI ML. Abbreviations: C = Clade; IC = Inter-Clade; NZ = New Zealand; SC = Sub Clade; SCS = South China Sea; TS = Tasman Sea.

Inter-Clade 1B within Sub-Clade 01 (Fig. 47B). The topology of the two ML trees was slightly different from each other (Sub-Clade 01). Genetic distance values are provided in Suppl. file 7 and Suppl. file 8.

Family Ophiactidae

A total of 18 COI sequences trimmed to 554 bp were obtained after removing ambiguous aligned sites and were used to reconstruct the ML tree (Fig. 48). Two main clades were detected within the family. Sub-Clade 02 represented all *Ophiactis* species recorded from the South China Sea. *Ophiactis* cf. *perplexa*,

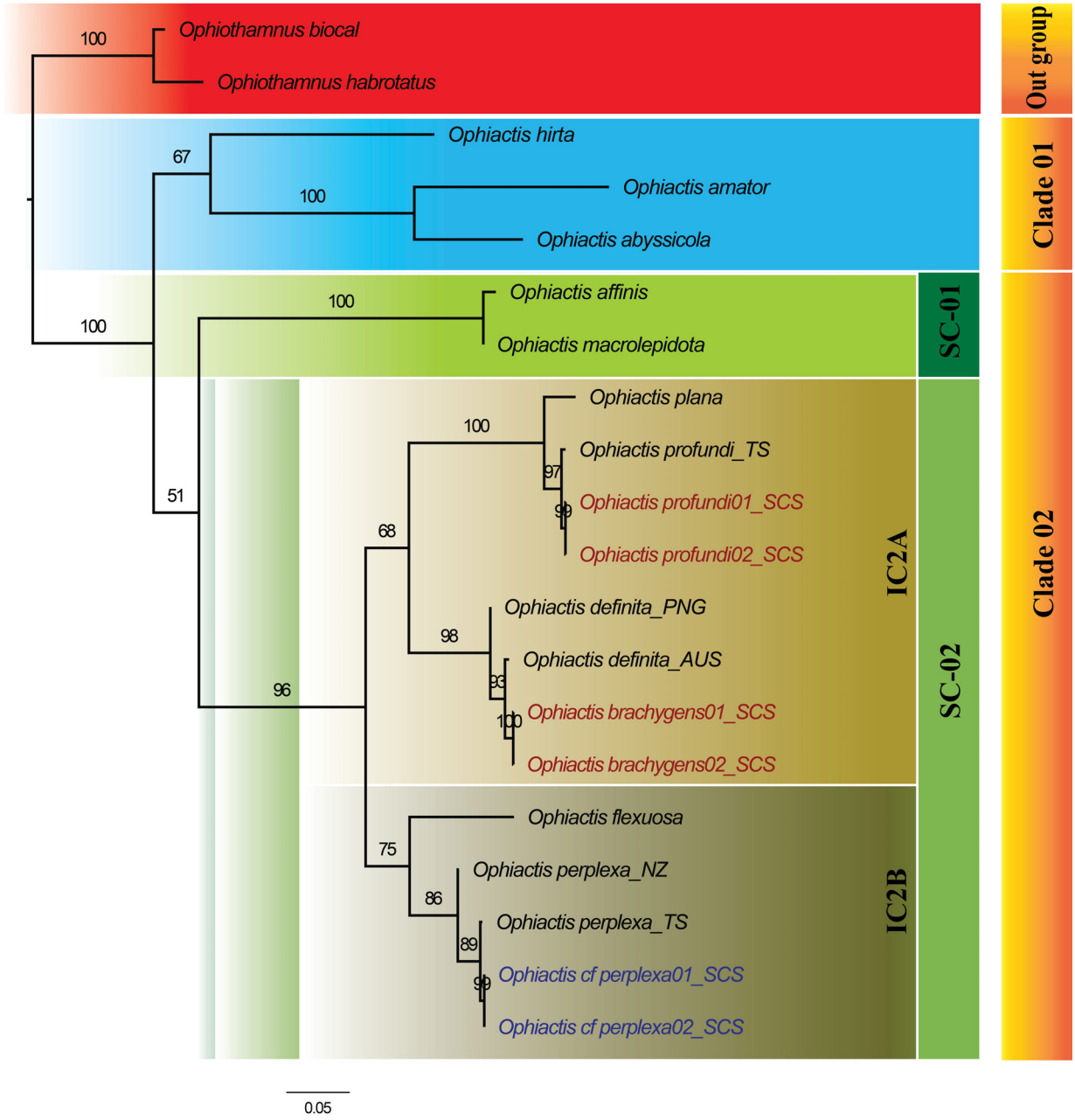

Fig. 48. Family Ophiactidae Matsumoto, 1915, Maximum likelihood (ML) tree based on partial COI sequences (bootstrap support values were generated with rapid bootstrapping algorithm for 1000 replicates). Abbreviations: AUS = Australia; IC = Inter-Clade; NZ = New Zealand; PNG = Papua New Guinea; SC = Sub-Clade; SCS = South China Sea; TS = Tasman Sea.

O. cf. *brachygenys* and *O*. *profundi* fell into two inter-clades within Sub-Clade 02 (Inter-Clades 2A and 2B) (Fig. 48). Genetic distance values are provided in Suppl. file 9.

Discussion

Taxonomy of deep-sea Ophiuroidea from the South China Sea

Our molecular phylogenetic analysis of the family Asteronychidae identified two main clades as genera *Asteronyx* and *Astrodia* Verrill, 1899 (Fig. 43). We prepared two different molecular phylogenetic trees using both the COI and 16S genes to represent the family Asteronychidae due to limited available published molecular data and to better understand the genetic distance variation among different mitochondrial genes. Previous studies suggested that interspecific genetic distances for COI within the class Ophiuroidea ranges from 5.6% to 31.6%, with a mean valve of 18.9% and intraspecific genetic distances from 0.5% to 6.4%, with a mean value of 2.2% according to the Kimura 2-parameter (K2P) (Boissin *et al.* 2017). The genetic distances from the COI of *Asteronyx loveni* and *Asteronyx reticulata* in this study fell within the ranges of these published values. We detected a more significant difference in genetic distance from the COI gene than from the 16S gene, and these results may be caused by a smaller substitution rate and lower base pair variation in the 16S gene than in the COI gene (Palumbi 1996b). We conclude that the COI gene was more suitable for interspecies identification than the 16S gene for the family Asteronychidae (Suppl. file 1 and Suppl. file 2). Cryptic speciation in the genus *Asteronyx* was difficult to recognize using only morphological details and the usefulness of some morphological characters may vary with the ontogenetic stage of a specimen. Recent studies suggested key morphological features to distinguish species of *Asteronyx*, such as features of the dorsal disc, and position and length of the genital slit (Okanishi *et al.* 2018). The holotype description of *Asteronyx luzonicus* by Döderlein (1927) mentioned distinguishing morphological features, such as characteristics of the ventralmost arm spine and sexually mature specimens appeared to have dark spots on the disc. Specimens in the present study were not mature, but appeared to have calcified scales on the disc, as mentioned by Baker *et al*. (2018). This study identified some morphological characters distinguishing *A*. *luzonicus* (13.5 mm disc diameter) from *A*. *loveni* (11 mm disc diameter), such as hook arm spines having a maximum of one secondary tooth, the disc surface being flattened, with a mesh-like center and calcified scales, and the first two to three ventral arm segments without an arm spine. Our molecular analysis of the family Asteronychidae was helpful to distinguish *A. luzonicus* from *A*. *loveni*, *A*. *longifissus* and *A*. *reticulata. Asteronyx luzonicus* is the second species of the genus *Asteronyx* recorded from the South China Sea. Previously, *A*. *luzonicus* had been recorded from neighboring seas and distant localities, such as Madagascar.

The molecular phylogenetic tree of the families Gorgonocephalidae and Euryalidae based on the COI gene (28 specimens) appear to be similar in topology and well in agreement with previous studies (Okanishi & Fujita 2013; Christodoulou *et al.* 2019; O'Hara *et al.* 2019). In this study, the genetic distance in *Asteroschema horridum* from Reunion Island and the South China Sea, and in *Gorgonocephalus chilensis* from New Zealand, the Antarctic, the Southern Ocean and the South China Sea, fell within the intraspecific genetic distance range of published values on Ophiuroidea and was well supported by the ML tree (Boissin *et al.* 2017) (Fig. 44). However, the genetic distance of COI was significantly lower in *Gorgonocephalus* than in *Asteroschema*. Therefore, we conclude that species of *Gorgonocephalus* had a slower genetic evolution, but comprehensive molecular analysis with more molecular data from different localities and species are needed to confirm this hypothesis (Suppl. file 3 and Suppl. file 4). The molecular phylogenetic analysis of Gorgonocephalidae identified two sub-clades within the genus *Gorgonocephalus* (Fig. 44). These clades were clearly distinguished by morphological differences. *Gorgonocephalus dolichodactylus*, *G*. *sundanus* and *G*. *pustulatum* fell into one clade and were distinguished morphologically from the other clade by having a wider, thin, intrabrachial peripheral ring, sparse, low granulation and a maximum of four arm spines (Baker 1980). The granulation pattern on the disc was not a suitable morphological feature to distinguish the species,

due to significant variation among individuals (Baker 1980). As an example, *G*. cf. *dolichodactylus* from the present study had naked skin on both sides of the disc, except on the radial shields (covered by a few scattered granules). Morphological analysis of *G. chilensis* s. lat. from different localities has indicated only a few differences and those depended on the size of the specimen (Döderlein 1927; Baker 1980; McKnight 2000; Olbers *et al.* 2019). *Gorgonocephalus chilensis* from New Zealand waters and the South China Sea had a significantly low genetic distance, but showed higher genetic distance from Antarctic/Subantarctic specimens of *G*. *chilensis*. According to the molecular phylogenetic tree, *G. chilensis* from the South China Sea and New Zealand fall into one clade that is sister to another clade with Antarctic/Subantarctic specimens (Fig. 44; Suppl. file 3), which prompted us to adopt a subspecific division. The molecular analysis indicated that *Astrodendrum sagaminum* falls within *Gorgonocephalus*, and genetic distances within *Astrodendrum sagaminum*, *G*. *pustulatum*, *G*. cf. *dolichodactylus* and *G*. *sundanus* ranged from 1.16% to 4.42%, but the genus *Astrodendrum* differs from *Gorgonocephalus* by having variously shaped external ossicles on the disc, a madreporite placed on the inner edge of the interradial lateral disc and by lacking calcareous scales on the lateral disc margin (Baker 1980; Okanishi & Fujita 2018a). This study suggests that the sequence of *A*. *sagaminum* downloaded from GenBank may be based on a misidentified specimen or the species belongs in the genus *Gorgonocephalus.* We suggest that the genus *Astrodendrum* should be revised using a combination of molecular and morphological data and material from different localities.

The molecular phylogenetic analysis of Euryalidae identified a sub-clade that belongs to the genus *Asteroschema* (Fig. 44). The genetic distance of *A*. *horridum* from Reunion Island to the South China Sea was higher than that of *Gorgonocephalus*, but they fall within previously published values (Okanishi *et al.* 2011a; Okanishi & Fujita 2013) (Suppl. file 3 and Suppl. file 4). Intraspecific and interspecific COI genetic distances were much lower in *Gorgonocephalus* than in *Asteroschema* (Suppl. file 3 and Suppl. file 4). Therefore, the COI gene appears to be more suitable for *Asteroschema* than for *Gorgonocephalus*, for species identification and classification. The results of COI from the ML tree suggested that *Asteroschema horridum* was closely related to *A*. *edmondsoni* (12.51%) and *Gorgonocephalus chilensis* is closely related to *G*. *eucnemis* (4.07%). *Asteroschema horridum* can clearly be distinguished within the genus *Asteroschema* by its having a small, flat disc with scales bearing conical granules. The present study and previous studies indicated that *A*. *horridum* may have few morphological variations, which depend on the size of the specimens. However, most species of *Asteroschema* have high morphological variation and cryptic species complexes occur among them (Baker 1980). Therefore, a combination of morphological and molecular analysis is needed to identify and revise the genus *Asteroschema*.

Our molecular phylogenetic analysis suggests three sub-clades within the family Ophiomusaidae. *Ophiomusa lymani* from the South China Sea fell into Sub-Clade 02 and genetic distance values between the South China Sea and New Zealand fell within published intraspecific genetic distance values (Ward *et al.* 2008; Boissin *et al.* 2017). *Ophiomusa lymani* was recently placed in the resurrected genus *Ophiomusa* and the new family Ophiomusaidae, because the type species of *Ophiomusium* (*O*. *eburneum*) was found to belong to a different clade (Christodoulou *et al.* 2019). However, molecular analysis in the present study and recent studies suggest the presence of two main clades within the family Ophiomusaidae (Christodoulou *et al.* 2019; O'Hara *et al.* 2019) (Fig. 45, Suppl. file 5).

The molecular analysis of the family Ophiotomidae identified an inter-clade that consisted of the genera *Ophiotreta* and *Ophiopristis*. Morphologically, *Ophiopristis shenhaiyongshii* sp. nov., *O*. *luctosa* and *O*. *procera* are clearly grouped together by having a series of thorny spines on the distal margin of the oral shield and by characteristics of the tentacle scale. Interspecific genetic distances in Ophiotomidae from this study determined *O*. *shenhaiyongshii* sp. nov. as a new species in the genus *Ophiopristis* (Suppl. file 6). *Ophiopristis shenhaiyongshii* sp. nov. was clearly distinguished within this clade by characteristics of the tentacle scale and the disc spines. In this study, the ML phylogenetic tree of the family Ophiotomidae

suggests that *Ophiacantha spectabilis* belongs to Ophiotomidae within the clade for *Ophiopristis*, confirming recent studies (Christodoulou *et al.* 2019; O'Hara *et al.* 2019) (Fig. 46). However, we refrain from transferring *O. spectabilis* to *Ophiopristis* without a comprehensive examination of specimens and sufficient molecular data (only one sequence in GenBank).

The molecular phylogenetic analysis of the family Ophiacanthidae identified two main sub-clades in both the 16S ML tree and the COI ML tree (Fig. 47). However, those two sub-clades did not possess clear distinguishing external morphological characters, but could clearly be distinguished by using characters of the vertebrae articulation appearance, such as streptospondylous articulation (*Ophioplinthaca plicata*, *Ophiacantha aster* sp. nov., *Ophiurothamnus clausa* and *Ophiomoeris petalis* sp. nov.) and zygospondylous articulation (*Ophientrema scolopendrica*, *Ophiacantha bathybia* and *O. vorax*). In this study, we prepared two different molecular phylogenetic trees by using both COI and 16S genes to represent the family Ophiacanthidae due to limited published molecular data, unsuccessful molecular data generation and to better understand the genetic distance variation among mitochondrial genes. We detected significantly higher genetic distances in COI than in the 16S gene at both intraspecific and interspecific levels.

Our phylogenetic analysis suggests that *Ophiacantha aster* sp. nov. is related to *O. antarctica*, *Ophiomoeris petalis* sp. nov. is related to *O. obstricta*, and *Ophioplinthaca rudis* (Koehler, 1897) is related to *O. plicata*. *Ophiacantha bathybia* fell between *O. vorax* and *Ophientrema scolopendrica* (Suppl. file 7 and Suppl. file 8). *Ophientrema scolopendrica*, *Ophiacantha bathybia* and *O. aster* sp. nov. appear to have a slightly lower variation in intraspecific genetic distances within the South China Sea (Suppl. file 7 and Suppl. file 8). Our molecular analysis found the genus *Ophiacantha* as polyphyletic, *Ophioplinthaca* and *Ophiomoeris* as monophyletic and previous studies suggest that the genera *Ophiomitrella* and *Ophiolebes* may also be polyphyletic. Previous studies have suggested that Ophiacanthidae needs to be revised to obtain a better understanding and many genera of Ophiacanthidae may be polyphyletic as well (O'Hara *et al.* 2018, 2019; Christodoulou *et al.* 2019; Lee *et al.* 2019). Molecular and morphological analysis using literature data on Ophiacanthidae suggests that *O. aster* sp. nov. belongs to the *Ophiacantha antarctica* clade. *Ophiacantha aster* sp. nov. can clearly be distinguished within this clade by having a unique color pattern on the arms and dorsal disc, four to five spiniform lateral oral papillae, sparse disc spines and deeper interradial disc excavations.

Species of the genus *Ophiomoeris* are difficult to identify when relying only on morphological analysis due to high morphological variation among individuals. Therefore, a combined molecular and morphological analysis of specimens from different localities will help to better understand the species limits within this genus (O'Hara & Stöhr 2006; Stöhr 2011). In this study, we identified *O. petalis* sp. nov. with the help of both molecular and morphological analysis. *Ophiomoeris petalis* sp. nov. falls within the clade of *Ophiomoeris* and genetic distance values support its differentiation from *O. obstricta* and *Ophiomoeris* sp. (Fig. 47A, Suppl. file 7). Morphologically, *O. petalis* sp. nov. can be distinguished within *Ophiomoeris* by having seven arms, large radial shields with a straight distal margin and a few low granules on the disc scales around the centrodorsal plate.

The genus *Ophientrema* was represented by only two species, *O. euphylactea* and *O. scolopendrica*, but *O. euphylactea* has not been recorded since its original description. Therefore, understanding the genus *Ophientrema* has been limited to *O. scolopendrica* in recent molecular and morphological studies. *Ophientrema* is clearly distinguished within Ophiacanthidae by having thin skin with small granules and by characteristics of the ventral arm spines along the arm. The molecular analysis indicates that *Ophiomitrella conferta* Koehler, 1922 may be closely related to the genus *Ophientrema*, but interspecific genetic distances between these two species were higher than previously published values (Ward *et al.* 2008; Boissin *et al.* 2017). The morphological analysis in this study and previous studies also

indicate significantly different morphological features between those species (O'Hara & Stöhr 2006) (Suppl. file 8).

According to the molecular analysis in the present study, *Ophiacantha bathybia* and *O. vorax* fall into the same clade within Ophiacanthidae. Genetic relationships between these species cannot yet be understood completely, due to the lack of molecular data for the species of *Ophiacantha*. *Ophiacantha bathybia* was the first abyssal species of the genus recorded from the South China Sea (depth 3563 m). The combination of morphological and molecular analysis in the present and previous studies suggest that *O. bathybia* is related to *O. pacifica, O. sollicita, O. levispina* Lyman, 1878 and *O. frigida* (Christodoulou *et al.* 2019; O'Hara *et al.* 2019), as well as *O. sociabilis* and *O. cosmica* (Stöhr & O'Hara 2021). Species of *Ophiacantha* from this clade have only been recorded from abyssal depths and appear to have similar morphological features. Stöhr & O'Hara (2021) proposed to apply the name *O. pacifica* to the Northern/Central/East Pacific populations and the name *O. cosmica* to the Southern Pacific/Antarctic/South Atlantic populations.

In this study, the genus *Ophioplinthaca* had different topologies in the COI gene and 16S gene ML phylogenetic trees. This may be caused by the evolution rates of 16S and COI and by the accuracy of sequences used in the phylogenetic tree (Palumbi 1996b). However, the inter-clade of *Ophioplinthaca* was in the same sub-clade on both trees (Fig. 47). Our phylogenetic analysis suggests that *O. rudis* (Koehler, 1897) may be related to *O. plicata* (4.12 ± 0.96% SE). The genetic distance within *O. plicata* using COI fell at the high end of published intraspecies values (Boissin *et al.* 2017). *Ophioplinthaca plicata* had a significantly high genetic distance among specimens from nearest localities at 0.9% (Tasmania and New Zealand). Therefore, the genetic distance values of *O. plicata* from the South China Sea to Tasmania and New Zealand (2.26%) suggest that the genus *Ophioplinthaca* has higher intraspecific genetic distances or that *O. plicata* may be a species complex. Previous studies suggest that *O. plicata* is difficult to identify and is often misidentified as *O. pulchra,* due to highly variable and overlapping morphological characters in these species. The present morphological analysis and previous studies indicate that the morphology of *O. plicata* tends to vary somewhat across biogeographic regions. We suggest a combination of molecular and morphological analysis of *O. plicata* from different localities to understand whether these morphological variations indicate a single species or a cryptic species complex (O'Hara & Stöhr 2006) (Suppl. file 7 and Suppl. file 8).

The molecular analysis of the Ophiactidae indicates four sub-clades within the family. Species of *Ophiactis* from the South China Sea fell into Sub-Clade 02 (*O.* cf. *perplexa*, *O. profundi* and *O.* cf. *brachygenys*) (Fig. 48). Species of *Ophiactis* were difficult to distinguish by morphological analysis alone, due to high morphological similarity between species and high morphological variation among individuals (Lyman 1879; H.L. Clark 1911; Koehler 1922a). Therefore, combining morphological and molecular analysis will help to understand the species complexity. The morphology of *O. perplexa* varied among individuals, especially the characteristics of disc spines (Fig. 36). Molecular analysis suggests two sister clades within *O. perplexa* due to a wide range of intraspecific genetic distances along the South China Sea to New Zealand waters (0.55% to 2.39%). *Ophiactis perplexa* from the South China Sea and Tasman Sea fall into one sister clade with another clade around New Zealand. However, we could not determine whether specimens in these two clades belong to a single species or a species complex without sufficient molecular data collection of *O. perplexa* from different localities. *Ophiactis brachygenys* from this study was the first record of a heptamerous and hexamerous species that was previously known only from pentamerous individuals. This finding added another problem to the taxonomy of *Ophiactis*. *Ophiactis definita* and *O. brachygenys* were synonymized by Liao (2004). Morphologically both species share similar features, except separated arm plates, but this character can vary due to the size of the specimen or the appearance of the arm (Fig. 42G–H). Species of *Ophiactis* were harder to identify by key morphological characters that delimit species, when considering morphological variation among individuals. The molecular analysis of Ophiactidae identified two sister clades among *O. definita* and

O. brachygenys due to broad intraspecific genetic distances from the South China Sea to Australian waters (1.09% to 2.02%). However, whether this result indicates a single species or a species complex could not be determined from this study, due to insufficient data collection and the small number of localities (Suppl. file 9). We suggest a population genetic study for the genus *Ophiactis* to better understand the species complexity.

Among morphological characters, arm skeleton characters have become key features to identify families among Ophiuroidea, especially vertebrae in the families Ophiotomidae, Ophiactidae, Ophiomusaidae (*Ophiomusa*) and some Ophiacanthidae (*Ophientrema*, most species of *Ophiacantha*) with zygospondylous articulation and in the families Asteronychidae, Euryalidae, Gorgonocephalidae and some Ophiacanthidae (*Ophiurothamnus*, *Ophiomoeris*, *Ophioplinthaca* and some species of *Ophiacantha*) with streptospondylous articulation.

The overall intraspecific genetic distance variation among families included in this study was 0.5% to 2.47% along the South Pacific region to the South China Sea. Genetic distances among families suggested that COI was better than 16S to understand interspecific molecular complexity (Suppl. file 10). The order Euryalida had a low interspecific genetic distance variation among all Ophiuroidea (Suppl. file 10). Our molecular analysis suggests that species from the genera *Ophiacantha* and *Ophiactis* have to be revised by constructing a concatenated ML tree with additional mitochondrial and nucleic genes (COI, 16S, 18S and 28S) to better understand the species complexity and evolutionary radiation among families (Liu *et al.* 2018).

Biogeography and species diversity of ophiuroids in the South China Sea

The ophiuroid fauna of the South China Sea is widespread across several biogeographic regions, but most of them are tropical Indo-Pacific species. A total of 304 species have been recorded from the South China Sea, including our study (Lane *et al.* 2000; Liao 2004; Putchakarn & Sonchaeng 2004; Sirenko *et al.* 2019; Chen *et al.* 2020; Li *et al.* 2021) (Suppl. file 11). Of the South China Sea ophiuroids, 44.55% (135) have been recorded from the Philippines and Indonesian seas, 69.97% (212) from Australia and New Zealand waters, 44.55% (135) from the Northwest Pacific region and only few of them (15) have been recorded from South Africa and the Indian Ocean. The South China Sea may be recognized as one of the species richest localities in the Indo-Pacific region. The recorded species belong to all six orders, 29 out of 33 families and 93 out of 259 genera within the class Ophiuroidea and represent 14.37% of global ophiuroid diversity (Table 3). The South China Sea harbors a great diversity of ophiuroid species, most of them in the order Amphilepidida, but also Ophiacanthida

Table 3. Species diversity in all six current orders of Ophiuroidea in the South China Sea (sources: Lane *et al.* 2000; Liao 2004; Putchakarn & Sonchaeng 2004; Sirenko *et al.* 2019; Chen *et al.* 2020; Li *et al.* 2021). Note: some species were removed due to uncertainty of location, especially near Philippine seas; see Lane *et al.* (2000).

Order	Family	Genus	Species	Species diversity (%)
Euryalida	3	14	27	13.7
Ophiurida	5	4	24	5.8
Amphilepidida	11	37	165	17.8
Ophiacanthida	8	32	85	17.6
Ophioleucida	1	2	2	6.9
Ophioscolcida	1	1	1	0.2
Total	**29**	**90**	**304**	**14.4**

(Lane *et al.* 2000; Liao 2004; Putchakarn & Sonchaeng 2004; Liu 2008; Sirenko *et al.* 2019; Chen *et al.* 2020; OBIS 2021; Stöhr *et al.* 2021; Li *et al.* 2021) (Table 3). The rate of endemicity in the South China Sea is high with 7.59% (23) of the ophiuroid fauna, and 37.96% (112) are endemic to the Indo-Pacific region. A possible reason for the prominence of endemics in the South China Sea may be that it has periodically been enclosed by land during glacial low sea level stands (Lane *et al.* 2000). Most of the high biodiversity areas within the South China Sea are still lacking in data (Nansha Islands reef system), and given the complex species diversity of ophiuroids, further sampling from those areas should record additional taxa, some of which may increase the number of endemic ophiuroids in the South China Sea.

According to the depth gradient, 168 (55.4%) species were recorded only from shallow waters, 60 (19.8%) species only from bathyal depths, 69 (22.4%) species from both shallow and bathyal waters, and two (0.7%) species from both bathyal and abyssal waters in the South China Sea. A high percentage of the shallow water species was recorded in the order Amphilepidida (Lane *et al.* 2000; Liao 2004; Putchakarn & Sonchaeng 2004; Sirenko *et al.* 2019; Chen *et al.* 2020; Li *et al.* 2021). A significant number of species was recorded from both shallow and bathyal depths, which shows that most of the ophiuroid species are eurybathic (e.g., *Ophiomusa lymani*: 200–4000 m), or they may harbor unrecognized cryptic diversity. In general, most of the species have been recorded from shallow waters (77.9%), few have been recorded only from deep waters (20.4%), and a significant number of species have been recorded from a wider depth range (22.4%) in the South China Sea (Lane *et al.* 2000; Liao 2004; Putchakarn & Sonchaeng 2004; Sirenko *et al.* 2019; Chen *et al.* 2020; Li *et al.* 2021).

There is a high chance of finding new records on the deep-sea seamounts in the South China Sea, and more deep-sea expeditions are required to analyze the biodiversity of deep-sea ophiuroids. However, the sample collection in the present study was restricted to only a few localities from the South China Sea, including near the Xisha and Zhongsha Islands, and Hainan Island. The actual number of species recorded from the deep waters of the South China Sea will likely increase, because some of the specimens in our collection were impossible to identify.

Station records and observations from the present study suggest that *Ophientrema scolopendrica* has a parasitic or mutualistic relationship with glass sponge species (Porifera: Hexactinellidea), but this needs to be studied further by repeated observation or gut content analysis to better understand their relationship (Henkel *et al.* 2008; Girard *et al.* 2016). Previous literature and our observations suggest that *O. scolopendrica* may be epizoic at depths of 1000–2000 m, because water depth is considered to have a high impact on biogeographic patterns on seamounts (O'Hara 2007). *Ophiacantha aster* sp. nov. was found on a seamount, living as a colony of more than a hundred specimens attached to a dead coral branch, but its relationship with coral species and its feeding behavior remain unknown.

Gorgonocephalus chilensis and *Asteroschema horridum* were recorded from deep waters in the South China Sea (1070–1550 m). *Asteroschema horridum* had previously been recorded as a deep-water species, but *Gorgonocephalus chilensis* had been recorded from a wide bathymetric range without any significant morphological variations (Olbers *et al.* 2019) The present study suggests a high possibility of recording species of Euryalida and *Gorgonocephalus* from the South China Sea that have previously been recorded from the South-Pacific region and confirms a high probability of a wider distribution of species of *Asteroschema* and *Gorgonocephalus* around the Indo-Pacific region than previously expected.

Acknowledgments

The authors want to thank the crews of the vessel 'Tansuo 1' and the pilots of the HOV 'Shenhaiyongshi'. The authors also thank the members of the marine ecology and evolutionary biology laboratory at the Institute of Deep-sea Science and Engineering, Chinese Academy of Sciences for their help in sample

collection and analysis. Many thanks to Dr Hou Xue and Dr Zhi Zheng for their help in acquiring SEM images of specimens. The authors would also like to thank Dr Timothy D. O'Hara and Dr Masanori Okanishi for their help in identifying species. We are grateful to two anonymous referees, who helped to improve the manuscript with constructive comments. This work was supported by the Major Scientific and Technological Projects of Hainan Province (ZDKJ2019011), the National Key Research and Development Program of China (2016YFC0304905, 2018YFC0309804) and the Strategic Priority Research Program of the Chinese Academy of Sciences (XDA22040502).

References

Baker A.N. 1980. Euryalinid Ophiuroidea (Echinodermata) from Australia, New Zealand, and the South-west Pacific Ocean. *New Zealand Journal of Zoology* 7 (1): 11–83. https://doi.org/10.1080/03014223.1980.10423763

Baker A.N., Okanishi M. & Pawson D.L. 2018. Euryalid brittle stars from the international Indian Ocean Expedition 1963–64 (Echinodermata: Ophiuroidea: Euryalida). *Zootaxa* 4392 (1): 1–27. https://doi.org/10.11646/zootaxa.4392.1.1

Bell F.J. 1909. Report on the Echinoderma (other than holothurians) collected by Mr. J. Stanley Gardiner in the western parts of the Indian Ocean. *Transactions of the Linnean Society of London, Series 2* 2: 17–22. Available from https://www.biodiversitylibrary.org/page/16398922 [accessed 16 Feb. 2022].

Boissin E., Feral J. & Chenuile A. 2008. Defining reproductively isolated units in a cryptic and syntopic species complex using mitochondrial and nuclear markers: the brooding brittle star, *Amphipholis squamata* (Ophiuroidea). *Molecular Ecology* 17 (7): 1732–1744. https://doi.org/10.1111/j.1365-294X.2007.03652.x

Boissin E., Stöhr S. & Chenuile A. 2011. Did vicariance and adaptation drive cryptic speciation and evolution of brooding in *Ophioderma longicauda* (Echinodermata: Ophiuroidea), a common Atlanto-Mediterranean ophiuroid? *Molecular Ecology* 20 (22): 4737–4755. https://doi.org/10.1111/j.1365-294X.2011.05309.x

Boissin E., Hoareau T.B., Paulay G. & Bruggemann J.H. 2017. DNA barcoding of reef brittle stars (Ophiuroidea, Echinodermata) from the southwestern Indian Ocean evolutionary hot spot of biodiversity. *Ecology and Evolution* 7 (24): 11197–11203. https://doi.org/10.1002/ece3.3554

Chang F.Y., Liao Y.L. & Wu B.L. 1962. Euryaliae of the China Sea. *Acta Zoologica Sinica* 14: 53–68.

Chen W.Y., Zhang D. & Wang C. 2020. Two new records of genus *Ophiurothamnus* (Ophiuroidea, Ophiacanthidae) from a deep-sea seamount of the South China Sea. *Oceanologia et Limnologia Sinica* 51 (3): 649–655. https://doi.org/10.11693/hyhz20191100232

Cho W. & Shank T.M. 2010. Incongruent patterns of genetic connectivity among four ophiuroid species with differing coral host specificity on North Atlantic seamounts. *Marine Ecology* 31 (Suppl. 1): 121–143. https://doi.org/10.1111/j.1439-0485.2010.00395.x

Christodoulou M., O'Hara T.D., Hugall A.F. & Arbizu P.M. 2019. Dark ophiuroid biodiversity in a prospective abyssal mine field. *Current Biology* 29 (22): 3909–3912. https://doi.org/10.1016/j.cub.2019.09.012

Clark H.L. 1911. North Pacific ophiurans in the collection of the United States National Museum. *United States National Museum Bulletin* 75: 1–302.

Clark H.L. 1915. Catalogue of recent ophiurans, based on the collection of the Museum of Comparative Zoology. *Memoirs of the Museum of Comparative Zoology at Harvard College* 25 (4): 164–376.

Clark H.L. 1923. The echinoderm fauna of South Africa. *Annals of the South African Museum* 13 (7): 221–438.

Corstorphine E.A. 2010. *DNA Barcoding of Echinoderms: Species Diversity and Patterns of Molecular Evolution.* MSc thesis, University of Guelph, Canada.

Döderlein L. 1902. Japanische Euryaliden. *Zoologischer Anzeiger* 25: 320–326.

Döderlein L. 1911. Über japanische und andere Euryalae. *Abhandlungen der Bayerischen Akademie der Wissenschaften, Mathematisch-physikalische Klasse* Suppl. 5 (2): 1–123.

Döderlein L. 1927. Indopacifische Euryalae. *Abhandlungen der Bayerischen Akademie der Wissenschaften, Mathematisch-physikalische Klasse* 31 (6): 1–106.

Edler D., Klein J., Antonelli A. & Silvestro D. 2021. raxmlGUI 2.0: a graphical interface and toolkit for phylogenetic analyses using RAxML. *Methods in Ecology and Evolution* 12 (2): 373–377. https://doi.org/10.1111/2041-210X.13512

Frensel R., Barboza C.A.M., Moura R.B. & Campos L.S. 2010. Southwest Atlantic deep-sea brittle stars (Echinodermata: Ophiuroidea) from Campos Basin, Brazil. *In*: Harris L.G., Boetger S.A., Walker C.W. & Lesser M.P. (eds) *Echinoderms: Durham – Proceedings of the 12th International Echinoderm Conference*: 173–180. CRC Press, Boca Raton, FL, USA. https://doi.org/10.1201/9780203869543-c27

Gallego R., Lavery S. & Sewell M.A. 2014. The meroplankton community of the oceanic Ross Sea during late summer. *Antarctic Science* 26 (4): 345–360. https://doi.org/10.1017/S0954102013000795

Galaska M.P., Li Y., Kocot K.M., Mahon A.R. & Halanych K.M. 2019. Conservation of mitochondrial genome arrangements in brittle stars (Echinodermata, Ophiuroidea). *Molecular Phylogenetics and Evolution* 130: 115–120. https://doi.org/10.1016/j.ympev.2018.10.002

Girard F., Fu B. & Fisher C.R. 2016. Mutualistic symbiosis with ophiuroids limited the impact of the Deepwater Horizon oil spill on deep-sea octocorals. *Marine Ecology Progress Series* 549: 89–98. https://doi.org/10.3354/meps11697

Guille A. 1981. Echinodermes: Ophiurides. *In*: Forest J. (ed.) *Résultats des Campagnes MUSORSTOM: 1. Philippines.* Mémoires ORSTOM 91: 413–456. Muséum national d'histoire naturelle, Paris.

Hendler G. 1988. Ophiuroid skeleton ontogeny reveals homologies among skeletal plates of adults: a study of *Amphiura filiformis*, *Amphiura stimpsonii* and *Ophiophragmus filograneus* (Echinodermata). *The Biological Bulletin* 174 (1): 20–29. https://doi.org/10.2307/1541755

Hendler G. 2018. Armed to the teeth: a new paradigm for the buccal skeleton of brittle stars (Echinodermata: Ophiuroidea). *Contributions in Science* 526 (December): 189–311.

Henkel T.P., Bruno J., Posey M. & Scharf F. 2008. *Ecology of the Obligate Sponge-dwelling Brittlestar Ophiothrix lineata.* PhD thesis, University of North Carolina Wilmington, USA.

Hertz M. 1927. Die Ophiuroiden der Deutschen Tiefsee-Expedition. I. Chilophiurida Matsumoto (Ophiolepididae, Ophioleucidae, Ophiodermatidae, Ophiocomidae). *Wissenschaftliche Ergebnisse der Deutschen Tiefsee-Expedition auf dem Dampfer Valdivia, 1898–1899* 22 (3): 59–122.

Hoareau T.B. & Boissin E. 2010. Design of phylum-specific hybrid primers for DNA barcoding: addressing the need for efficient COI amplification in the Echinodermata. *Molecular Ecology Resources* 10 (6): 960–967. https://doi.org/10.1111/j.1755-0998.2010.02848.x

Hunter R.L., Brown L.M., Alexander Hill C., Kroeger Z.A. & Rose S.E. 2016. Additional insights into phylogenetic relationships of the Class Ophiuroidea (Echinodermata) from rRNA gene sequences. *Journal of Zoological Systematics and Evolutionary Research* 54 (4): 269–275. https://doi.org/10.1111/jzs.12135

International Hydrographic Organization (I.H.O.) & Sieger R. 2012. Names of oceans and seas as digitized table. Alfred Wegener Institute, Helmholtz Centre for Polar and Marine Research, Bremerhaven, PANGAEA. https://doi.org/10.1594/PANGAEA.777976

Irimura S. 1991. Ophiuroidea. *In*: Imaoka T., Irimura S., Okutani T., Oguro C., Oji T. & Kanazawa K. (eds) *Echinoderms from Continental Shelf and Slope Around Japan: The Intensive Research of Unexploited Fishery Resources on Continental Slopes.* Japan Fisheries Resource Conservation Association, Tokyo.

Kim D. & Shin S. 2015. A newly recorded basket star of genus *Gorgonocephalus* (Ophiuroidea: Euryalida: Gorgonocephalidae) from the East Sea, Korea. *Animal Systematics, Evolution and Diversity* 31 (4): 311–315. https://doi.org/10.5635/ased.2015.31.4.311

Kimura M. 1980. A simple method for estimating evolutionary rates of base substitutions through comparative studies of nucleotide sequences. *Journal of Molecular Evolution* 16 (2): 111–120. https://doi.org/10.1007/BF01731581

Koehler R. 1895. Dragages profonds exécutés à bord du Caudan dans le Golfe de Gascogne. Rapport préliminaire sur le échinodermes. *Revue biologique du Nord de la France* 7: 439–49.

Koehler R. 1897. Echinodermes recueillis par "l'Investigator" dans l'Océan Indien. I. Les ophiures de mer profonde. *Annales des Sciences naturelles Zoologie* 8 (4): 277–372.

Koehler R. 1899. *An Account of the Deep-Sea Ophiuroidea Collected by the Royal Indian Marine Survey*. Trustees of the Indian Museum, Calcutta.

Koehler R. 1900. Note préliminaire sur les échinides et les ophiures de l'Expédition Antarctique Belge. *Bulletin de l'Academie royale de Belgique* 11 (3): 814–820.

Koehler R. 1904. Ophiures de l'expédition du Siboga. Part 1. Ophiures de mer profonde. *Siboga Expeditie* 45A: 1–176.

Koehler R. 1905. Ophiures de l'expédition du Siboga. Part 2. Ophiures littorales. *Siboga Expeditie* 45B: 1–140.

Koehler R. 1907. Note préliminaire sur quelques astéries et ophiures provenant des campagnes de la Princesse Alice. *Bulletin de l'Institut oceanographique* 99: 1–47.

Koehler R. 1922a. Ophiurans of the Philippine seas and adjacent waters. *United States National Museum Bulletin* 5 (100): 1–480.

Koehler R. 1922b. Echinodermata: Ophiuroidea. *Australasian Antarctic Expedition 1911–1914, Scientific Report Series C* 8 (2): 5–98.

Koehler R. 1930. Ophiures recueillies par le Docteur Th. Mortensen dans les Mers d'Australie et dans l'Archipel Malais. Papers from Dr. Th. Mortensen's Pacific Expedition 1914–16. LIV. *Videnskabelige Meddelelser fra Dansk naturhistorisk Forening* 89: 1–295.

Kumar S., Stecher G. & Tamura K. 2016. MEGA7: Molecular Evolutionary Genetics Analysis version 7.0 for bigger datasets. *Molecular Biology and Evolution* 33 (7): 1870–1874. https://doi.org/10.1093/molbev/msw054

Kumar S., Stecher G., Li M., Knyaz C. & Tamura K. 2018. MEGA X: Molecular Evolutionary Genetics Analysis across computing platforms. *Molecular Biology and Evolution* 35 (6): 1547–1549. https://doi.org/10.1093/molbev/msy096

Lane D.J.W., Marsh L.M., VandenSpiegel D. & Rowe F.W.E. 2000. Echinoderm fauna of the South China Sea: an inventory and analysis of distribution patterns. *Raffles Bulletin of Zoology* 48 (Suppl. 8): 459–493.

Lee T., Stöhr S., Jae Bae Y. & Shin S. 2019. A new fissiparous brittle star, *Ophiacantha scissionis* sp. nov. (Echinodermata, Ophiuroidea, Ophiacanthida), from Jeju Island, Korea. *Zoological Studies* 58: 1–17. https://doi.org/10.6620/ZS.2019.58-08

Li G. 1987. Deep-sea ophiurans in the South China Sea. *Nanhai Studia Marina Sinica* 8: 143–153.

Li Q., Li Y., Na J., Han X., Paterson G.L.J., Liu K., Zhang D. & Qiu J.-W. 2021. Description of a new species of *Histampica* (Ophiuroidea: Ophiothamnidae) from cold seeps in the South China Sea and analysis of its mitochondrial genome. *Deep-Sea Research Part I: Oceanographic Research Papers* 178: e103658. https://doi.org/10.1016/j.dsr.2021.103658

Li X. 2017. Taxonomic research on deep-sea macrofauna in the South China Sea using the Chinese deep-sea submersible Jiaolong. *Integrative Zoology* 12 (4): 270–282. https://doi.org/10.1111/1749-4877.12254

Liao Y. 2004. *Echinodermata: Ophiuroidea.* Fauna Sinica: Zoology of China Invertebrates 40. Science Press, Beijing.

Liao Y. & Clark A.M. 1995. *The Echinoderms of Southern China*. Science Press, Beijing.

Litvinova N.M. 1998. Two new species of the genus *Ophiuraster* (Ophiurinae, Ophiuroidea, Echinodermata) from French collections and some remarks on the genus. *Zoosystema* 20 (3): 439–444.

Liu J., Liu H. & Zhang H. 2018. Phylogeny and evolutionary radiation of the marine mussels (Bivalvia: Mytilidae) based on mitochondrial and nuclear genes. *Molecular Phylogenetics and Evolution* 126: 233–240. https://doi.org/10.1016/j.ympev.2018.04.019

Liu R. (ed.) 2008. *Checklist of Marine Biota of China Seas. China Science Press* 1267: 1–1289.

Lütken C.F. & Mortensen T. 1889. Reports on an exploration off the west coasts of Mexico, Central and Southern America and off the Galapagos Islands. XXV. The Ophiuridae. *Memoirs of the Museum of Comparative Zoology* 23 (2): 97–208.

Lyman T. 1869. Preliminary report on the Ophiuridae and Astrophytidae dredged in deep water between Cuba and Florida Reef. *Bulletin of the Museum of Comparative Zoology* 1: 309–354.

Lyman T. 1875. Zoological Results of the Hassler Expedition. 2. Ophiuridae and Astrophytidae. *Illustrated Catalogue of the Museum of Comparative Zoology at Harvard College* 8 (2): 1–34.

Lyman T. 1878. Ophiuridae and Astrophytidae of the "Challenger" expedition. Part I. *Bulletin of the Museum of Comparative Zoology* 5 (7): 65–168.

Lyman T. 1879. Ophiuridae and Astrophytidae of the "Challenger" expedition. Part II. *Bulletin of the Museum of Comparative Zoology* 6 (2): 17–83.

Lyman T. 1882. Report on the Ophiuroidea. *Report of the Scientific Results of the Voyage of H.M.S. Challenger 1873–76, Zoology* 5 (1): 1–386.

Lyman T. 1883. Reports on the results of dredging, under the supervision of Alexander Agassiz, in the Carribbean Sea (1878–79), and on the east coast of the United States, during the summer of 1880, by the U.S. coast survey steamer "Blake", commander J.R. Bartlett, U.S. *Bulletin of the Museum of Comparative Zoology* 10 (6): 227–287.

Martynov A. 2010. Reassessment of the classification of the Ophiuroidea (Echinodermata), based on morphological characters. I. General character evaluation and delineation of the families Ophiomyxidae and Ophiacanthidae. *Zootaxa* 2697 (1): 1–54. https://doi.org/10.11646/zootaxa.2697.1.1

Matsumoto H. 1915. A new classification of the Ophiuroidea: with descriptions of new genera and species. *Proceedings of the Academy of Natural Sciences of Philadelphia* 67: 43–92.

Matsumoto H. 1917. A monograph of Japanese Ophiuroidea, arranged according to a new classification. *Journal of the College of Science, Imperial University, Tokyo* 38: 1–408.

McKnight D.G. 2000. The marine fauna of New Zealand: basket-stars and snake-stars (Echinodermata: Ophiuroidea: Euryalinida). *NIWA Biodiversity Memoir* 115: 1–79.

Mortensen T. 1924. Echinoderms of New Zealand and the Auckland-Campbell Islands. II. Ophiuroidea. Papers from Dr Th. Mortensen's Pacific Expedition 1914–16. *Videnskabelige Meddelelser fra Dansk naturhistorisk Forening* 77: 91–177.

Mortensen T. 1936. *Discovery Reports: Echinoidea and Ophiuroidea*. Cambridge University Press, Cambridge, UK.

Müller J. & Troschel F.H. 1842. *System der Asteriden. 1. Asteriae. 2. Ophiuridae.* Vieweg, Braunschweig, Germany.

Muths D., Davoult D., Gentil F. & Jollivet D. 2006. Incomplete cryptic speciation between intertidal and subtidal morphs of *Acrocnida brachiata* (Echinodermata: Ophiuroidea) in the Northeast Atlantic. *Molecular Ecology* 15 (11): 3303–3318. https://doi.org/10.1111/j.1365-294X.2006.03000.x

Muths D., Jollivet D., Gentil F. & Davoult D. 2009. Large-scale genetic patchiness among NE Atlantic populations of the brittle star *Ophiothrix fragilis*. *Aquatic Biology* 5 (2): 117–132. https://doi.org/10.3354/ab00138

Na J., Chen W., Zhang D., Zhang R., Lu B., Shen C., Zhou Y. & Wang C. 2022. Morphological description and population structure of an ophiuroid species from cobalt-rich crust seamounts in the Northwest Pacific: implications for marine protection under deep-sea mining. *Acta Oceanologica Sinica* 40: 79–89. https://doi.org/10.1007/S13131-020-1666-1

OBIS 2021. *Ocean Biodiversity Information System.* Available from www.obis.org [accessed 15 Aug. 2021].

O'Hara T.D. 2007. Seamounts: centres of endemism or species richness for ophiuroids? *Global Ecology and Biogeography* 16 (6): 720–732. https://doi.org/10.1111/j.1466-8238.2007.00329.x

O'Hara T.D. & Stöhr S. 2006. Deep water Ophiuroidea (Echinodermata) of New Caledonia : Ophiacanthidae and Hemieuryalidae. *In*: Richer de Forges B. & Justine J.-L. (ed.) *Tropical Deep-Sea Benthos* 24: 33–141. Muséum national d'histoire naturelle, Paris.

O'Hara T.D., Smith P.J., Mills V.S., Smirnov I. & Steinke D. 2013. Biogeographical and phylogeographical relationships of the bathyal ophiuroid fauna of the Macquarie Ridge, Southern Ocean. *Polar Biology* 36 (3): 321–333. https://doi.org/10.1007/s00300-012-1261-9

O'Hara T.D., Hugall A.F., Thuy B. & Moussalli A. 2014. Phylogenomic resolution of the class Ophiuroidea unlocks a global microfossil record. *Current Biology* 24 (16): 1874–1879. https://doi.org/10.1016/j.cub.2014.06.060

O'Hara T.D., Hugall A.F., Hunjan S., Nilsen R. & Moussalli A. 2016. An exon-capture system for the entire class Ophiuroidea. *Molecular Biology and Evolution* 33 (1): 281–294. https://doi.org/10.1093/molbev/msv216

O'Hara T.D., Hugall A.F., Thuy B., Stöhr S. & Martynov A.V. 2017. Restructuring higher taxonomy using broad-scale phylogenomics: the living Ophiuroidea. *Molecular Phylogenetics and Evolution* 107: 415–430. https://doi.org/10.1016/j.ympev.2016.12.006

O'Hara T.D., Stöhr S., Hugall A.F., Thuy B. & Martynov A. 2018. Morphological diagnoses of higher taxa in Ophiuroidea (Echinodermata) in support of a new classification. *European Journal of Taxonomy* 416: 1–35. https://doi.org/ 10.5852/ejt.2018.416

O'Hara T.D., Hugall A.F., Woolley S.N.C., Bribiesca-Contreras G. & Bax N.J. 2019. Contrasting processes drive ophiuroid phylodiversity across shallow and deep seafloors. *Nature* 565 (7741): 636–639. https://doi.org/10.1038/s41586-019-0886-z

Okanishi M. & Fujita T. 2013. Molecular phylogeny based on increased number of species and genes revealed more robust family-level systematics of the order Euryalida (Echinodermata: Ophiuroidea). *Molecular Phylogenetics and Evolution* 69 (3): 566–580. https://doi.org/10.1016/j.ympev.2013.07.021

Okanishi M. & Fujita T. 2018a. A taxonomic review of the genus *Astrodendrum* (Echinodermata, Ophiuroidea, Euryalida, Gorgonocephalidae) with description of a new species from Japan. *Zootaxa* 4392 (2): 289–310. https://doi.org/10.11646/zootaxa.4392.2.4

Okanishi M. & Fujita T. 2018b. Description of a new subfamily, Astrocloninae (Ophiuroidea : Euryalida : Gorgonocephalidae), based on molecular phylogeny and morphological observations. *Zoological Science* 35 (2): 179–187. https://doi.org/10.2108/zs170090

Okanishi M., O'Hara T.D. & Fujita T. 2011a. Molecular phylogeny of the order Euryalida (Echinodermata: Ophiuroidea), based on mitochondrial and nuclear ribosomal genes. *Molecular Phylogenetics and Evolution* 61 (2): 392–399. https://doi.org/10.1016/j.ympev.2011.07.003

Okanishi M., O'Hara T.D. & Fujita T. 2011b. A new genus *Squamophis* of Asteroschematidae (Echinodermata, Ophiuroidea, Euryalida) from Australia. *ZooKeys* 129: 1–15. https://doi.org/10.3897/zookeys.129.1202

Okanishi M., Yamaguchi K., Horii Y. & Fujita T. 2011c. Ophiuroids of the Order Euryalida (Echinodermata) from Hachij'jima Island and Ogasawara Islands, Japan. *Bulletin of the National Museum of Nature and Science, Series B* (*Botany*)*, Tokyo* (47): 367–385.

Okanishi M., Sentoku A., Martynov A. & Fujita T. 2018. A new cryptic species of *Asteronyx* Müller and Troschel, 1842 (Echinodermata: Ophiuroidea), based on molecular phylogeny and morphology, from off Pacific coast of Japan. *Zoologischer Anzeiger* 274: 14–33. https://doi.org/10.1016/j.jcz.2018.03.001

Olbers J.M., Griffiths C.L., O'Hara T.D. & Samyn Y. 2019. Field guide to the brittle and basket stars (Echinodermata: Ophiuroidea) of South Africa. *Abc Taxa* 19: 1–354. Available from http://www.abctaxa.be/volumes/volume_19_fieldguide-brittle-and-basket-stars [accessed 16 Feb. 2022].

Palumbi S.R. 1996a. Nucleic Acids II: the polymerase chain reaction. *In*: Hillis D.M., Moritz C. & Mable B.K. (eds) *Molecular Systematics*: 205–247. Sinauer Press, Sunderland, MA, USA.

Palumbi S.R. 1996b. What can molecular genetics contribute to marine biogeography? An urchin's tale. *Journal of Experimental Marine Biology and Ecology* 203 (1): 75–92. https://doi.org/10.1016/0022-0981(96)02571-3

Paterson G.L.J. 1985. The deep-sea Ophiuroidea of the North Atlantic Ocean. *Bulletin of the British Museum* (*Natural History*) 49 (1): 1–162.

Pérez-Portela R., Almada V. & Turon X. 2013. Cryptic speciation and genetic structure of widely distributed brittle stars (Ophiuroidea) in Europe. *Zoologica Scripta* 42 (2): 151–169. https://doi.org/10.1111/j.1463-6409.2012.00573.x

Putchakarn S. & Sonchaeng P. 2004. Echinoderm fauna of Thailand: history and inventory reviews. *ScienceAsia* 30: 417–428. https://doi.org/10.2306/scienceasia1513-1874.2004.30.417

Richards V.P., DeBiasse M.B. & Shivji M.S. 2015. Genetic evidence supports larval retention in the Western Caribbean for an invertebrate with high dispersal capability (*Ophiothrix suensonii*: Echinodermata, Ophiuroidea). *Coral Reefs* 34 (1): 313–325. https://doi.org/10.1007/s00338-014-1237-z

Rodrigues C.F., Paterson G.L.J., Cabrinovic A. & Cunha M.R. 2011. Deep-sea ophiuroids (Echinodermata: Ophiuroidea: Ophiurida) from the Gulf of Cadiz (NE Atlantic). *Zootaxa* 2754 (1): 1–26. https://doi.org/10.11646/zootaxa.2754.1.1

Rodriguez F., Oliver J.L. & Marin A. 1990. The general stochastic model of nucleotide substitution. *Journal of Theoretical Biology* 142 (4): 485–501. https://doi.org/10.1016/S0022-5193(05)80104-3

Sands C.J., O'Hara T.D., Barnes D.K.A. & Martín-Ledo R. 2015. Against the flow: evidence of multiple recent invasions of warmer continental shelf waters by a Southern Ocean brittle star. *Frontiers in Ecology and Evolution* 3: e63. https://doi.org/10.3389/fevo.2015.00063

Seno J. & Irimura S. 1968. Ophiuroidea collected from around the Ross Sea in 1964 with description of a new species. *Journal of the Tokyo University of Fisheries* 9 (2): 147–154.

Sirenko B.I., Smirnov I.S., Stepanjants S.D., Poltaruha O.P. & Savinkin O.V. 2019. First record of symbiosis of the brittle star *Ophiocnemis marmorata* (Echinodermata: Ophiuroidea: Ophiotrichidae) on jellyfish of the genus *Rhopilema* (Cnidaria: Scyphozoa) in Vietnamese waters. *Zoosymposia* 15 (1): 141–145. https://doi.org/10.11646/zoosymposia.15.1.16

Stöhr S. 2005. Who's who among baby brittle stars (Echinodermata: Ophiuroidea): postmetamorphic development of some North Atlantic forms. *Zoological Journal of the Linnean Society* 143 (4): 543–576. https://doi.org/10.1111/j.1096-3642.2005.00155.x

Stöhr S. 2011. New records and new species of Ophiuroidea (Echinodermata) from Lifou, Loyalty Islands, New Caledonia. *Zootaxa* 50 (1): 1–50. https://doi.org/10.11646/zootaxa.3089.1.1

Stöhr S. 2012. Ophiuroid (Echinodermata) systematics—where do we come from, where do we stand and where should we go? *Zoosymposia* 7 (1): 147–162. https://doi.org/10.11646/zoosymposia.7.1.14

Stöhr S. & O'Hara T.D. 2021. Deep-sea Ophiuroidea (Echinodermata) from the Danish Galathea II Expedition, 1950–52, with taxonomic revisions. *Zootaxa* 4963 (3): 505–529. https://doi.org/10.11646/zootaxa.4963.3.6

Stöhr S., O'Hara T.D. & Thuy B. 2012. Global diversity of brittle stars (Echinodermata: Ophiuroidea). *PLoS One* 7 (3): e31940. https://doi.org/10.1371/journal.pone.0031940

Stöhr S., O'Hara T. & Thuy B. (eds) 2021. *The World Ophiuroidea Database*. https://doi.org/10.14284/358

Studer T. 1884. Verzeichnis der während der Reise S.M.S. 'Gazelle' um die Erde, 1874-76 gesammelten Asteriden und Euryaliden. *Abhandlungen der preussischen Akademie der Wissenschaften* 2: 1–64.

Summers M.M. & Rouse G.W. 2014. Phylogeny of Myzostomida (Annelida) and their relationships with echinoderm hosts. *BMC Evolutionary Biology* 14 (1): 1–15. https://doi.org/10.1186/s12862-014-0170-7

Tavaré S. 1986. Some probabilistic and statistical problems in the analysis of DNA sequences. *American Mathematical Society: Lectures on Mathematics in the Life Sciences* 17: 57–86.

Teh L., Cashion T., Alava Saltos J., Cheung W. & Sumaila U. 2019. Status, Trends, and the Future of Fisheries in the East and South China Seas. *Fisheries Centre Research Reports* 27 (1): 1–101.

Thompson J.D., Higgins D.G. & Gibson T.J. 1994. CLUSTAL W: improving the sensitivity of progressive multiple sequence alignment through sequence weighting, position-specific gap penalties and weight matrix choice. *Nucleic Acids Research* 22 (22): 4673–4680. https://doi.org/10.1093/nar/22.22.4673

Thomson C.W. 1873. *The Depths of the Sea*. Macmillan and Co., London.

Thuy B. & Stöhr S. 2016. A new morphological phylogeny of the Ophiuroidea (Echinodermata) accords with molecular evidence and renders microfossils accessible for cladistics. *PLoS One* 11 (5): e156140. https://doi.org/10.1371/journal.pone.0156140

Turner R.L., Boucher J.M., O'Neill B.O. & Becker N.W. 2021. Brittlestars with a bite: a new kind of pedicellaria in echinoderms. *Zoomorphology* 140 (4): 505–525. https://doi.org/10.1007/s00435-021-00542-4

Ward R.D., Holmes B.H. & O'Hara T.D. 2008. DNA barcoding discriminates echinoderm species. *Molecular Ecology Resources* 8 (6): 1202–1211. https://doi.org/10.1111/j.1755-0998.2008.02332.x

Manuscript received: 28 May 2021
Manuscript accepted: 16 December 2021
Published on: 6 April 2022
Section editors: Rudy Jocqué, Didier VandenSpiegel
Desk editor: Danny Eibye-Jacobsen

Printed versions of all papers are also deposited in the libraries of the institutes that are members of the *EJT* consortium: Muséum national d'histoire naturelle, Paris, France; Meise Botanic Garden, Belgium; Royal Museum for Central Africa, Tervuren, Belgium; Royal Belgian Institute of Natural Sciences, Brussels, Belgium; Natural History Museum of Denmark, Copenhagen, Denmark; Naturalis Biodiversity Center, Leiden, the Netherlands; Museo Nacional de Ciencias Naturales-CSIC, Madrid, Spain; Real Jardín Botánico de Madrid CSIC, Spain; Zoological Research Museum Alexander Koenig, Bonn, Germany; National Museum, Prague, Czech Republic.

Overview of supplementary files

Supplementary file 1. Family Asteronychidae, pairwise distance values based on 443 bp mitochondrial 16S sequences, calculated using the Kimura 2-parameter method with 1000 bootstrap replicates (values in blue represent Standard Error).

Supplementary file 2. Family Asteronychidae, pairwise distance values based on 601 bp mitochondrial COI sequences, calculated using the Kimura 2-parameter method with 1000 bootstrap replicates (values in blue represent Standard Error).

Supplementary file 3. Family Gorgonocephalidae, pairwise distance values based on 608 bp mitochondrial COI sequences, calculated using the Kimura 2-parameter method with 1000 bootstrap replicates (values in blue represent Standard Error). Abbreviations: AN = Antarctica; NZ = New Zealand; SO = Southern Ocean; SCS = South China Sea.

Supplementary file 4. Family Euryalidae, pairwise distance values based on 608 bp mitochondrial COI sequences, calculated using the Kimura 2-parameter method with 1000 bootstrap replicates (values in blue represent Standard Error). Abbreviations: RI = Reunion Island; SCS = South China Sea.

Supplementary file 5. Family Ophiomusaidae, pairwise distance values based on 568 bp mitochondrial COI sequences, calculated using the Kimura 2-parameter method with 1000 bootstrap replicates (values in blue represent Standard Error). Abbreviations: NZ = New Zealand; SCS = South China Sea.

Supplementary file 6. Family Ophiotomidae, pairwise distance values based on 623 bp mitochondrial COI sequences, calculated using the Kimura 2-parameter method with 1000 bootstrap replicates (values in blue represent Standard Error). Abbreviation: SCS = South China Sea.

Supplementary file 7. Family Ophiacanthidae, pairwise distance values based on 608 bp mitochondrial 16S sequences, calculated using the Kimura 2-parameter method with 1000 bootstrap replicates (values in blue represent Standard Error). Abbreviation: SCS = South China Sea.

Supplementary file 8. Family Ophiacanthidae, pairwise distance values based on 449 bp mitochondrial COI sequences, calculated using the Kimura 2-parameter method with 1000 bootstrap replicates (values in blue color represent Standard Error). Abbreviations: AUS = Australia; NP = North Pacific; NZ = New Zealand; PNG = Papua New Guinea; SCS = South China Sea; TS = Tasman Sea.

Supplementary file 9. Family Ophiactidae, pairwise distance values based on 593 bp mitochondrial COI sequences, calculated using the Kimura 2-parameter method with 1000 bootstrap replicates (values in blue represent Standard Error). Abbreviations: AUS = Australia; NZ = New Zealand; PNG = Papua New Guinea; SCS = South China Sea; TS = Tasman Sea.

Supplementary file 10. Percentage of average Kimura 2-parameter model genetic distances between species within each family analyzed in this study (values in parentheses are ranges of genetic distance between species). Abbreviation: SE = Standard Error.

Supplementary file 11. The ophiuroid fauna of the South China Sea (sources: Lane *et al.* 2000; Liao 2004; Putchakarn & Sonchaeng 2004; Sirenko *et al.* 2019; Chen *et al.* 2020; Li *et al.* 2021). Note: some species were removed due to uncertainty of location, especially near Philippine seas; see Lane *et al.* (2000).

ZOBODAT - www.zobodat.at

Zoologisch-Botanische Datenbank/Zoological-Botanical Database

Digitale Literatur/Digital Literature

Zeitschrift/Journal: European Journal of Taxonomy

Jahr/Year: 2022

Band/Volume: 0810

Autor(en)/Author(s): Nethupul Hasitha, Stöhr Sabine, Zhang Haibin

Artikel/Article: New species, redescriptions and new records of deep-sea brittle stars (Echinodermata: Ophiuroidea) from the South China Sea, an integrated morphological and molecular approach 1-95